REPUBLIC OF TURKEY
ACIBADEM MEHMET ALI AYDINLAR UNIVERSITY
INSTITUTE OF HEALTH SCIENCES

TRANSCRIPTOMICS-BASED INVESTIGATION of DRUG RESISTANCE MECHANISMS in TRIPLE-NEGATIVE BREAST CANCER CELL LINES

RÜÇHAN EKREN
MASTER THESIS

DEPARTMENT of BIOSTATISTICS and BIOINFORMATICS

Thesis Supervisor:
Prof. O. UĞUR SEZERMAN

Thesis Co-Supervisor:
Assist. Prof. PERİNUR BOZAYKUT EKER

ISTANBUL – 2020

DECLARATION

I hereby declare that; this thesis study is solely my original work, I had no unethical behavior at any stage from planning to writing, I obtained all of the information in this thesis following academic and ethical rules, I have shown all the resources I have used in the bibliography and there is no violation of any patents and/or copyrights.

31/07/2020

Rüçhan Ekren

ACKNOWLEDGMENTS

Initially, I would like to express my sincere gratitude to my supervisor Prof. Dr. O. Uğur Sezerman, for his guidance that molds my early research career and the whole of my scientific insight, his endless patience, and continuous support when I feel confused and/or lost. He has been truly an idol for me, as a great scientist, as a great mentor, and as a kind and caring person. It has been a great privilege and honor for me to be one of his students. I would like to thank my co-advisor Asst. Prof. Dr. Perinur Bozaykut Eker for her positive energy that boosts me up whenever we meet and her valuable support. I also would like to thank my jury members, Prof. Dr. Meltem Müftüoğlu, Assoc. Prof. Dr. Emel Timuçin and Ph.D. Orhan Özcan for their scientific critics and constructive comments.

This thesis study is financially supported by the 117S013 enumerated International TUBITAK project I want to thank TUBITAK for funding this thesis study and Express my appreciation to GENENTECH authorities for providing full-access to a controlled study of EGAS00001000610 data to be utilized in this study.

My best friend, my greatest power-supplier, and my partner-in-crime Pınar seeing joy and love in your eyes kept me motivated all the time, especially when I am down. Thank you for your support for me.

Sezerman Lab friends and alumni, I am grateful to have worked side-by-side with them all; especially, MD. Ege Ülgen, Hüseyin Okan Soykam, Nogayhan Seymen, Begüm Özemek Güner, Ph.D. Ozan Özışık, and Ph.D. Orhan Özcan for all the brainstorm sessions we engaged and their enthusiasm to help me whenever I counsel them, I have learned a lot when I am working with them. Also, sincere thanks to Ph.D. Ceren Saygı, Ph.D. Melis Durası, Asst. Prof. Dr. Aslı Kutlu, Zehra Hazal Sezer, Tayyip Karaman, Narod Kebabcı, Eray Şahin, Umut Gerlevik, Sıla Karacan, Deniz Ece Kaya, Berk Gürdamar, Tuğçe Bozkurt and Fatma İşleyen for their friendship and advice in both scientific and non-scientific topics.

Moreover, I would like to especially thank my former supervisor -the person that greatly bend my scientific interest into bioinformatics- Prof. Dr. Jens Allmer and former lab mates of mine; Mehmet Direnç Mungan, Caner Bağcı, İlhan Erkin Acar, Mustafa Toprak, Rabia Suluyayla, Görkem Erdoğan, Mehmet Göktay, Ph.D. Canan Has and Asst. Prof. Dr. Müşerref Duygu Saçar Demirci for all the things we laughed and shared.

Additionally, I want to thank Prof. Dr. Devrim Pesen Okvur and C*iv*Ms Lab members/alumni; especially PhD Deniz Vurmaz, PhD Gizem Eyrilmez, PhD Tuğçe Oruç, Sevgi Önal and Hamdullah Yanık , that host me during my undergraduate years and helping me to become a better researcher. Also, I appreciate all the academics and friends that touched my life at least in some portion of my life.

Lastly, the greatest thanks to my family; I know I will always owe them, will try to become better and better in whatever I do to be worthy of their unconditional and infinite support, their belief, and their love for me. Dear Mom, Dad, I would be in a totally different spot without your perseverance and selfless sacrifice to support me.I feel very fortunate to have such a great family!

TABLE OF CONTENTS

LIST OF ABBREVIATIONS and SYMBOLS

TNBC	Triple-Negative Breast Cancer
ATCC	American Type Culture Collection
GDSC	Genomics of Drug Sensitivity in Cancer
CCLE	Cancer Cell Line Encyclopedia
EGA	European Genome-phenome Archive
IC50	Half-maximal inhibitory concentration
DEG	Differentially Expressed Gene
KEGG	Kyoto Encyclopedia of Genes and Genomes
SMILES	Simplified molecular-input line-entry system
FDR	False discovery rate

LIST OF FIGURES

LIST OF TABLES

SUMMARY

Breast cancer is the second leading cause of death in women and Triple-Negative breast cancer (TNBC) is one of the most aggressive cancer subtypes of breast cancer and highly resistant to most drugs. Even though the prevalence of TNBC cases among the patients is around 15-20 percent of the whole breast cancer cases; the survival lifespan of the patients is at least 3 times lesser than other sub-type having breast cancer patients.

To better understand the overall resistance mechanisms to a large pool of chemotherapeutic compounds, 52 different drugs' pharmacodynamics measurements on 17 TNBC cell lines were used, and then baseline gene expression profiles of these 17 TNBC cell lines were combined with pharmacodynamics data then assessed independently for each drug. Next, those 52 drugs investigated by their common targeted pathways and assessed together to unravel the most commonly affected DEGs and most commonly enriched pathways that take a significant role in the respective drugs' resistance mechanisms. Among 52 different chemotherapeutic compounds, it is observed that there are 15 common pathway target groups and among those target groups, many overlapping DEG trends that might have important effects on the regulatory network of the genes. Most prevalently found enriched pathways are MAPK signaling, ErbB signaling, and PI3K/MTOR signaling which are all greatly involved in tumorigenesis. The determined DEGs are highly differing for each of the drug response comparison but the enriched pathways are substantially consistent for especially the common pathway targeting drugs.

Keywords: Triple-Negative Breast Cancer, Drug Resistance, Baseline Gene Expression, Pathway Analysis

ÖZET

Üçlü-Negatif Meme Kanseri Hücre Hatlarının İlaç Direnç Mekanizmalarının Transkriptomiks-bazlı İncelenmesi

Meme kanseri, kadınlarda en fazla ölüme sebebiyet veren ikinci nedendir ve üçlü-negatif meme kanseri, meme kanseri tipleri arasında en agresif ve de çoğu ilaca karşı oldukça dirençli olan bir alt tipdir. Meme kanseri hastalarının yaklaşık olarak yüzde 15-20'si üçlü-negatif meme kanseri grubuna ait hücreler taşıyor olsa da, bu hastaların sağ kalımı; diğer meme kanseri alt tiplerini taşıyan hastalara kıyasla en az 3 kat daha az olmaktadır.

Üçlü-negatif meme kanseri hücrelerinin ilaç direnç mekanizmalarını daha iyi anlayabilmek amacıyla, 17 TNBC hücre hattının 52 ilaca karşı farmakodinamik verisi ile bu hücre hatlarının bazal gen ifadeleri birarada her bir ilaç için ayrı ayrı değerlendirildi. Bu aşamada diferansiyel gen ifadeleri belirlenmiş olan 52 ilaç için ortak hedeflenmiş metabolik yolaklar üzerinden analize devam edildi. İncelenmiş olan 52 kemoterapötik ilaç arasında hedeflenmiş metabolik yolaklar nezdinde ortak bir yolağı hedefleyen 15 ayrı grup gözlemlendi. Bu 15 hedeflenmiş yolaklar üzerinden ortak diferansiyel genler ve bu genlerin zenginleştirdiği; ilgili ilaçlara direnç gösterilmesinde etkili olduğu düşünülen istatistiki anlamlılıktaki yolaklar tespit edildi. Farklı farklı ilaçların yanıt grupları arasında yapılan yolak analizlerinde en yaygın karşılaşılan yolaklar; MAPK sinyal yolağı, ErbB sinyal yolağı ve PI3K/mTOR yolağı oldu. Tespit edilen diferansiyel ifade edilmiş genler farklı ilaç-yanıt gruplarının analizlerinde değişkenlik gösterse de ortak yolakları hedefleyen ilaçların analizinde, birbiri ile oldukça örtüşen nispette yolaklar seti önemli bulundu.

Anahtar Kelimeler: Üçlü-Negatif Meme Kanseri, İlaç Direnci, Bazal Gen İfadesi, Yolak Analizi

1. AIM OF THE STUDY and INTRODUCTION

American Cancer Society's 2020 report indicates that breast cancer is the second leading cause of death in women **(1)**. Even though not only females are stricken by breast cancer, according to the 2017 study of Jhan JR et al., one out of each eight women is diagnosed as a breast cancer patient, at least in a portion of their lifetime **(2)**. Although clinicians have been able to achieve more successful results against breast cancer in recent years, still we are losing 24% of patients diagnosed with breast cancer under 40 years of age. This high rate of patient loss leads to the highest cause of death in breast cancer patients under the age of 40 years **(1)**.On the other hand, we have a lot of insight into the heterogeneity of different types of breast cancer, as a result of deeply investigated and focused cancer studies **(3–7)**. Through these studies, subtypes of breast cancer are much clearly understood. In the battle against these breast cancer subtypes which are classified according to the status of their expression of certain receptors, widely used chemotherapy drugs designed to target those receptors **(8,9)**.

The triple-negative breast cancer (TNBC) cells do not contain the estrogen receptor (ER), progesterone receptor (PR), and do not overly express epidermal growth hormone 2 receptor (HER2) which are the fundamental differences of TNBC cells from other breast cancer cells **(10)**. Thus, the mode of action of most of the chemotherapy drugs fails on the targeting triple-negative breast cancer cells **(11)**. Triple-Negative Breast Cancer (TNBC) is the most lethal breast cancer with its more aggressive spread-pattern on the body and its difficulty to target by drugs due to the lack of hormone receptors. At the same time, most of the patients who showed improvement had a higher rate of progression than other subtypes **(11,12)**.

This study aims to investigate the drug resistance mechanisms in TNBC cell lines with the combined assessment of pharmacodynamics data of 52 chemotherapeutic compounds on TNBC cell lines and baseline transcriptomics data of TNBC cell lines.

2. BACKGROUND

This section is dedicated to introducing all fundamental information that is related to this thesis study to prepare even the most unfamiliar reader to easily understand what is unraveled in this study.

2.1. Cancer

All living beings are made of cells or just a single cell**(13,14)**. Aside from unicellular lives, the life cycle of multicellular livings starts with a single cell, an embryo, and continues with the division of that one cell to differentiate new types of cells and form body tissues and organs and later on organ systems**(15–17)**. The whole of these organ systems molds into a body that is called an organism. The growth of a single cell embryo to a complete organism happens with cellular multiplication by division, specifically mitotic division**(18–20)**. To the mitotic division of a cell, there are requirements to meet; having enough cellular materials to budding into another cell and proper command on a cell to initiate actual nuclear division**(21,22)**. This cellular division is scheduled by a certain molecular clock which is called the cell cycle**(23–26)**. Regulation of the cell cycle is essential for the healthiness of the cell and its daughter cells after division**(27–30)**.

Cancer mainly is the mere consequence of either genetic or environmental-based dysregulation and/or misregulation of the cell cycle**(31)**. There are lots of highly impactful metabolic pathways responsible for the controlled growth of a cell; like PI3K/mTOR signaling, Wnt signaling, MAPK signaling, p53 signaling, estrogen signaling, and so on**(32–40)**. The anomaly on gene products that are directly or indirectly related to any of those pathways may cause genomic instability, perturb the apoptosis mechanisms, induce enhanced blood vessel formation around the tissue, and even prevent telomere loss which is providing virtual immortality to the cells.

Cells divide without proper molecular checkpoint controls and form tumorogenic sites on body tissue. However, having tumors itself is not lethal usually, actual danger of the cancerous cells is when they gain excessive molecular characteristics and undock themselves to spread out and invade other body tissues. This phenomenon called metastasis and most of the fatality in cancer caused by the metastatic activity of cancer cells**(41–43)**.

2.1.1. Breast cancer

According to the body tissue of tumorigenesis takes place, there are a variety of differently named cancers present in the scientific literature. Breast cancer is one of them that uncontrolled cell division and abnormal mass-growth initially happen in breast tissue.

Breast cancer is one of the top lethal causes in females, apart from it's also hosting in males. There are striking recent statistics about how abundant breast cancer among the female population and how likely that a woman may face this problem eventually**(1,2)**.

The severity of breast cancer immensely attracted the scientific interest of scientists in the last 2-3 decades and deep investigation of this cancer type unearthed quite in detailed knowledge about it**(3–7)**. Through these studies, subtypes of breast cancer are much clearly understood. In the battle against these breast cancer subtypes which are generally classified according to the status of their expression of certain receptors, widely used chemotherapy drugs designed to target those receptors**(8,9)**.

One of the breast cancer subtype; the triple-negative breast cancer (TNBC) cells do not contain the estrogen receptor (ER), progesterone receptor (PR), and do not overly express epidermal growth hormone 2 receptor (HER2) which are the fundamental differences of TNBC cells from other breast cancer cell types **(10)**. Thus, the mode of action of most of the chemotherapy drugs fails on the targeting triple-negative breast cancer cells **(11)**.

Currently, TNBC is the most lethal breast cancer with its more aggressive spread-pattern on the body and its difficulty to target by drugs due to the lack of endocrine receptors. Additionally, most of the TNBC-bearing patients who showed improvement had a higher rate of progression than other subtypes **(11,12)**.

2.2. Pharmacodynamics

In pharmacy, medicine, and biochemistry therapeutic compounds tested to better understand the mode of action of those compounds, their activity trends, their toxicity, and certain different type of measurements calculated in this manner. All of those quantitative information gatherings about the therapeutics are considered as pharmacodynamics**(44–47)**.

There is one significant unit in pharmacodynamics that is highly adopted by other disciplines, especially in oncology, for the pragmatic reasons; IC50. IC50 is the concentration of the tested drug that causes the inhibitory effect at 50% of the tested population of the sample**(48,49)**.

Usage of the IC50 value of a drug on a certain population of sample is usually used in the machine learning-based approach with the generation of predictive drug-response models with ideally clinical usage or drug screening purposes**(50–52)**.

2.3. Gene Expression

Gene is the most fundamental virtual unit of DNA that may or may not code a protein. Gene expression is the production of transcripts from the respective gene with the control of cellular mechanisms**(53)**. If a gene doesn't code a protein, contrary to the "junk-DNA theory" it is responsible for the orchestration of other regulating elements like non-coding RNAs**(54,55).**

With the Human Genome Project and steep acceleration on the high-throughput sequencing advancements; measurement of gene expression became a highly popular source of evidence for the validation of the scientific hypothesis of scientists**(56–58)**.

There are constant developments on sequencing technologies, currently most abundantly used gene expression measurement technique is RNA-Seq which is sequencing the all of the converted mRNAs inside the cell/tissue as bulk, but there are also another next next-generation sequencing techniques arise like single-cell sequencing and single-nucleus sequencing to provide better resolution of the gene expression profile of the investigated samples to the researchers**(59–62)**. These single-cell approaches are quite promising with their precision however there is still a milestone to take in the raw data processing and normalization of the data for downstream analysis**(63–66)**

3. MATERIAL and METHODS

This section is dedicated to the explanation of the material and methods used in this thesis study for the sake of reproducibility by other researchers and a better understanding of the methods by the readers. In **Figure 1**, the overview workflow steps of the applied methodology in this study represented in a diagram scheme.

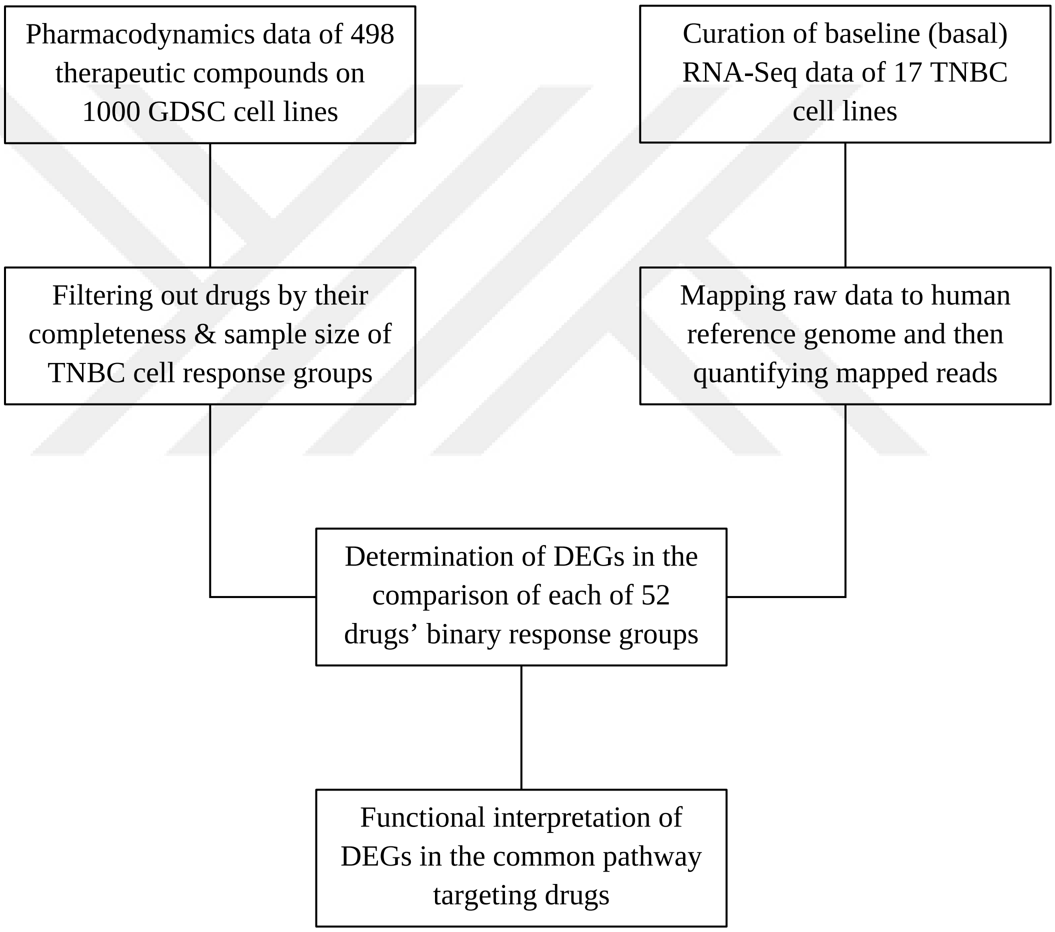

Figure 1: Overview representation of the methodology that is followed in this study.

Combined assesment of pharmacodynamics data of a large pool of chemotherapeutic compounds and baseline gene expression of 17 TNBC cell lines to understand how the resistant cell lines are differing from the sensitive cell lines.

3.1. TNBC Cell Lines

17 TNBC cell lines selected from a variety of cell lines, due to obtaining consistency on different data sources**(67)**. The cell lines selected for this study have greater data availability for the GDSC and CCLE consortiums. Official names of the selected TNBC cell lines are; BT-20, CAL-120, CAL-51, CAL-85-1, DU-4475, HCC1143, HCC1187, HCC1395, HCC1937, HCC2157, HCC38, HDQ-P1, Hs-578-T, MDA-MB-231, MDA-MB-436, MDA-MB-468, and MFM-223.

Adopted TNBC cell lines in this study, along with other 984 different cell lines, were properly grown and checked for possible co-culture contamination with the according to their ideal growth conditions which were explained in the GDSC1000 project's sample preparation procedure**(68)**.

3.2. Pharmacodynamics Data

GDSC database (GDSC v2) currently has drug screening data of 498 chemical compounds on 809 distinct cancer cell lines**(69,70)**. The primary aim in drug screening data collection was gathering as much as much drug's response data on TNBC cell lines in a curated data-pool to do a more comprehensive investigation. While drug response data is being curated, some drawbacks have been experienced.

First of all, not all of the TNBC cell lines had drug screening data for all 498 chemical compounds. Filtering the bulky drug response data for 17 TNBC cell lines out of 983 cell lines' diminished the data-pool from 498 to 266 chemotherapeutic compounds' drug screening measurements. Then, it didn't go unnoticed that some of the measurements among the 266 drugs' dose-response data from the GDSC dataset are lacking a full set of measurements of all TNBC cell lines and introduced some

"NA" (Not-Available) values in the dose-response data-pool. When we filtered "incomplete" drug-response measurement having chemical compounds out of the curated dose-response data-pool, the remaining drug number in total is 109 out of 266.

3.3. Classification of Drug Responses

In the case of this thesis study, TNBC cell lines which have resistant nature or mildly sensitive to a respective chemical compound classified as "resistant" and the ones that have a vulnerable characteristic to respective drug called as "sensitive".

The criterion on the determination of resistance/sensitivity is the evaluation of the half-maximal inhibitory concentration (IC50) and maximal dosage tested for drug molecules on that specific cell line. If the IC50 value of a drug on cell line is less than or equal to the maximum dosage tested of the chemical compound on that cell line, that cell line classified as "resistant"; if not, that cell line classified as "sensitive" to that drug molecule**(68)**.

After the binary classification ("resistant" or "sensitive") of the TNBC cell lines' to 109 therapeutic compounds, distributions of cell line numbers to each group are investigated. Both of the drug response categories must be comparable with each other concerning the sample size in populations to stand in a statistically logical base. When the distributions checked, some far-from being ideal cases observed in the drug response dataset of 109 drugs. A great portion of the data would consist of either all resistant or highly unequally distributed number of cell lines among sensitive response versus resistant response groups. To illustrate that; 16 of TNBC cell lines classified as resistant to one certain drug and only 1 other TNBC cell line classified as sensitive to that same drug. It is not statistically appropriate to compare a group consists of 16 samples and another group that has just one sample in it. Within the consideration of this fact, drug responses of TNBC cell lines filtered to meet the condition of sample size must be at least 3 cell lines for either of the response groups for each drug. At the end of this last step of filtering the drug response data, 52 therapeutic compounds remained in the dataset **(Table 1)**.

GDSC database also provides putative targets and affected metabolic pathways of each drug that is present in their dataset and these are categorically organized and sorted by the targeted pathways **(Table 2)** to provide visual easiness to readers.

Table 1: Binarized drug responses of 17 TNBC cell lines to 52 curated drugs.

Columns of the table are cell line names, rows are drug names resistant response abbreviated as "R" and sensitive response indicated as "S".

	BT-20	CAL-120	CAL-51	CAL-85-1	DU-4475	HCC1143	HCC1187	HCC1395	HCC1937	HCC2157	HCC38	HDQ-P1	Hs-578-T	MDA-MB-231	MDA-MB-436	MDA-MB-468	MFM-223
ABT737	R	S	R	R	S	S	R	R	S	S	S	S	S	S	R	S	S
Afatinib	R	R	R	R	S	S	R	S	R	S	R	S	S	S	R	S	R
Afuresertib	S	R	S	R	R	R	R	S	R	S	R	S	S	R	R	S	S
Alisertib	R	R	R	R	S	R	S	R	R	R	R	S	S	S	R	S	S
AT13148	R	R	R	R	R	R	S	R	R	R	R	S	S	R	R	R	R
AZ6102	R	R	S	R	S	R	R	R	R	R	R	S	S	R	R	S	S
AZD4547	R	R	S	R	S	R	S	S	R	R	S	R	R	S	R	R	S
AZD5363	S	R	S	R	R	R	R	S	R	S	R	S	S	R	R	R	S
AZD6482	S	R	R	R	R	R	R	S	R	R	R	S	S	R	R	S	R
AZD6738	R	R	S	S	S	S	R	S	R	R	S	S	S	R	R	S	S
AZD8055	S	S	R	S	S	R	R	S	R	R	R	S	S	S	R	S	S
AZD8186	R	R	R	R	R	S	R	S	R	S	R	S	S	R	R	S	R
BDP-00009066	R	R	S	S	S	R	S	S	R	S	R	R	S	S	R	R	R
BMS-536924	R	R	S	S	S	S	R	S	R	S	R	S	S	R	R	S	S
Camptothecin	R	R	S	R	S	R	R	S	R	R	R	R	R	R	R	S	R
Cediranib	R	R	S	S	S	R	R	S	S	S	R	S	S	R	R	S	S
Crizotinib	R	R	R	S	S	R	R	S	R	R	R	R	R	R	R	S	R
Dactolisib	S	S	S	S	S	S	R	S	R	S	R	S	S	S	R	S	R
Dasatinib	R	R	R	R	R	S	R	R	R	R	R	S	S	S	R	R	R
Entinostat	R	R	S	S	S	S	R	S	R	S	R	R	S	S	R	S	R
Epirubicin	R	S	S	R	S	R	R	R	R	S	S	S	S	S	R	S	R
Gemcitabine	R	S	S	S	S	R	R	R	R	R	S	S	S	S	S	S	R
GSK269962A	R	R	R	R	S	R	R	S	R	R	R	R	R	R	R	S	R
Ipatasertib	S	R	S	R	R	R	R	S	R	S	R	R	S	R	R	R	S
Irinotecan	R	R	S	R	S	R	R	R	R	R	R	R	R	R	R	S	R
JQ1	R	R	R	R	S	R	S	R	R	R	S	R	S	S	R	R	R
Lapatinib	S	R	S	R	S	S	R	S	R	S	R	S	S	R	R	S	R
MK-2206	S	R	R	R	S	R	R	S	R	S	R	R	S	R	R	R	S
Navitoclax	S	S	S	S	S	S	R	R	S	S	S	S	S	S	R	S	S
Nilotinib	R	R	S	R	S	R	R	R	R	R	R	S	S	S	R	S	R
NU7441	S	R	R	R	S	R	R	S	R	R	R	R	S	S	R	S	R
NVP-ADW742	R	R	R	R	S	S	R	S	R	S	R	S	R	R	R	R	R
OSI-027	S	S	S	S	S	R	R	S	S	S	R	S	S	S	S	S	S
Paclitaxel	S	R	R	S	S	S	S	S	R	R	S	R	S	S	R	S	S
Pevonedistat	S	S	S	S	S	R	R	R	R	S	S	S	R	S	R	S	R
RO-3306	R	R	R	R	S	R	R	R	R	R	R	R	S	R	R	S	R
Sapitinib	R	R	R	R	R	R	R	R	R	S	R	S	R	R	R	S	R
Sorafenib	S	R	S	R	S	R	S	R	R	R	R	R	S	S	R	S	S
Taselisib	S	R	S	S	R	S	R	S	S	S	R	S	S	R	R	R	S
Tozasertib	R	R	S	R	S	R	R	R	R	R	R	R	R	R	R	S	S
Trametinib	R	R	R	S	S	S	R	R	R	R	R	S	R	S	R	R	R
UMI-77	R	R	S	S	S	R	S	R	R	S	S	R	S	S	R	S	R
VE821	R	R	S	R	S	S	R	R	R	R	R	R	R	R	R	R	R
Vinblastine	R	R	S	R	S	R	R	S	R	S	R	S	S	S	R	S	S
Vinorelbine	R	S	S	R	S	R	S	S	R	R	S	R	S	S	R	S	R
Vorinostat	R	R	S	S	S	S	R	R	R	S	R	R	S	S	R	S	S
VX-11e	R	R	R	R	S	R	R	R	R	R	R	S	R	S	R	R	R
Wee1 Inhibitor	S	R	S	R	S	S	R	S	R	R	S	R	S	S	S	S	S
WEHI-539	R	S	R	R	S	S	R	R	R	S	S	S	R	R	R	R	R
WIKI4	R	R	R	R	R	S	R	R	R	S	R	S	R	R	R	R	R
YK-4-279	S	R	S	R	S	S	R	S	R	S	S	S	S	R	R	S	R
ZM447439	R	R	R	R	S	R	S	R	R	R	R	R	S	R	R	S	R

Table 2: Target genes and targeted metabolic pathways of curated 52 drugs included in this study.

Drug Name	Putative Target	Targeted Pathway
Nilotinib	ABL	ABL signaling
ABT737	BCL2, BCL-XL, BCL-W, BCL-B, BFL1	Apoptosis regulation
Navitoclax	BCL2, BCL-XL, BCL-W	Apoptosis regulation
UMI-77	MCL1	Apoptosis regulation
WEHI-539	BCL-XL	Apoptosis regulation
RO-3306	CDK1	Cell cycle
Wee1-Inhibitor	WEE1, CHEK1	Cell cycle
Entinostat	HDAC1, HDAC3	Chromatin histone acetylation
Vorinostat	HDAC inhibitor Class I, IIa, IIb, IV	Chromatin histone acetylation
JQ1	BRD2, BRD3, BRD4, BRDT	Chromatin other
BDP-00009066	MRCKB_HUMAN	Cytoskeleton
GSK269962A	ROCK1, ROCK2	Cytoskeleton
Camptothecin	TOP1	DNA replication
Epirubicin	Anthracycline	DNA replication
Gemcitabine	Pyrimidine antimetabolite	DNA replication
Irinotecan	TOP1	DNA replication
Afatinib	ERBB2, EGFR	EGFR signaling
Lapatinib	EGFR, ERBB2	EGFR signaling
Sapitinib	EGFR, ERBB2, ERBB3	EGFR signaling
Trametinib	MEK1, MEK2	ERK MAPK signaling
VX-11e	ERK2	ERK MAPK signaling
AZD6738	ATR	Genome integrity
NU7441	DNA-PK	Genome integrity
VE821	ATR	Genome integrity
BMS-536924	IGF1R, IR	IGF1R signaling
NVP-ADW742	IGF1R	IGF1R signaling
Alisertib	AURKA	Mitosis
Paclitaxel	Microtubule stabiliser	Mitosis
Tozasertib	AURKA, AURKB, AURKC, others	Mitosis
Vinblastine	Microtubule destabiliser	Mitosis
Vinorelbine	Microtubule destabiliser	Mitosis
ZM447439	AURKA, AURKB	Mitosis
Afuresertib	AKT1, AKT2, AKT3	PI3K/MTOR signaling
AT13148	AKT1	PI3K/MTOR signaling
AZD6482	PI3Kbeta	PI3K/MTOR signaling
AZD8055	MTORC1, MTORC2	PI3K/MTOR signaling
AZD8186	PI3Kalpha, PI3Kbeta	PI3K/MTOR signaling
Dactolisib	PI3K (class 1), MTORC1, MTORC2	PI3K/MTOR signaling
Ipatasertib	AKT1, AKT, AKT3	PI3K/MTOR signaling
MK-2206	AKT1, AKT2	PI3K/MTOR signaling
OSI-027	MTORC1, MTORC2	PI3K/MTOR signaling
Taselisib	PI3K (beta sparing)	PI3K/MTOR signaling
AZD4547	FGFR1, FGFR2, FGFR3	RTK signaling
Cediranib	VEGFR, FLT1, FLT2, FLT3, FLT4, KIT, PDGFRB	RTK signaling
Crizotinib	MET, ALK, ROS1	RTK signaling
AZ6102	TNKS1, TNKS2	WNT signaling
WIKI4	TNKS1, TNKS2	WNT signaling
Pevonedistat	NAE	Other
YK-4-279	RNA helicase A	Other
AZD5363	AKT1, AKT2, AKT3, ROCK2	Other, kinases
Dasatinib	ABL, SRC, Ephrins, PDGFR, KIT	Other, kinases
Sorafenib	PDGFR, KIT, VEGFR, RAF	Other, kinases

3.4. Baseline Gene Expression Data

Baseline gene expression is the snapshot of under the ideal growth condition of a cell. There is no stimulant effect on the samples, just basal cell metabolism on the investigated samples. TNBC cell lines' baseline gene expression data obtained as raw RNA-Seq .fastq files to be processed in the downstream transcriptome analysis. 16 of 17 TNBC cell lines' raw data were in CCLE's study and publicly available in SRA, under the project ID of PRJNA523380**(71,72)**. The last TNBC cell line's raw data had found in the EGAS00001000610 dataset and obtained from EGA with the special permission taken from Genentech authorities to be used in this thesis study**(73,74)**.

Table 3: Accession IDs of the raw RNA-Seq data of TNBC cell lines.

Accession numbers of the TNBC cell lines and other relevant information about the raw data.

Cell Line Name	Accession ID	Sequencing Technology	Sequencing Type	Data Provider
BT-20	SRR8616124	Illumina HiSeq 2500	Paired-end	SRA
CAL-120	SRR8615270	Illumina HiSeq 2500	Paired-end	SRA
CAL-51	SRR8615264	Illumina HiSeq 2500	Paired-end	SRA
CAL-85-1	SRR8615528	Illumina HiSeq 2500	Paired-end	SRA
DU-4475	SRR8615297	Illumina HiSeq 2500	Paired-end	SRA
Hs-578-T	SRR8615420	Illumina HiSeq 2500	Paired-end	SRA
HCC38	SRR8615458	Illumina HiSeq 2500	Paired-end	SRA
HCC1143	SRR8615819	Illumina HiSeq 2500	Paired-end	SRA
HCC1187	SRR8615817	Illumina HiSeq 2500	Paired-end	SRA
HCC1395	SRR8615822	Illumina HiSeq 2500	Paired-end	SRA
HCC1937	SRR8616179	Illumina HiSeq 2500	Paired-end	SRA
HCC2157	SRR8615891	Illumina HiSeq 2500	Paired-end	SRA
HDQ-P1	SRR8615278	Illumina HiSeq 2500	Paired-end	SRA
MDA-MB-231	SRR8615767	Illumina HiSeq 2500	Paired-end	SRA
MDA-MB-436	SRR8615584	Illumina HiSeq 2500	Paired-end	SRA
MDA-MB-468	SRR8615578	Illumina HiSeq 2500	Paired-end	SRA
MFM-223	ERR413710	Illumina HiSeq 2000	Paired-end	EGA

3.5. Pre-processing Gene Expression Data

Downloaded RNA-Seq raw data (.fastq) files require pre-processing to be properly utilized on the downstream analysis pipeline. This pre-processing usually includes cleaning of adapter sequences and removal of “bad quality” reads from the sequence reads. Quality check of “.fastq” files of TNBC cell lines was done via FASTQC software, version 0.11.9 **(75)**. Then removal of adapter sequences and sequencing artifacts were removed with the usage of the “bbduk.sh” bash script of BBTools suite BBMap software, version0.38.86 **(76)**.

3.6. Mapping RNA-seq Reads

“Cleaned” paired-end RNA-seq baseline expression files of TNBC cell lines were aligned to the reference human genome with the usage of Spliced Transcripts Alignment to a Reference (STAR) software version 2.7.3.a**(77)**. The alignment of RNA-Seq reads to reference is usually named as mapping. In this part, Broad Institute's The Genotype-Tissue Expression (GTEx) consortium’s RNA-Seq pipeline is adapted and then modified to obtain better coverage in the mapping procedure**(78)**. STAR requires a generated genome reference as the reference to align RNA-Seq reads. “Homo_sapiens.GRCh38.dna.toplevel.fasta” file was downloaded and used to generate the software-required genome, from Ensembl’s FTP web server, release version was 99 at the moment of analysis taking place**(79)**. To prevent redundancy in the mapping process, some modifications were done on the obtained reference genome file. “ALT” contigs that carry alternative genomic variation information as haplotypes were removed with filtering out “_alt” suffix bearing sequences from the reference fasta file. At the end of this trimming stage non-redundant and most recent, the human reference genome is ready to be utilized within the STAR. STAR is a splice-aware aligner and in the alignment process, to provide better guidance on alternative splicing machinery; the user can feed the STAR algorithm with a different type of additional reference. This additional reference file can be “gtf”, “gff” or “gff3”, all of them contains the same positional genomic annotation information with different formatting. During the time of analysis, the most current version of the annotation reference was “Homo_sapiens.GRCh38.99.chr_patch_hapl_scaff.gff3” file**(79)**. Henceforth, that annotation reference from Ensembl was used to build splice-aware software-specific reference human genome “which is so-called transcriptome” in the dynamics of the STAR software.

3.7. Quantification of the Mapped Reads

After doing the mapping RNA-seq reads of TNBC cell lines to reference human genome, obtained ”binary alignment map (bam)” files contain all the alignment information to reference in an unordered and intangible way. To interpret bam files, the usage of a quantification tool is required. In this thesis study, the Salmon quantification tool is used to quantify each bam file of respective TNBC cell lines to unravel human and machine-readable, tabular formatted and also library-length and transcript length normalized counts of each RNA products of each sample. Salmon quantification tool has a feature to quantify either from mapped-reads (bam files) or directly from raw data (fastq files) with pseudo-mapping. In this study, we used the mapped reads mode of Salmon tool, version 1.2**(80)**.

All of the quantified outputs for mapped TNBC cell lines were generated into the “quants” folder with the respective sample names of the bam files. As a next stage of the analysis, R statistical computing software **(81)** and a handful of special R packages will be used to continue towards the down-stream analysis.

3.8. Importing Quantification Results

To import Salmon’s quantification outputs into R, a specialized R package can be used to maintain consistency and provide easiness “tximport” R package can import these quantifications and convert transcript accession ids (i.e. ENST00000XXXX) to proper gene accession ids (ENSG00000XXXX) with the guidance of human reference gff file**(82)**. Then, imported normalized “counts” of transcripts assigned to their responsible genes and at the end data table is formed with 67140 (coding & non-coding) ENSEMBL genes for the TNBC cell lines.

3.9. Differential Expression Analysis

Baseline gene expression is the basal-level gene expression on the controlled and ideally, the same cell-cycle stage’s momentarily snapshotted gene expression profile. This baseline gene expression data is ideal for either providing a control group on the comparison of the effects of different stimulants on cells or generating predictive statistical models with the utilization of each gene’s expression values as mathematical coefficients like the coefficients of linear regression models.

Apart from those two mainstream approaches, baseline gene expression can be used to investigate the steady-state activity of the cells, and with this information characteristic nature of each cell line can be differentiated with the focus of the inquired scientific question. In this study, binarized drug responses of the TNBC cell lines investigated with the baseline gene expression.

To achieve that, normalized counts of each gene product (transcripts) of the samples gathered in a large data table of 67140 (coding & non-coding) ENSEMBL genes within the proper framework of R. Then each cell lines’ drug response to each of 52 drugs is bonded as side-by-side columns (**Table 2**). After that, each column of the respective drug's response is treated as the "design matrix" of that respective drug's within the DESeq2 differential expression analysis package**(83)**. Next, the "contrast" function of DESeq2 is run for the determination of DEGs in the comparison of resistant TNBC cell lines gene expression versus sensitive TNBC cell lines gene expression.

There is one tricky aspect of the interpretation of the outputs; the output of this contrast on DEG analysis with DESeq2 is giving $\log_2$-fold change for the comparison groups in the reverse order. To clarify that further; example code of the function is

```
contrast=c("Afatinib","Resistant","Sensitive")
```

"Resistant" is the resistantly classified group of TNBC cells to Afatinib drug and "Sensitive" is the sensitively classified group of TNBC cells to Afatinib. The output of this contrast code is given as "$\log_2$ fold-change of Resistant vs Sensitive" but the actual interpretation of the upregulation/downregulation is opposite of the indication. "contrast" function calculates of $\log_2$ fold-change to the second group that is given in the function over the first group which is fed into the function. Practically, the upregulation of a "gene X" in the contrast output of the DESeq2 is serviced as the "$\log_2$ fold-change of Resistant vs Sensitive" but in reality, it means that that "gene X" is upregulated on the sensitive group compared to the resistant group of TNBC cells. This is a little misleading output serving by the DESeq2 package itself on the DEG results.

To clarify, all of the calculated $\log_2$ fold-changes and up-regulation/down-regulation acclaims are exclusively valid for "sensitive response giving TNBC cells to the drug of interest" over "resistant response giving TNBC cells to the same drug of interest". Applied DEG cutoff of false discovery rate (FDR) < 0.05 and absolute fold change ≥ 1.5 during this thesis study. In-detail parameter settings and code availability can be found in the relevant part of section 6. Supplementary Appendix.

3.10. Pathway Analysis

To functionally interpret the DEGs in the comparison of sensitive cell lines' gene expression versus resistant cell lines' gene expression for each of 52 drugs, gene enrichment is one of the suitable approaches to be performed. For this thesis study, the pathfindR gene enrichment R package which is based on an "active sub-network" search algorithm is preferred**(84)**. DEGs in each response comparison group of TNBC cells for 52 drugs were respectively given as input. Then, KEGG pathways are used as the main metabolic pathway database for enrichment and pathway analysis.

Intersection analyses for the comparison of the most enriched pathways between two pathway enrichment analyses results were done with the combined assessment of the p-values by Fisher's method. If a DEG is commonly upregulated/downregulated in the compared drug's enrichment results that DEG is highlighted as green/red color respectively. In the case of a DEG is contradictorily found expressed in an enriched pathway or not present in both drugs' DEG result; then that DEG is indicated as a gray node and labeled as "Conflict or Not Present in Both (NPiB)".

3.11. Drug Similarity Analysis

Chemical structure and canonical formula of the therapeutic compounds can be represented with SMILES notation. SMILES notations of the curated 52 drugs are gathered from PubChem **(85)** and fed into a web-based drug similarity algorithm of ChemMineTools **(86,87)**. Generated drug similarity hierarchical clustering parameters were properties color and display values: Z-scores, linkage method: complete, heatmap: distance matrix, physicochemical properties heatmap: ChemmineR properties.

4. RESULTS

This section is dedicated to express the refined forms of all findings in this study. To see all unrefined results, section 6. Supplementary Appendix can be visited.

4.1. Drug Similarity by SMILES

Physicochemical properties of 52 drugs were investigated by ChemMine tools via their SMILES notation(**Figure 2**).

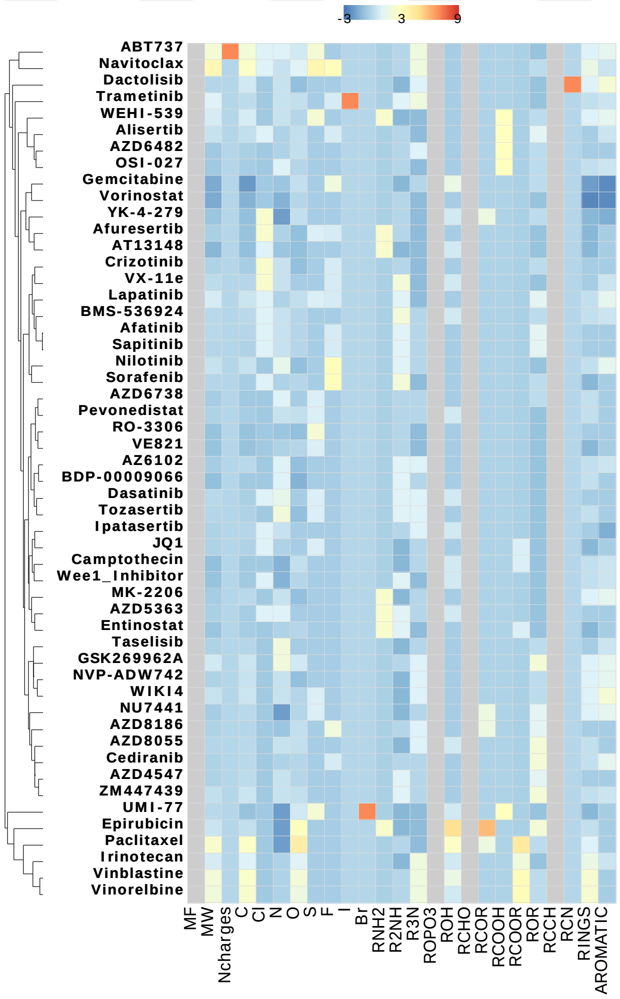

Figure 2: Hierarchical clustering of the drug similarity of 52 curated drugs by their respective physicochemical properties.

Most similar drugs among the closely neighboring branches on the dendrogram of **Figure 2** were investigated for commonly most enriched pathways for the sensitive response giving TNBC cells versus resistant response giving TNBC cells (**Figure 3**, **Figure 4**, **Figure 5**, and **Figure 30**).

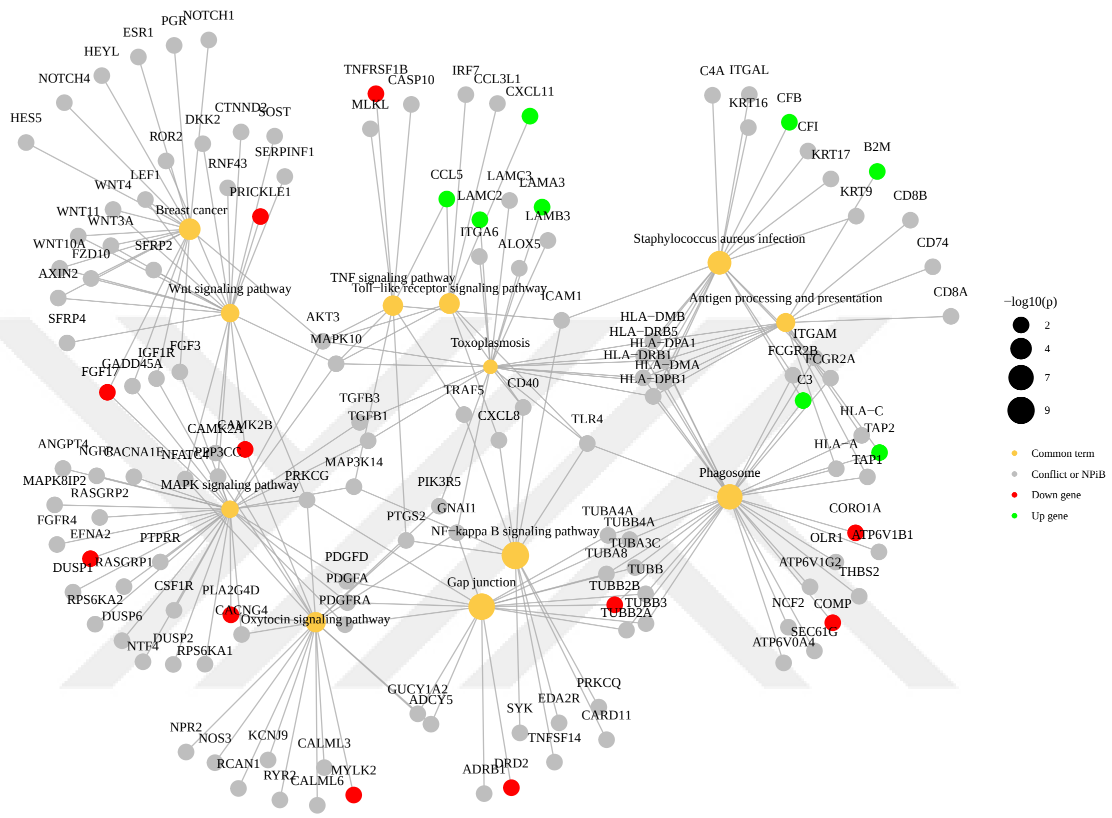

Figure 3: Intersection of most enriched pathways from the determined DEGs of AZD4547 and ZM447439 differential expression analysis**.**

In this figure, the intersection of the most significant (combined p-value assessment by Fisher's method, p-value $\leq$ 0.05) commonly enriched KEGG pathways are visualized as yellow hubs. The nodes are representing commonly upregulated DEGs (green), commonly down-regulated DEGs (red), and "conflict or NPiB (Not Present in Both)" DEGs (grey) which were involved in the enrichment of the connected pathway hub. Preferred DEG cutoff of false discovery rate (FDR) < 0.05 and $\log_2$ absolute fold change $\geq$ 1.5. The size of the hubs is reversely proportional with their respective combined p-values for the commonly enriched pathways in the comparison of the two above mentioned drug comparisons.

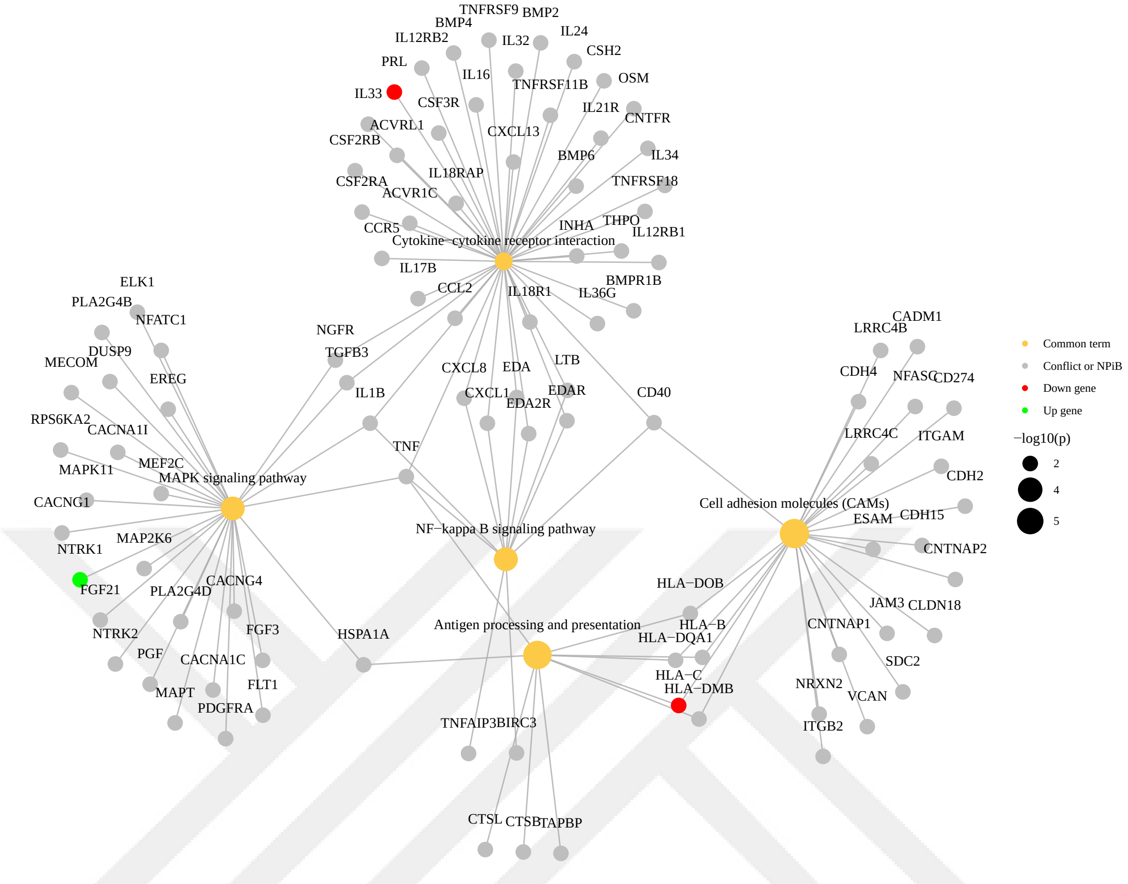

Figure 4: Intersection of most enriched pathways from the determined DEGs of AZD6738 and Pevonedistat differential expression analysis**.**

In this figure, the intersection of the most significant (combined p-value assessment by Fisher's method, p-value ≤ 0.05) commonly enriched KEGG pathways are visualized as yellow hubs. The nodes are representing commonly upregulated DEGs (green), commonly down-regulated DEGs (red), and "conflict or NPiB (Not Present in Both)" DEGs (grey) which were involved in the enrichment of the connected pathway hub. Preferred DEG cutoff of false discovery rate (FDR) < 0.05 and $\log_2$ absolute fold change ≥ 1.5. The size of the hubs is reversely proportional with their respective combined p-values for the commonly enriched pathways in the comparison of the two above mentioned drug comparisons.

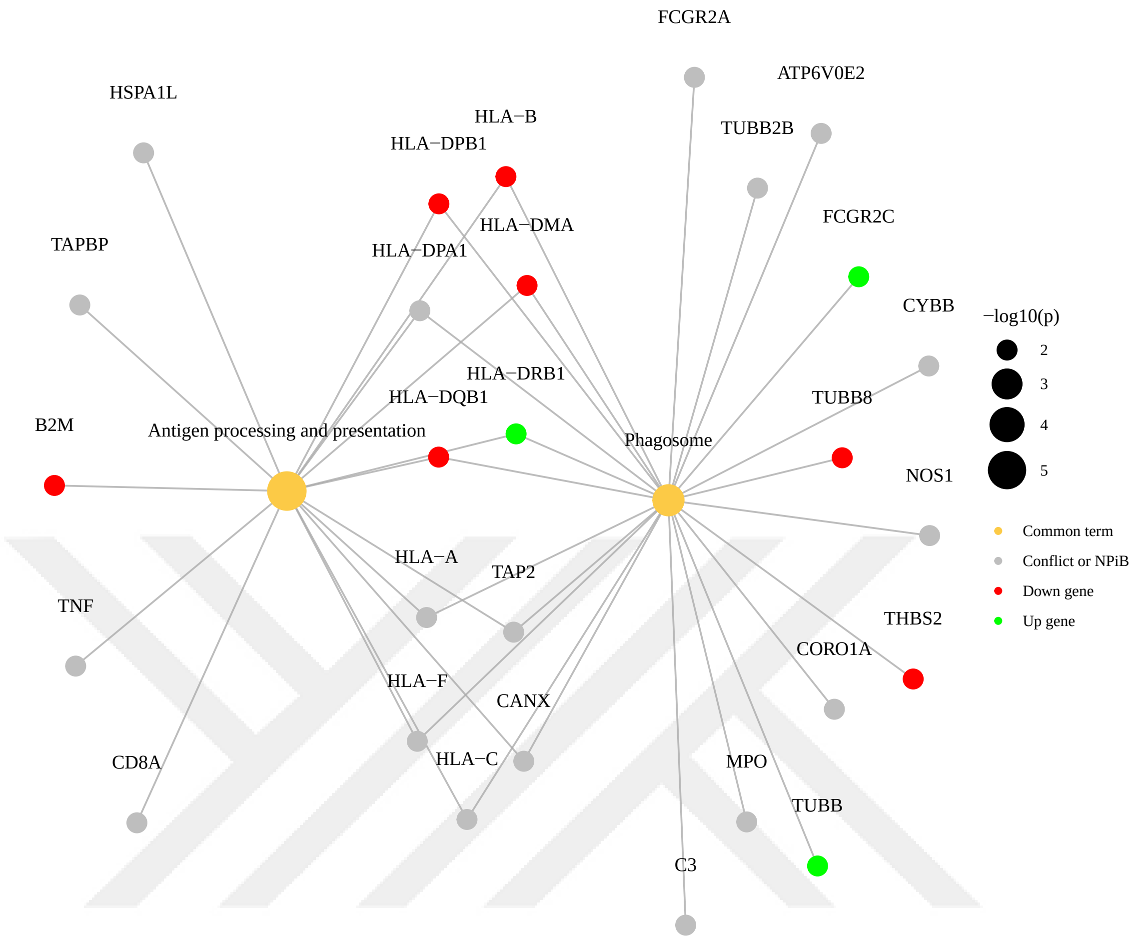

Figure 5: Intersection of most enriched pathways from the determined DEGs of AZD6738 and Pevonedistat differential expression analysis.

In this figure, the intersection of the most significant (combined p-value assessment by Fisher's method, p-value ≤ 0.05) commonly enriched KEGG pathways are visualized as yellow hubs. The nodes are representing commonly upregulated DEGs (green), commonly down-regulated DEGs (red), and "conflict or NPiB (Not Present in Both)" DEGs (grey) which were involved in the enrichment of the connected pathway hub. Preferred DEG cutoff of false discovery rate (FDR) < 0.05 and $\log_2$ absolute fold change ≥ 1.5. The size of the hubs is reversely proportional with their respective combined p-values for the commonly enriched pathways in the comparison of the two above mentioned drug comparisons.

4.2. ABL Signaling Targeting Drug

There is only one drug that targets the ABL signaling among the curated pool of 52 drugs. The following result is an interpretation of the detailed gene expression profile of sensitive TNBC cells versus resistant TNBC cells to that drug.

4.2.1. Nilotinib results

Differential expression analysis results yielded 933 DEGs in the comparison of Nilotinib sensitive 6 TNBC cell lines versus resistant 11 cell lines. Active sub-network based pathway enrichment analysis found 37 enriched KEGG pathways. The most significantly enriched 10 pathways and included DEGs are visualized in **Figure 6**.

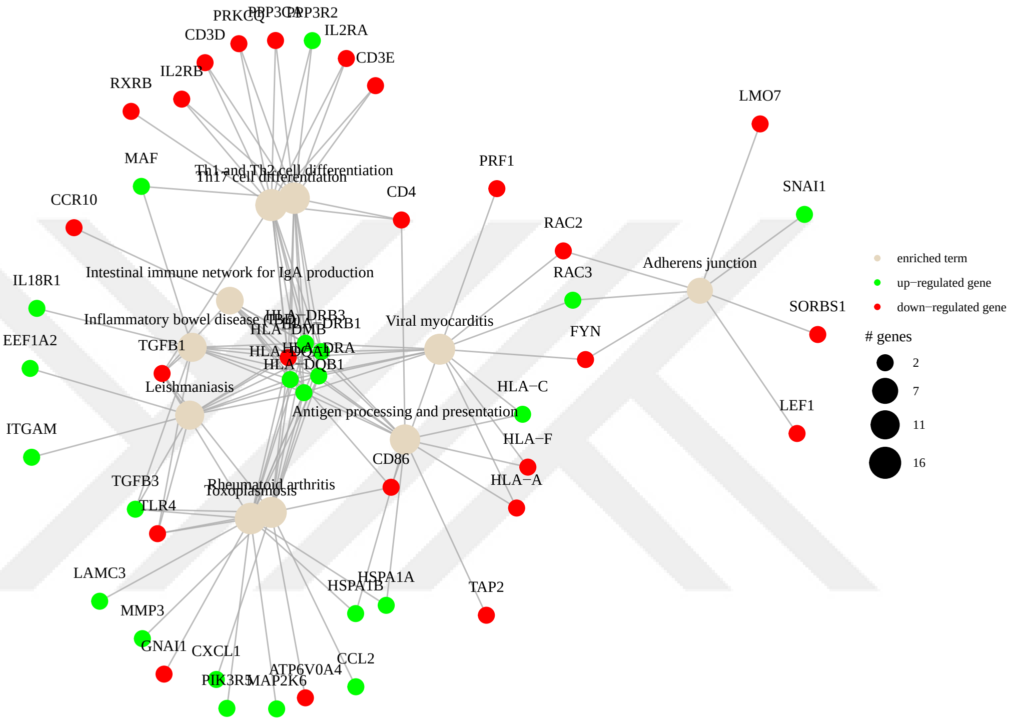

Figure 6: Reduced network of most enriched pathways for the sensitive TNBC cells versus resistant TNBC cells to Nilotinib.

In this figure significantly enriched top10 KEGG pathways are visualized as gray hubs (p-value < 0.05). Nodes are representing either upregulated DEGs (green) or down-regulated DEGs (red) which were involved in the enrichment of the connected hub pathway. Preferred DEG cutoff of false discovery rate (FDR) < 0.05 and $\log_2$ absolute fold change ≥ 1.5. These hubs and nodes are not all of the found significant elements. For full list, please look up the relevant section of the supplemental appendix.

4.3. Apoptosis Regulation Targeting Drugs

There are 4 drugs that target apoptosis regulation among the curated pool of 52 drugs. The following results are interpretations of the detailed gene expression profile of sensitive TNBC cells versus resistant TNBC cells to those 4 drugs.

4.3.1. ABT737 results

Differential expression analysis results yielded 935 DEGs in the comparison of ABT737 sensitive 11 TNBC cell lines versus resistant 6 cell lines. Active sub-network based pathway enrichment analysis found 39 enriched KEGG pathways. The most significantly enriched 10 pathways and included DEGs are visualized in **Figure 7**.

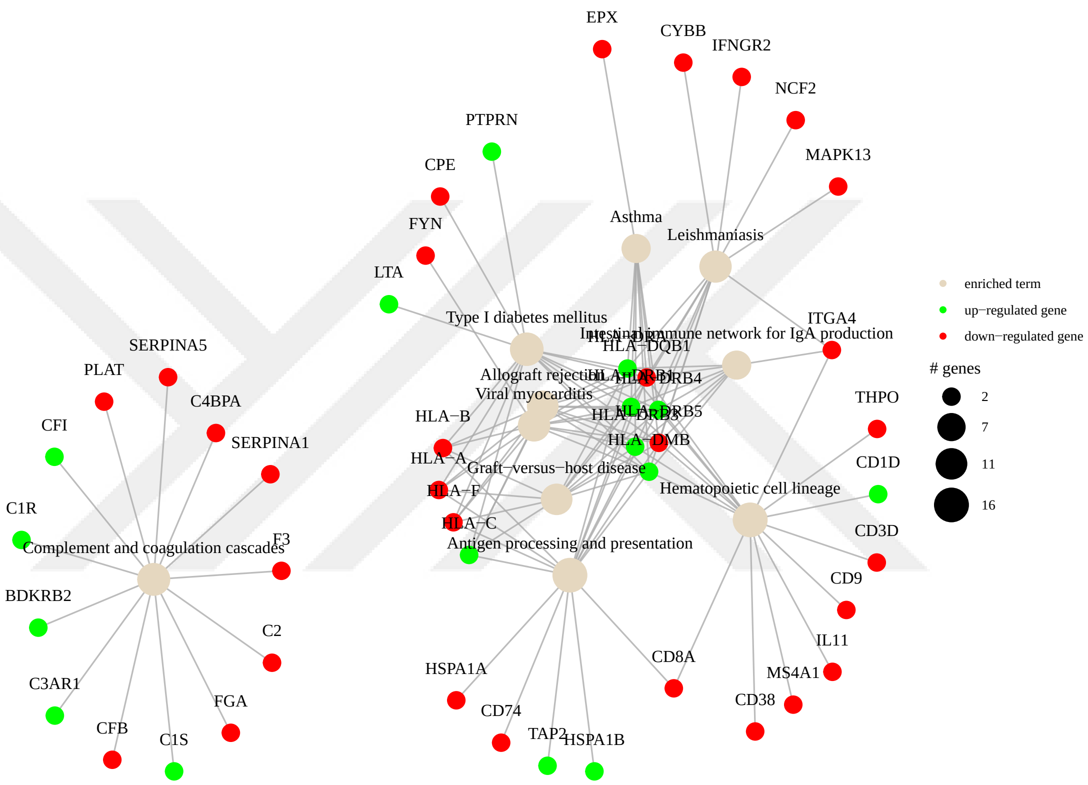

Figure 7: Reduced network of most enriched pathways for the sensitive TNBC cells versus resistant TNBC cells to ABT737.

In this figure significantly enriched top10 KEGG pathways are visualized as gray hubs (p-value < 0.05). Nodes are representing either upregulated DEGs (green) or down-regulated DEGs (red) which were involved in the enrichment of the connected hub pathway. Preferred DEG cutoff of false discovery rate (FDR) < 0.05 and $\log_2$ absolute fold change $\geq$ 1.5. These hubs and nodes are not all of the found significant elements. For full list, please look up the relevant section of the supplemental appendix.

4.3.2. Navitoclax results

Differential expression analysis results yielded 611 DEGs in the comparison of Navitoclax sensitive 6 TNBC cell lines versus resistant 11 cell lines. Active sub-network based pathway enrichment analysis found 28 enriched KEGG pathways. The most significantly enriched 10 pathways and included DEGs are visualized in **Figure 8.**

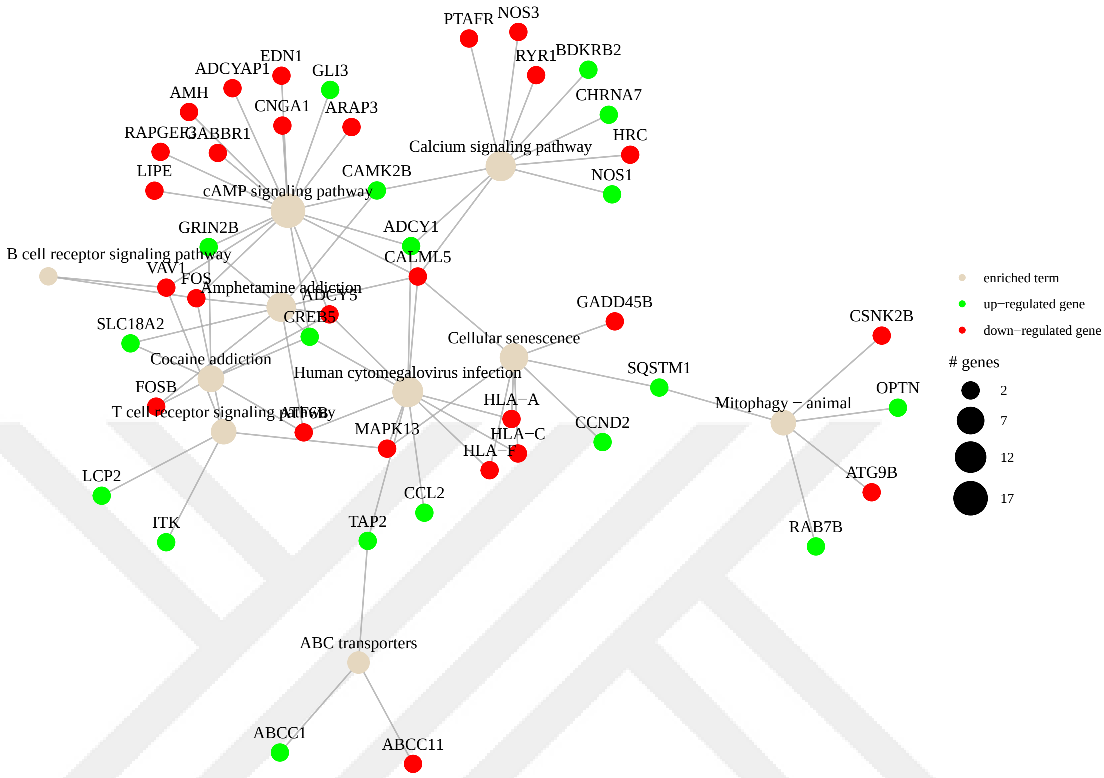

Figure 8: Reduced network of most enriched pathways for the sensitive TNBC cells versus resistant TNBC cells to Navitoclax.

In this figure significantly enriched top10 KEGG pathways are visualized as gray hubs (p-value < 0.05). Nodes are representing either upregulated DEGs (green) or down-regulated DEGs (red) which were involved in the enrichment of the connected hub pathway. Preferred DEG cutoff of false discovery rate (FDR) < 0.05 and $\log_2$ absolute fold change ≥ 1.5. These hubs and nodes are not all of the found significant elements. For full list, please look up the relevant section of the supplemental appendix.

4.3.3. UMI-77 results

Differential expression analysis results yielded 581 DEGs in the comparison of UMI-77 sensitive 9 TNBC cell lines versus resistant 8 cell lines. Active sub-network based pathway enrichment analysis found 9 enriched KEGG pathways. These enriched pathways and included DEGs are visualized in **Figure 9**.

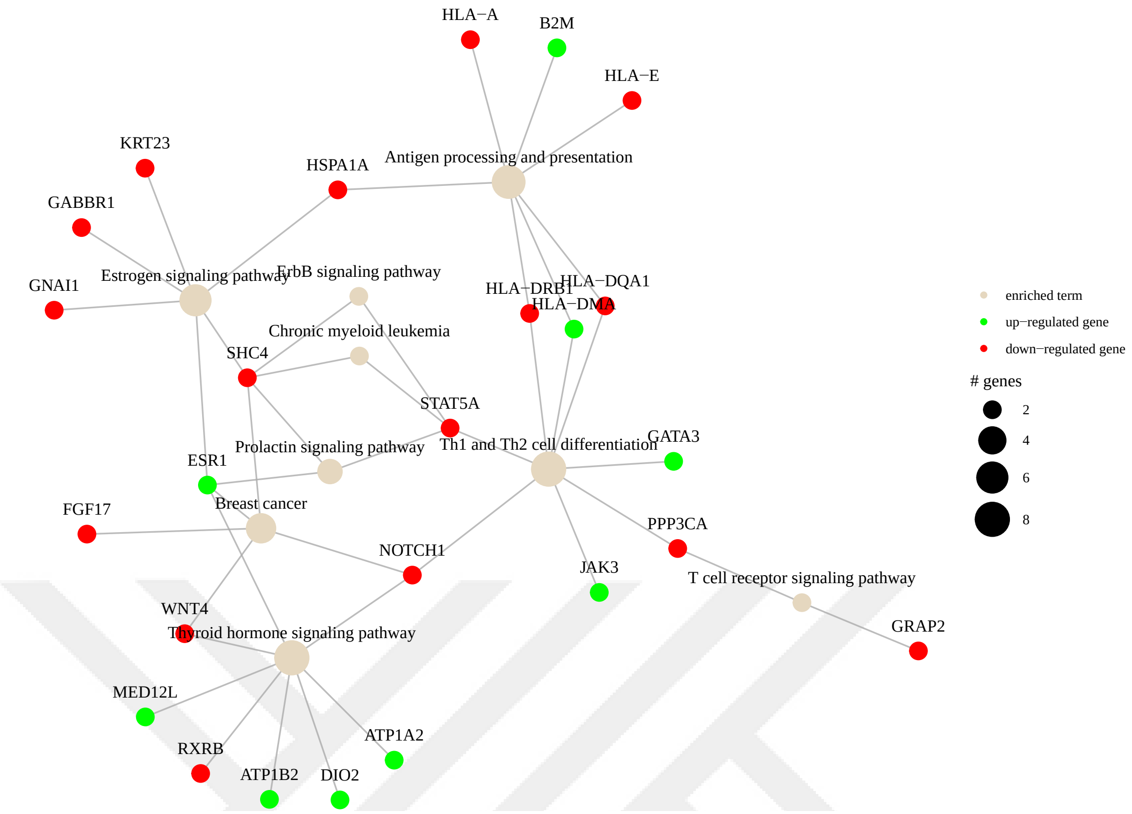

Figure 9: Network of most enriched pathways for the sensitive TNBC cells versus resistant TNBC cells to UMI-77.

In this figure significantly enriched KEGG pathways are visualized as gray hubs (p-value < 0.05). Nodes are representing either upregulated DEGs (green) or down-regulated DEGs (red) which were involved in the enrichment of the connected hub pathway. Preferred DEG cutoff of false discovery rate (FDR) < 0.05 and $\log_2$ absolute fold change ≥ 1.5. These hubs and/or nodes are not all of the found significant elements. For full list, please look up the relevant section of the supplemental appendix.

4.3.4. WEHI-539 results

Differential expression analysis results yielded 825 DEGs in the comparison of WEHI-539 sensitive 6 TNBC cell lines versus resistant 11 cell lines. Active sub-network based pathway enrichment analysis found 25 enriched KEGG pathways. The most significantly enriched 10 pathways and included DEGs are visualized in **Figure 10**.

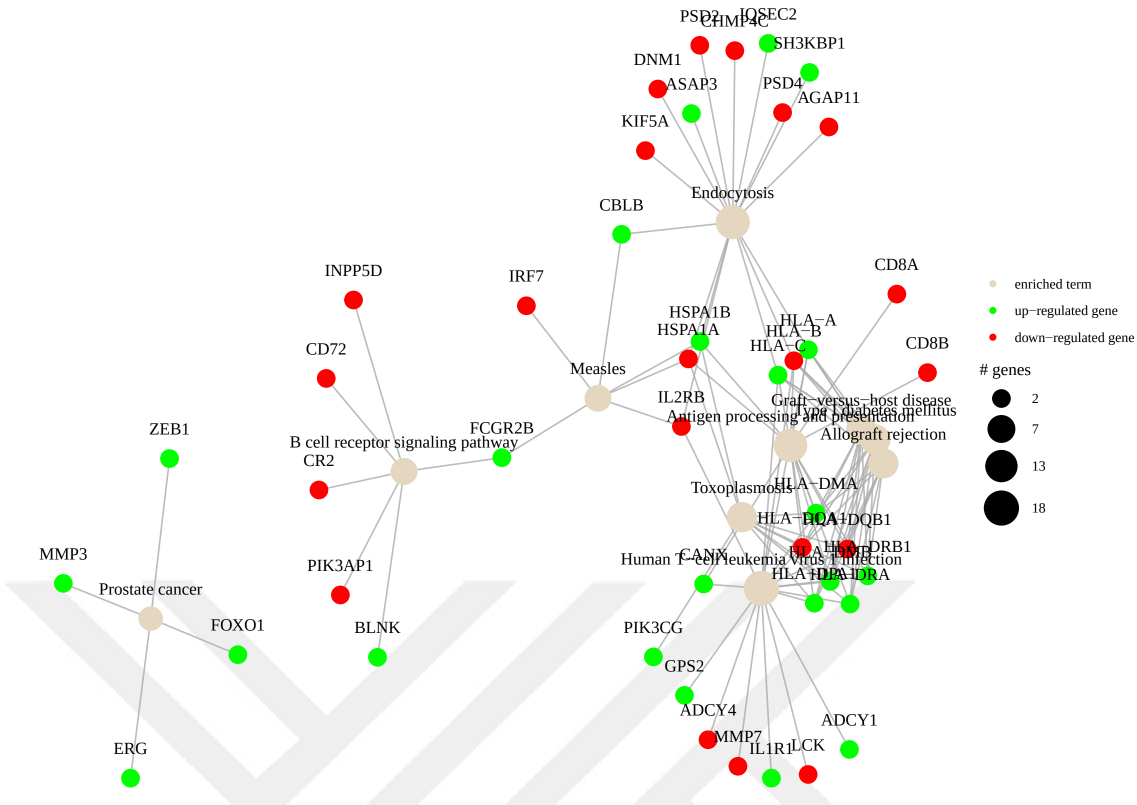

Figure 10: Reduced network of most enriched pathways for the sensitive TNBC cells versus resistant TNBC cells to WEHI-539.

In this figure significantly enriched top10 KEGG pathways are visualized as gray hubs (p-value < 0.05). Nodes are representing either upregulated DEGs (green) or down-regulated DEGs (red) which were involved in the enrichment of the connected hub pathway. Preferred DEG cutoff of false discovery rate (FDR) < 0.05 and $\log_2$ absolute fold change ≥ 1.5. These hubs and nodes are not all of the found significant elements. For full list, please look up the relevant section of the supplemental appendix.

4.3.5. The intersection of ABT737 and Navitoclax

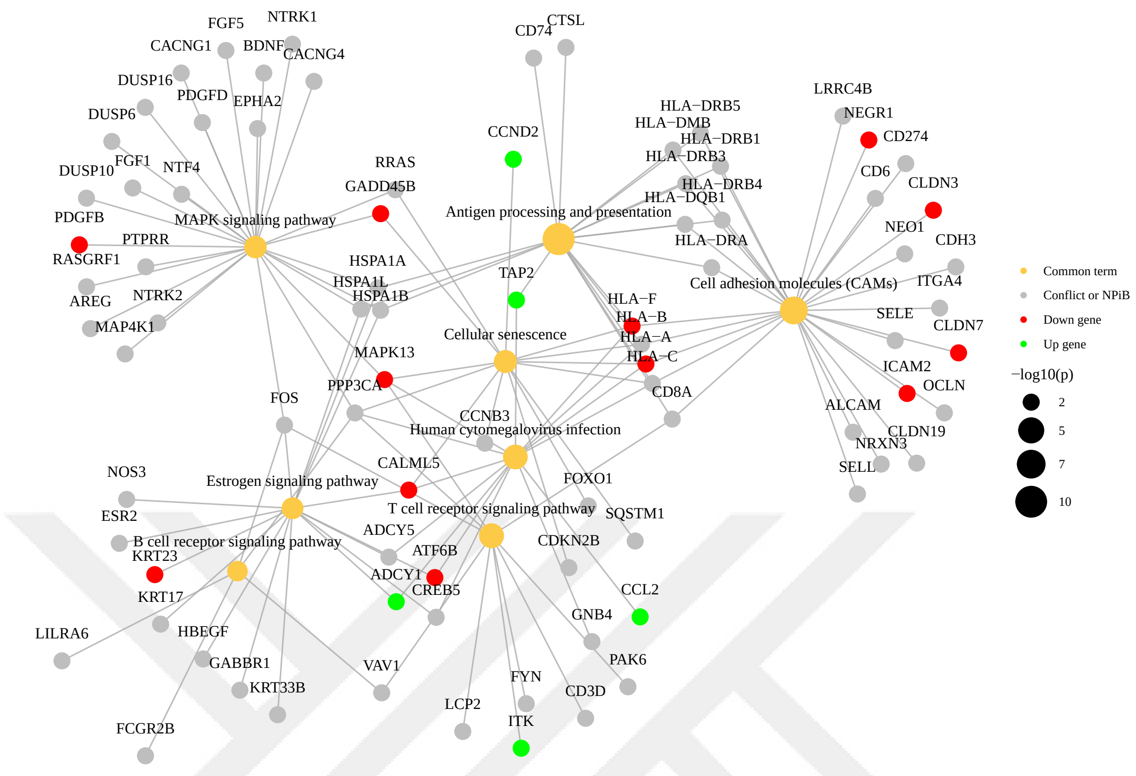

Figure 11: Intersection of most enriched pathways from the determined DEGs of ABT737 and Navitoclax differential expression analysis.

In this figure, the intersection of the most significant (combined p-value assessment by Fisher's method, p-value ≤ 0.05) commonly enriched KEGG pathways are visualized as yellow hubs. The nodes are representing commonly upregulated DEGs (green), commonly down-regulated DEGs (red), and "conflict or NPiB (Not Present in Both)" DEGs (grey) which were involved in the enrichment of the connected pathway hub. Preferred DEG cutoff of false discovery rate (FDR) < 0.05 and absolute fold change ≥ 1.5. The size of the hubs is reversely proportional with their respective combined p-values for the commonly enriched pathways in the comparison of the two above mentioned drug comparisons.

4.4. Cell Cycle Targeting Drugs

There are 2 drugs that target cell cycle regulation among the curated pool of 52 drugs. The following results are interpretations of the detailed gene expression profile of sensitive TNBC cells versus resistant TNBC cells to those 2 drugs.

4.4.1. RO-3306 results

Differential expression analysis results yielded 846 DEGs in the comparison of RO-3306 sensitive 3 TNBC cell lines versus resistant 14 cell lines. Active sub-network based pathway enrichment analysis found 46 enriched KEGG pathways. The most significantly enriched 10 pathways and included DEGs are visualized in **Figure 12**.

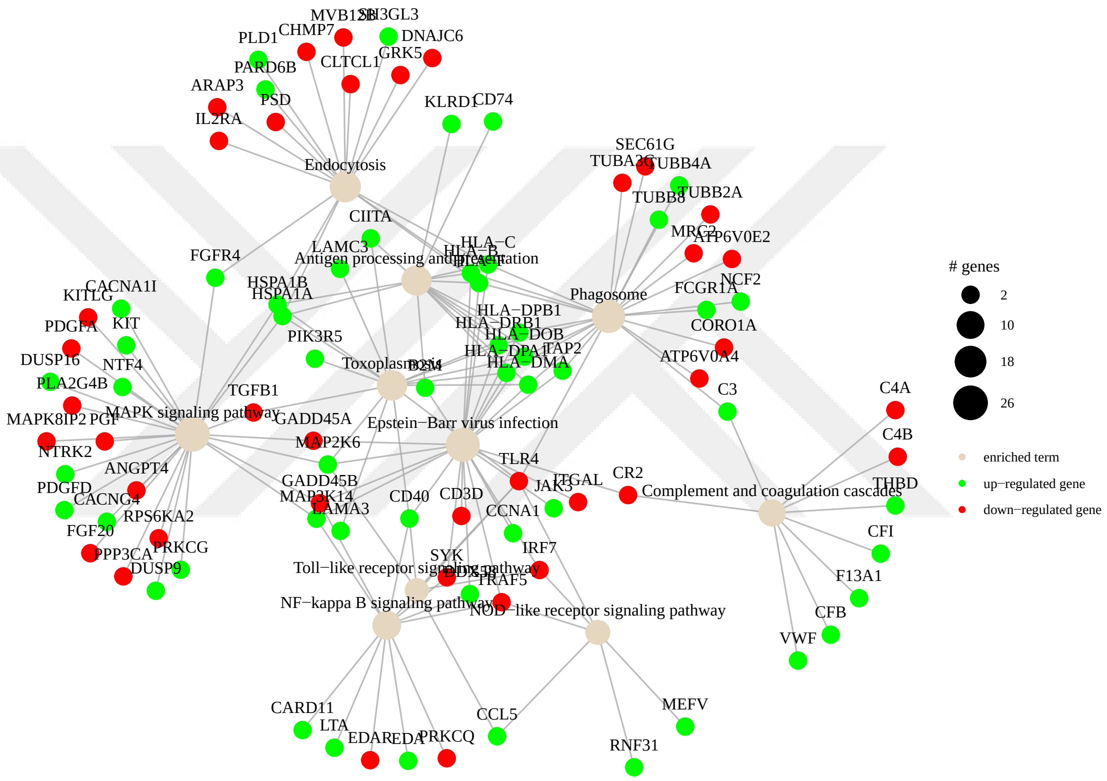

Figure 12: Reduced network of most enriched pathways for the sensitive TNBC cells versus resistant TNBC cells to RO-3306.

In this figure significantly enriched top10 KEGG pathways are visualized as gray hubs (p-value < 0.05). Nodes are representing either upregulated DEGs (green) or down-regulated DEGs (red) which were involved in the enrichment of the connected hub pathway. Preferred DEG cutoff of false discovery rate (FDR) < 0.05 and $\log_2$ absolute fold change ≥ 1.5. These hubs and nodes are not all of the found significant elements. For full list, please look up the relevant section of the supplemental appendix.

4.4.2. Wee1-Inhibitor results

Differential expression analysis results yielded 541 DEGs in the comparison of Wee1-Inhibitor sensitive 11 TNBC cell lines versus resistant 6 cell lines. Active sub-network based pathway enrichment analysis found 10 enriched KEGG pathways. These pathways and included DEGs are visualized in **Figure 13**.

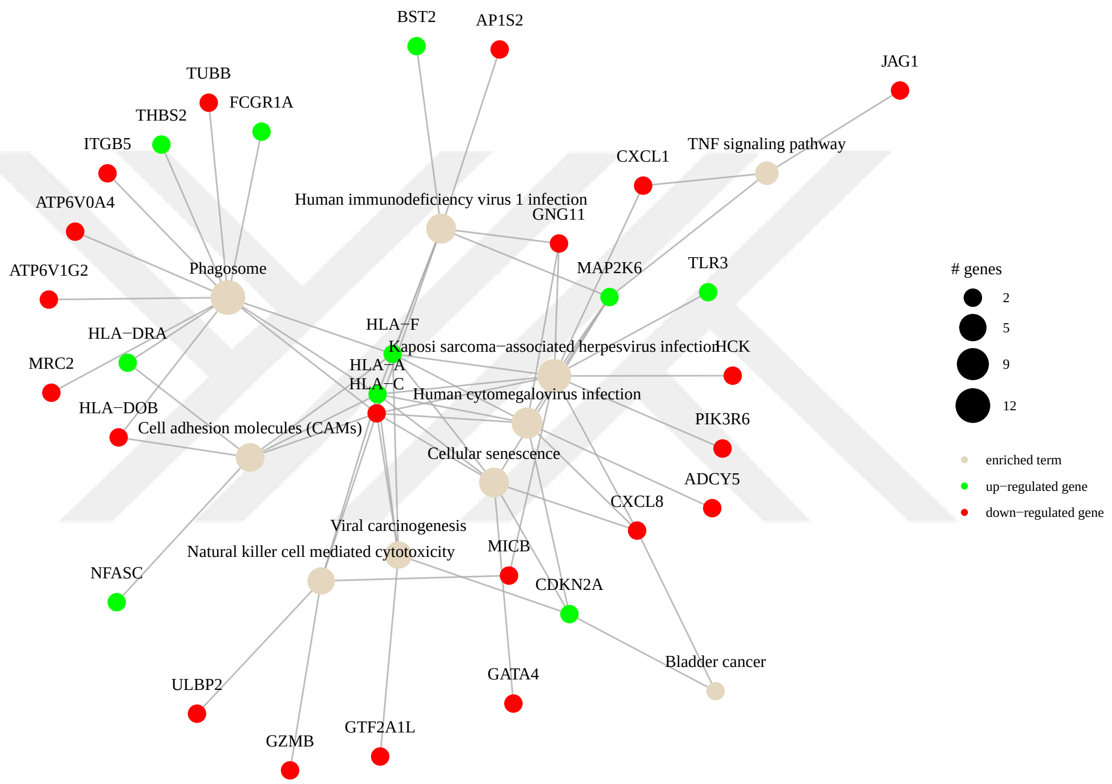

Figure 13: Network of most enriched pathways for the sensitive TNBC cells versus resistant TNBC cells to Wee1-Inhibitor.

In this figure significantly enriched top10 KEGG pathways are visualized as gray hubs (p-value < 0.05). Nodes are representing either upregulated DEGs (green) or down-regulated DEGs (red) which were involved in the enrichment of the connected hub pathway. Preferred DEG cutoff of false discovery rate (FDR) < 0.05 and $\log_2$ absolute fold change ≥ 1.5. These hubs and/or nodes are not all of the found significant elements. For full list, please look up the relevant section of the supplemental appendix.

4.4.3. The intersection of RO-3306 and Wee1-Inhibitor

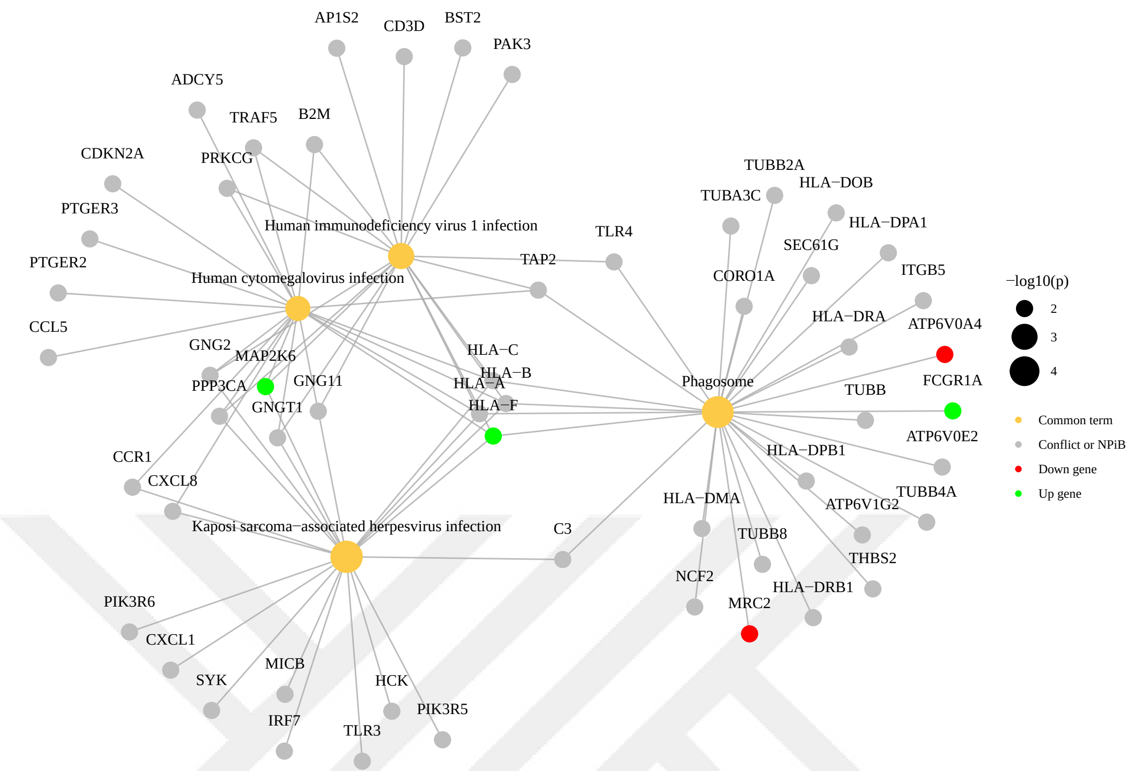

Figure 14: Intersection of most enriched pathways from the determined DEGs of RO-3306 and Wee1-Inhibitor differential expression analysis.

In this figure, the intersection of the most significant (combined p-value assessment by Fisher's method, p-value ≤ 0.05) commonly enriched KEGG pathways are visualized as yellow hubs. The nodes are representing commonly upregulated DEGs (green), commonly down-regulated DEGs (red), and "conflict or NPiB (Not Present in Both)" DEGs (grey) which were involved in the enrichment of the connected pathway hub. Preferred DEG cutoff of false discovery rate (FDR) < 0.05 and absolute fold change ≥ 1.5. The size of the hubs is reversely proportional with their respective combined p-values for the commonly enriched pathways in the comparison of the two above mentioned drug comparisons.

4.5. Chromatin Histone Acetylation Targeting Drugs

There are 2 drugs that target histone acetylation among the curated pool of 52 drugs. The following results are interpretations of the detailed gene expression profile of sensitive TNBC cells versus resistant TNBC cells to those 2 drugs.

4.5.1. Entinostat results

Differential expression analysis results yielded 709 DEGs in the comparison of Entinostat sensitive 9 TNBC cell lines versus resistant 8 cell lines. Active sub-network based pathway enrichment analysis found 26 enriched KEGG pathways. The most significantly enriched 10 pathways and included DEGs are visualized in **Figure 15**.

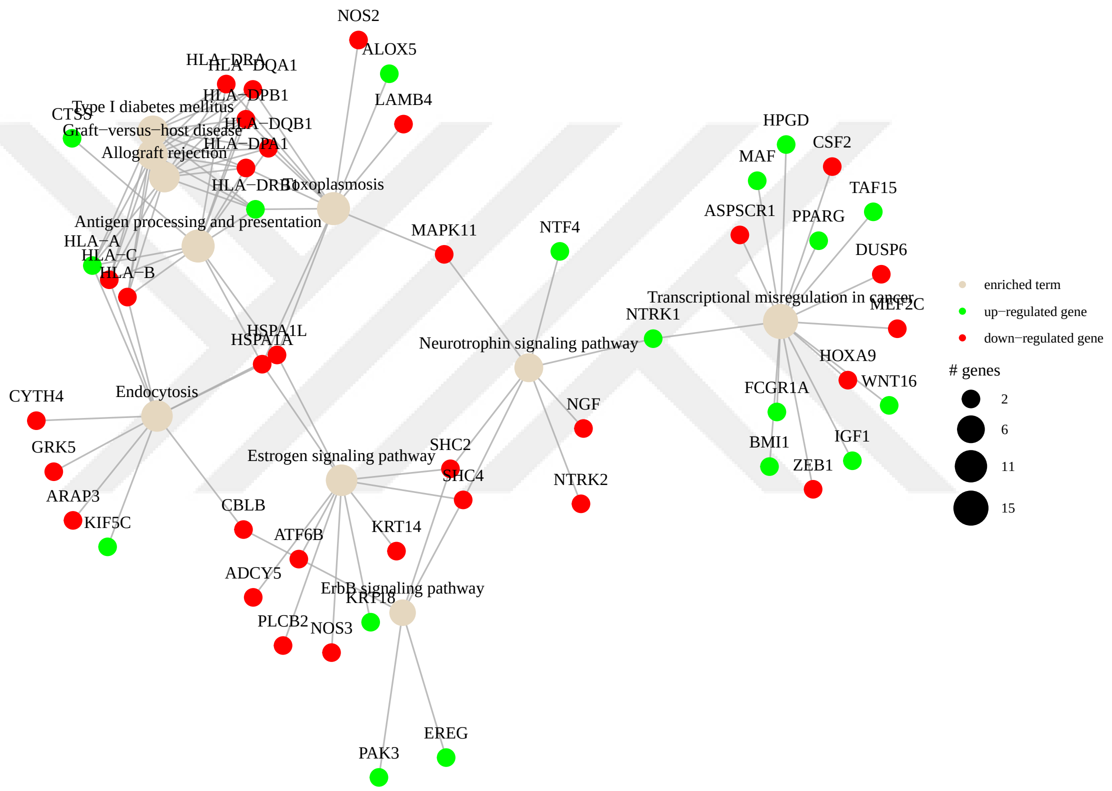

Figure 15: Reduced network of most enriched pathways for the sensitive TNBC cells versus resistant TNBC cells to Entinostat.

In this figure significantly enriched top10 KEGG pathways are visualized as gray hubs (p-value < 0.05). Nodes are representing either upregulated DEGs (green) or down-regulated DEGs (red) which were involved in the enrichment of the connected hub pathway. Preferred DEG cutoff of false discovery rate (FDR) < 0.05 and $\log_2$ absolute fold change ≥ 1.5. These hubs and nodes are not all of the found significant elements. For full list, please look up the relevant section of the supplemental appendix.

4.5.2. Vorinostat results

Differential expression analysis results yielded 481 DEGs in the comparison of Vorinostat sensitive 9 TNBC cell lines versus resistant 8 cell lines. Active sub-network based pathway enrichment analysis found 16 enriched KEGG pathways. The most significantly enriched 10 pathways and included DEGs are visualized in **Figure 16**.

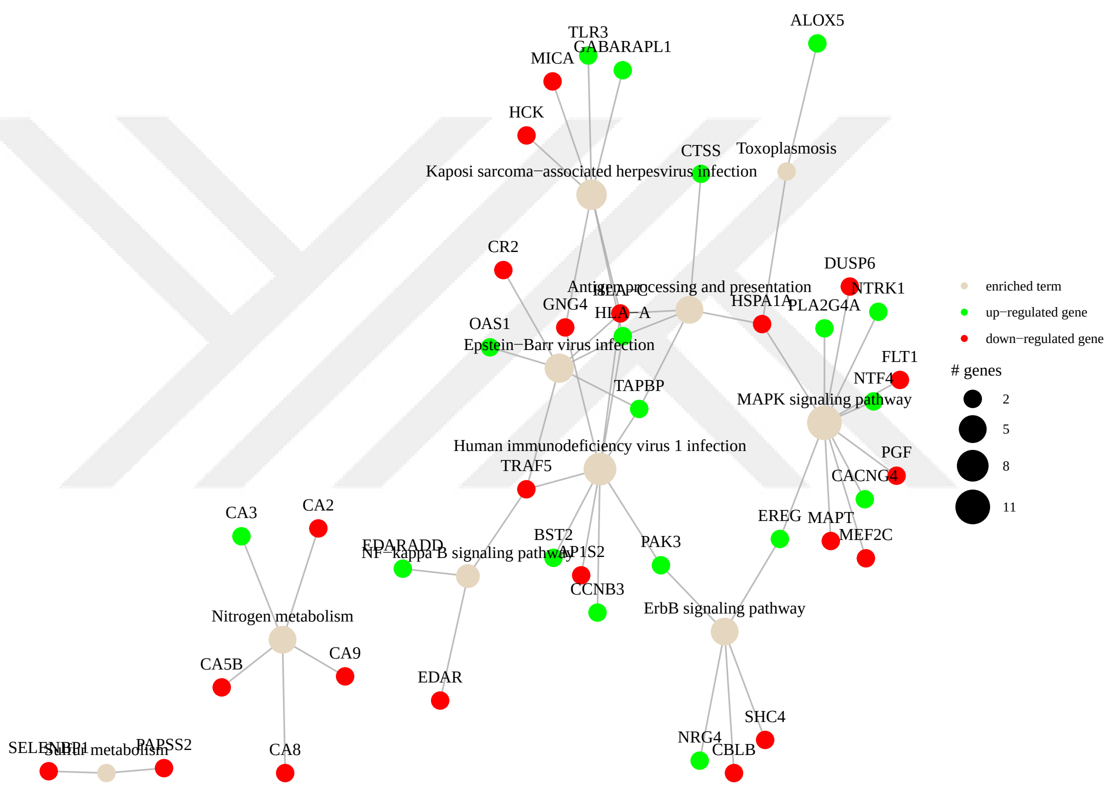

Figure 16: Reduced network of most enriched pathways for the sensitive TNBC cells versus resistant TNBC cells to Vorinostat.

In this figure significantly enriched top10 KEGG pathways are visualized as gray hubs (p-value < 0.05). Nodes are representing either upregulated DEGs (green) or down-regulated DEGs (red) which were involved in the enrichment of the connected hub pathway. Preferred DEG cutoff of false discovery rate (FDR) < 0.05 and $\log_2$ absolute fold change ≥ 1.5. These hubs and nodes are not all of the found significant elements. For full list, please look up the relevant section of the supplemental appendix.

4.5.3. The intersection of Entinostat and Vorinostat

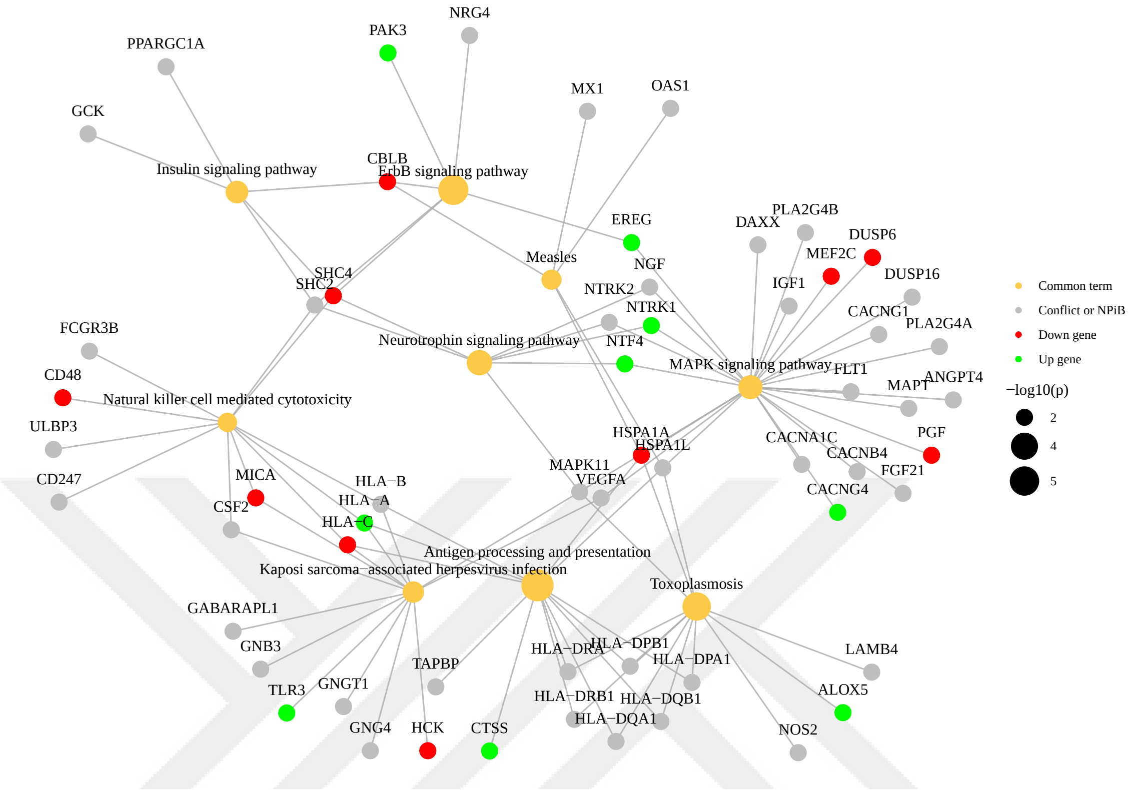

Figure 17: Intersection of most enriched pathways from the determined DEGs of Entinostat and Vorinostat differential expression analysis.

In this figure, the intersection of the most significant (combined p-value assessment by Fisher's method, p-value ≤ 0.05) commonly enriched KEGG pathways are visualized as yellow hubs. The nodes are representing commonly upregulated DEGs (green), commonly down-regulated DEGs (red), and "conflict or NPiB (Not Present in Both)" DEGs (grey) which were involved in the enrichment of the connected pathway hub. Preferred DEG cutoff of false discovery rate (FDR) < 0.05 and absolute fold change ≥ 1.5. The size of the hubs is reversely proportional with their respective combined p-values for the commonly enriched pathways in the comparison of the two above mentioned drug comparisons.

4.6. Chromatin Targeting Drug

There is only one drug that targets chromatin structure among the curated pool of 52 drugs. The following result is an interpretation of the detailed gene expression profile of sensitive TNBC cells versus resistant TNBC cells to that drug.

4.6.1. JQ1 results

Differential expression analysis results yielded 869 DEGs in the comparison of JQ1 sensitive 6 TNBC cell lines versus resistant 12 cell lines. Active sub-network based pathway enrichment analysis found 59 enriched KEGG pathways. The most significantly enriched 10 pathways and included DEGs are visualized in **Figure 18**.

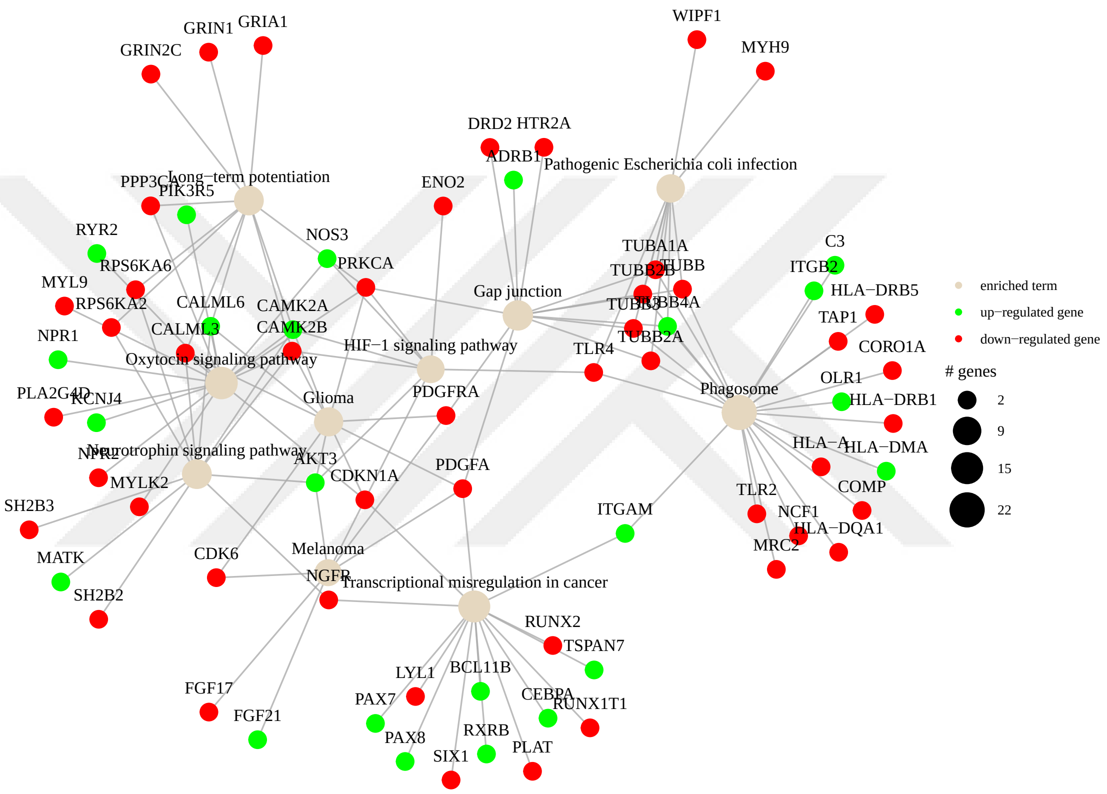

Figure 18: Reduced network of most enriched pathways for the sensitive TNBC cells versus resistant TNBC cells to JQ1.

In this figure significantly enriched top10 KEGG pathways are visualized as gray hubs (p-value < 0.05). Nodes are representing either upregulated DEGs (green) or down-regulated DEGs (red) which were involved in the enrichment of the connected hub pathway. Preferred DEG cutoff of false discovery rate (FDR) < 0.05 and $\log_2$ absolute fold change ≥ 1.5. These hubs and nodes are not all of the found significant elements. For full list, please look up the relevant section of the supplemental appendix.

4.7. Cytoskeleton Targeting Drugs

There are 2 drugs that target the cytoskeleton structure among the curated pool of 52 drugs. The following results are interpretations of the detailed gene expression profile of sensitive TNBC cells versus resistant TNBC cells to those 2 drugs.

4.7.1. BDP-00009066 results

Differential expression analysis results yielded 870 DEGs in the comparison of BDP-00009066 sensitive 8 TNBC cell lines versus resistant 9 cell lines. Active sub-network based pathway enrichment analysis found 48 enriched KEGG pathways. The most significantly enriched 10 pathways and included DEGs are visualized in **Figure 19**.

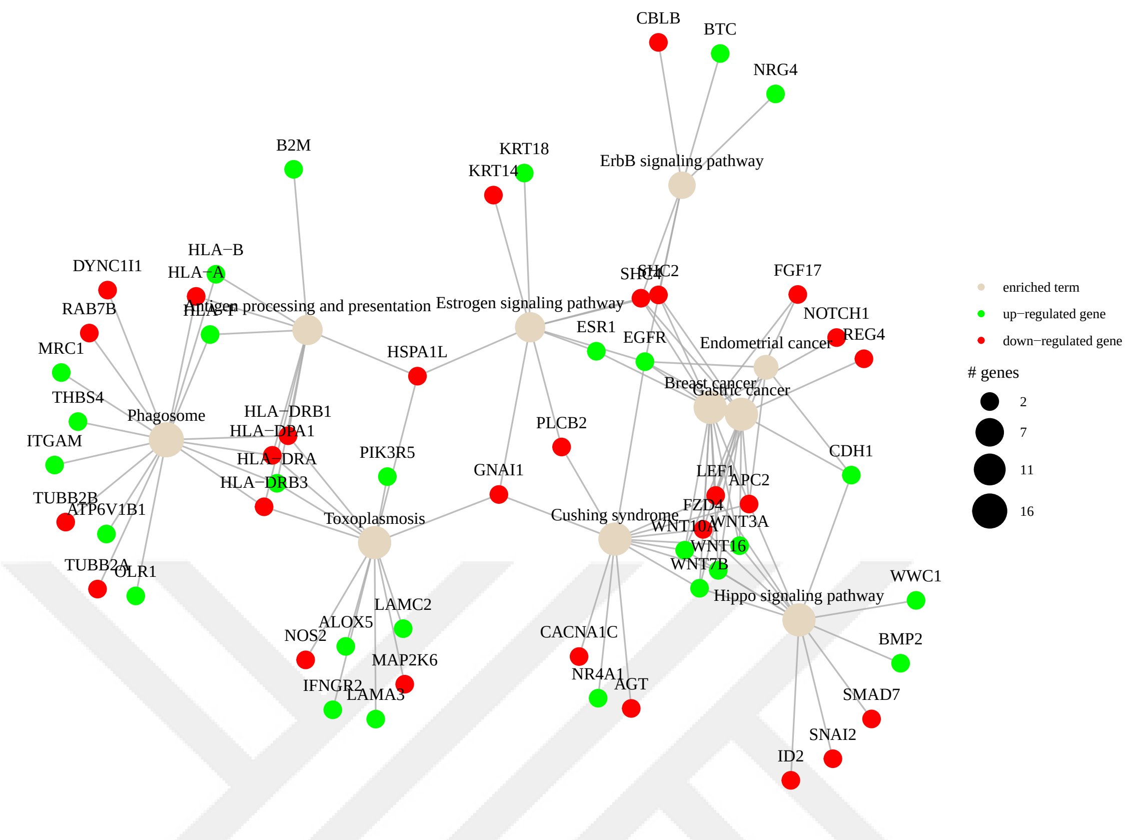

Figure 19: Reduced network of most enriched pathways for the sensitive TNBC cells versus resistant TNBC cells to BDP-00009066.

In this figure significantly enriched top10 KEGG pathways are visualized as gray hubs (p-value < 0.05). Nodes are representing either upregulated DEGs (green) or down-regulated DEGs (red) which were involved in the enrichment of the connected hub pathway. Preferred DEG cutoff of false discovery rate (FDR) < 0.05 and $\log_2$ absolute fold change $\geq$ 1.5. These hubs and nodes are not all of the found significant elements. For full list, please look up the relevant section of the supplemental appendix.

4.7.2. GSK269962A results

Differential expression analysis results yielded 574 DEGs in the comparison of GSK269962A sensitive 3 TNBC cell lines versus resistant 14 cell lines. Active sub-network based pathway enrichment analysis found 52 enriched KEGG pathways. The most significantly enriched 10 pathways and included DEGs are visualized in **Figure 20**.

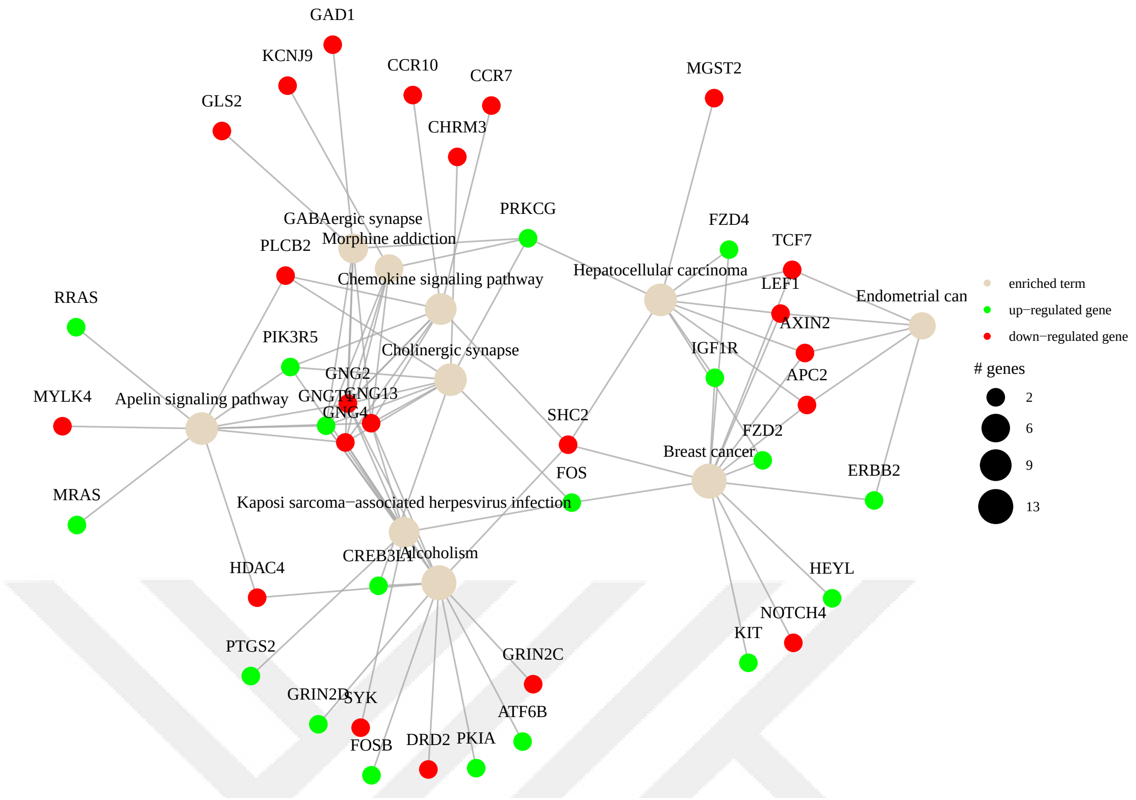

Figure 20: Reduced network of most enriched pathways for the sensitive TNBC cells versus resistant TNBC cells to GSK269962A.

In this figure significantly enriched top10 KEGG pathways are visualized as gray hubs (p-value < 0.05). Nodes are representing either upregulated DEGs (green) or down-regulated DEGs (red) which were involved in the enrichment of the connected hub pathway. Preferred DEG cutoff of false discovery rate (FDR) < 0.05 and $\log_2$ absolute fold change ≥ 1.5. These hubs and nodes are not all of the found significant elements. For full list, please look up the relevant section of the supplemental appendix.

4.7.3. The intersection of GSK269962A and BDP-00009066

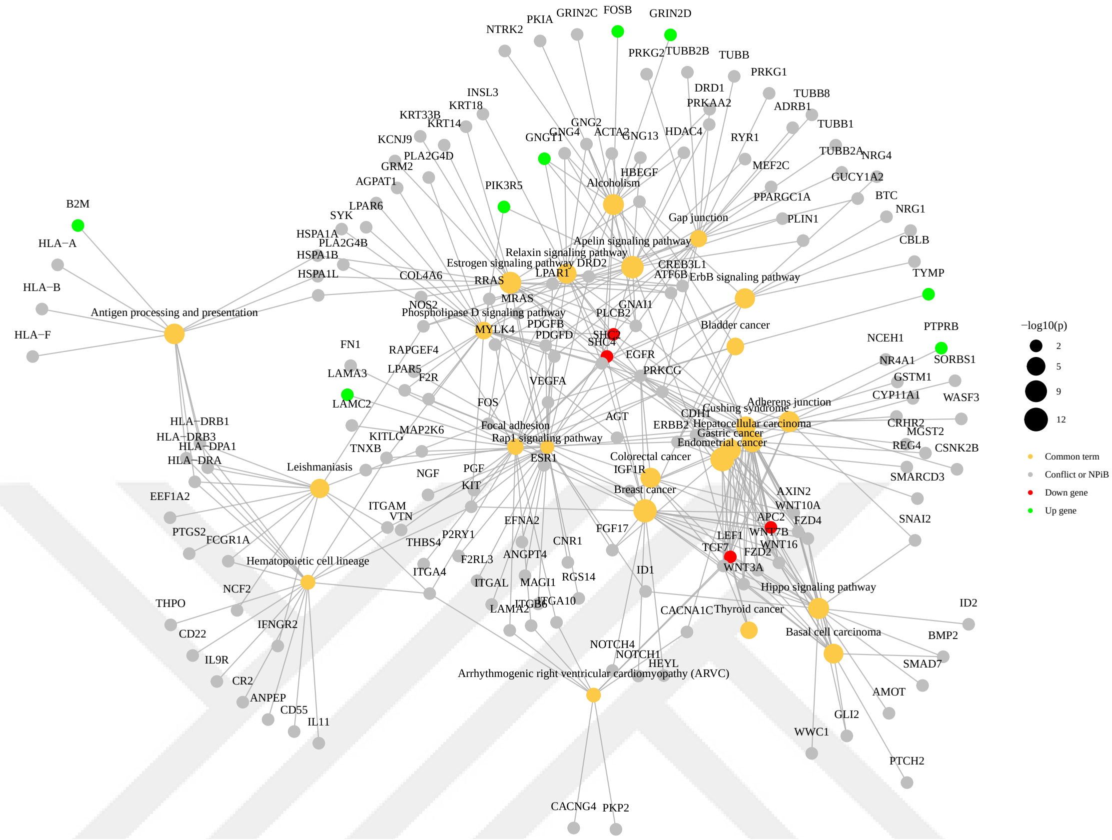

Figure 21: Intersection of most enriched pathways from the determined DEGs of BDP-00009066 and GSK269962A differential expression analysis.

In this figure, the intersection of the most significant (combined p-value assessment by Fisher's method, p-value ≤ 0.05) commonly enriched KEGG pathways are visualized as yellow hubs. The nodes are representing commonly upregulated DEGs (green), commonly down-regulated DEGs (red), and "conflict or NPiB (Not Present in Both)" DEGs (grey) which were involved in the enrichment of the connected pathway hub. Preferred DEG cutoff of false discovery rate (FDR) < 0.05 and absolute fold change ≥ 1.5. The size of the hubs is reversely proportional with their respective combined p-values for the commonly enriched pathways in the comparison of the two above mentioned drug comparisons.

4.8. DNA Replication Targeting Drugs

There are 4 drugs that target DNA replication machinery among the curated pool of 52 drugs. The following results are interpretations of the detailed gene expression profile of sensitive TNBC cells versus resistant TNBC cells to those 4 drugs.

4.8.1. Camptothecin results

Differential expression analysis results yielded 608 DEGs in the comparison of Camptothecin sensitive 4 TNBC cell lines versus resistant 13 cell lines. Active sub-network based pathway enrichment analysis found 19 enriched KEGG pathways. The most significantly enriched 10 pathways and included DEGs are visualized in **Figure 22**.

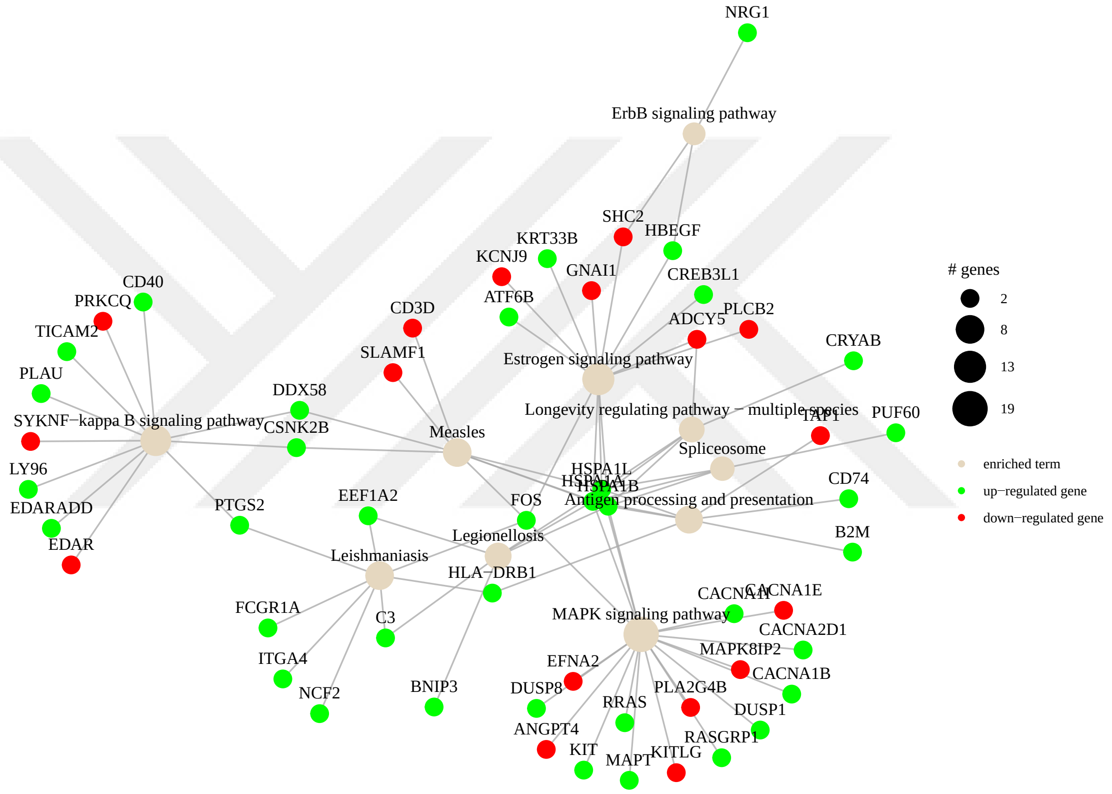

Figure 22: Reduced network of most enriched pathways for the sensitive TNBC cells versus resistant TNBC cells to Camptothecin.

In this figure significantly enriched top10 KEGG pathways are visualized as gray hubs (p-value < 0.05). Nodes are representing either upregulated DEGs (green) or down-regulated DEGs (red) which were involved in the enrichment of the connected hub pathway. Preferred DEG cutoff of false discovery rate (FDR) < 0.05 and $\log_2$ absolute fold change ≥ 1.5. These hubs and nodes are not all of the found significant elements. For full list, please look up the relevant section of the supplemental appendix.

4.8.2. Epirubicin results

Differential expression analysis results yielded 712 DEGs in the comparison of Epirubicin sensitive 9 TNBC cell lines versus resistant 8 cell lines. Active sub-network based pathway enrichment analysis found 37 enriched KEGG pathways. The most significantly enriched 10 pathways and included DEGs are visualized in **Figure 23**.

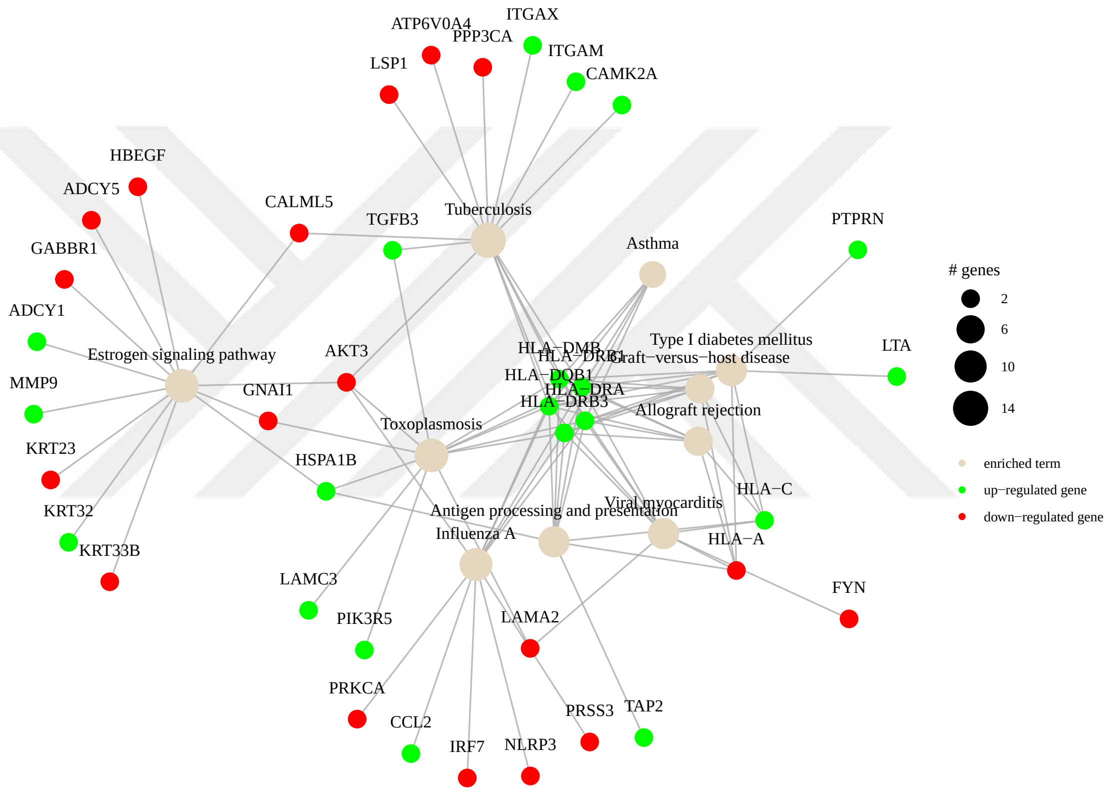

Figure 23: Reduced network of most enriched pathways for the sensitive TNBC cells versus resistant TNBC cells to Epirubicin.

In this figure significantly enriched top10 KEGG pathways are visualized as gray hubs (p-value < 0.05). Nodes are representing either upregulated DEGs (green) or down-regulated DEGs (red) which were involved in the enrichment of the connected hub pathway. Preferred DEG cutoff of false discovery rate (FDR) < 0.05 and $\log_2$ absolute fold change $\geq$ 1.5. These hubs and nodes are not all of the found significant elements. For full list, please look up the relevant section of the supplemental appendix.

4.8.3. Gemcitabine results

Differential expression analysis results yielded 718 DEGs in the comparison of Gemcitabine sensitive 10 TNBC cell lines versus resistant 7 cell lines. Active sub-network based pathway enrichment analysis found 24 enriched KEGG pathways. The most significantly enriched 10 pathways and included DEGs are visualized in **Figure 24**.

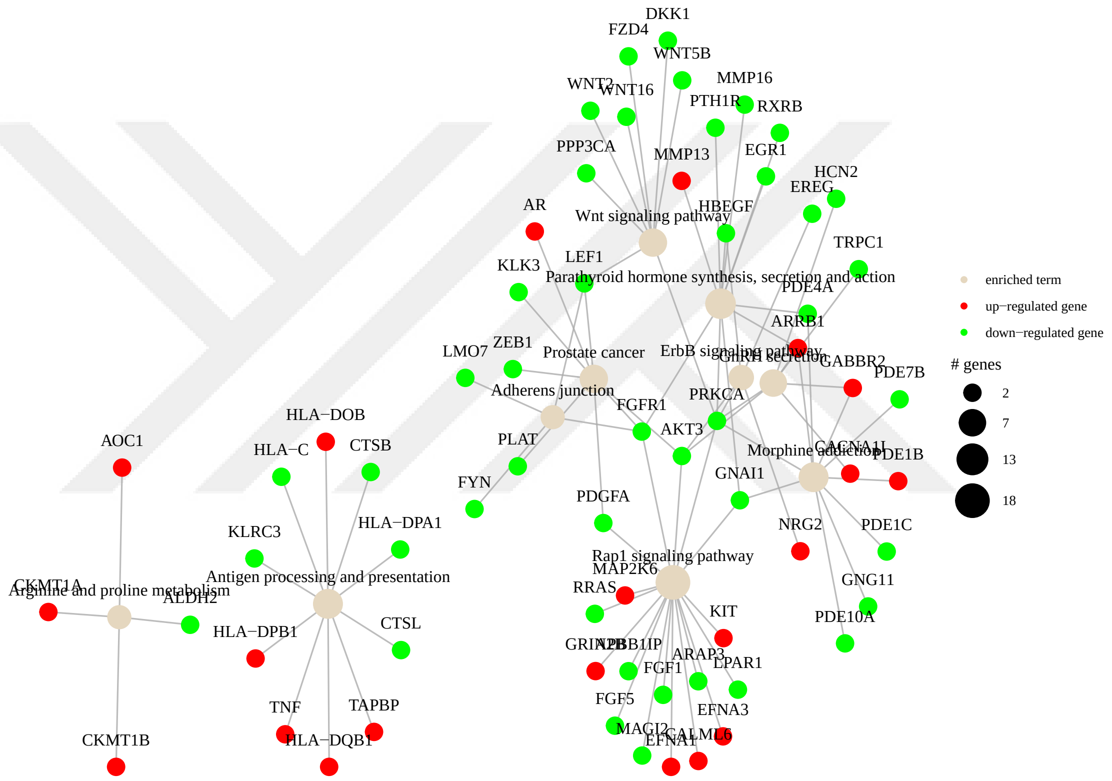

Figure 24: Reduced network of most enriched pathways for the sensitive TNBC cells versus resistant TNBC cells to Gemcitabine.

In this figure significantly enriched top10 KEGG pathways are visualized as gray hubs (p-value < 0.05). Nodes are representing either upregulated DEGs (green) or down-regulated DEGs (red) which were involved in the enrichment of the connected hub pathway. Preferred DEG cutoff of false discovery rate (FDR) < 0.05 and $\log_2$ absolute fold change ≥ 1.5. These hubs and nodes are not all of the found significant elements. For full list, please look up the relevant section of the supplemental appendix.

4.8.4. Irinotecan results

Differential expression analysis results yielded 987 DEGs in the comparison of Irinotecan sensitive 3 TNBC cell lines versus resistant 14 cell lines. Active sub-network based pathway enrichment analysis found 60 enriched KEGG pathways. The most significantly enriched 10 pathways and included DEGs are visualized in **Figure 25**.

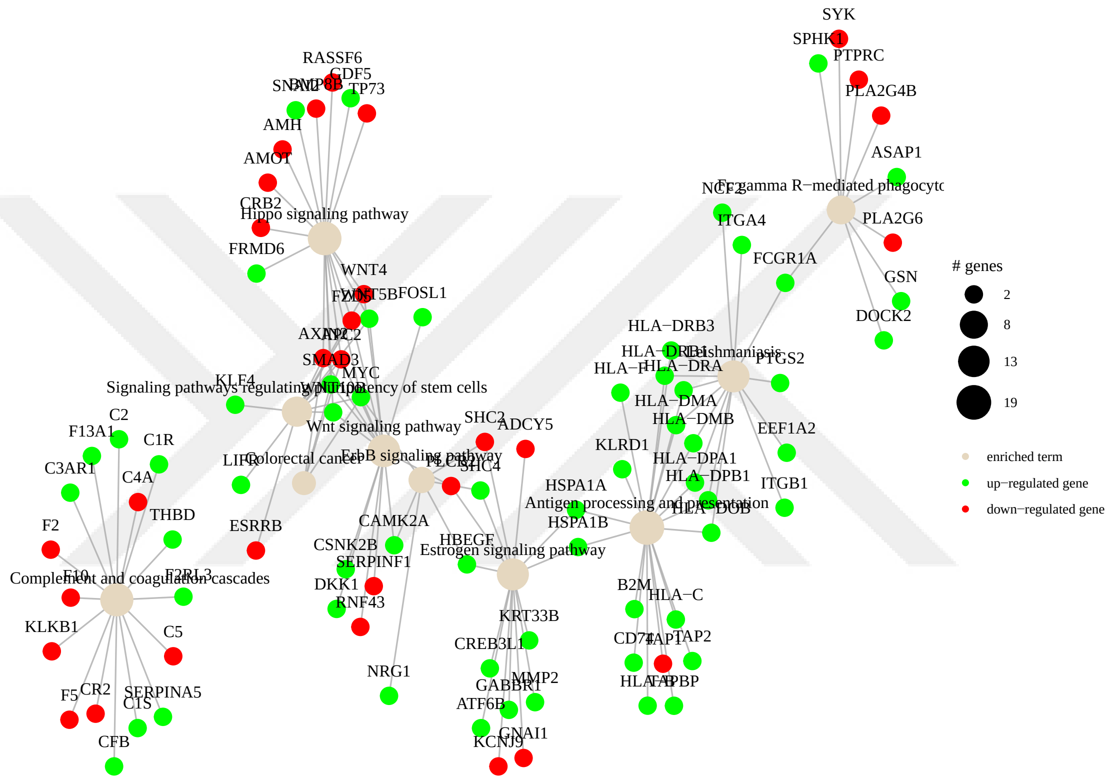

Figure 25: Reduced network of most enriched pathways for the sensitive TNBC cells versus resistant TNBC cells to Irinotecan.

In this figure significantly enriched top10 KEGG pathways are visualized as gray hubs (p-value < 0.05). Nodes are representing either upregulated DEGs (green) or down-regulated DEGs (red) which were involved in the enrichment of the connected hub pathway. Preferred DEG cutoff of false discovery rate (FDR) < 0.05 and $\log_2$ absolute fold change ≥ 1.5. These hubs and nodes are not all of the found significant elements. For full list, please look up the relevant section of the supplemental appendix.

4.8.5. The intersection of Epirubicin and Irinotecan

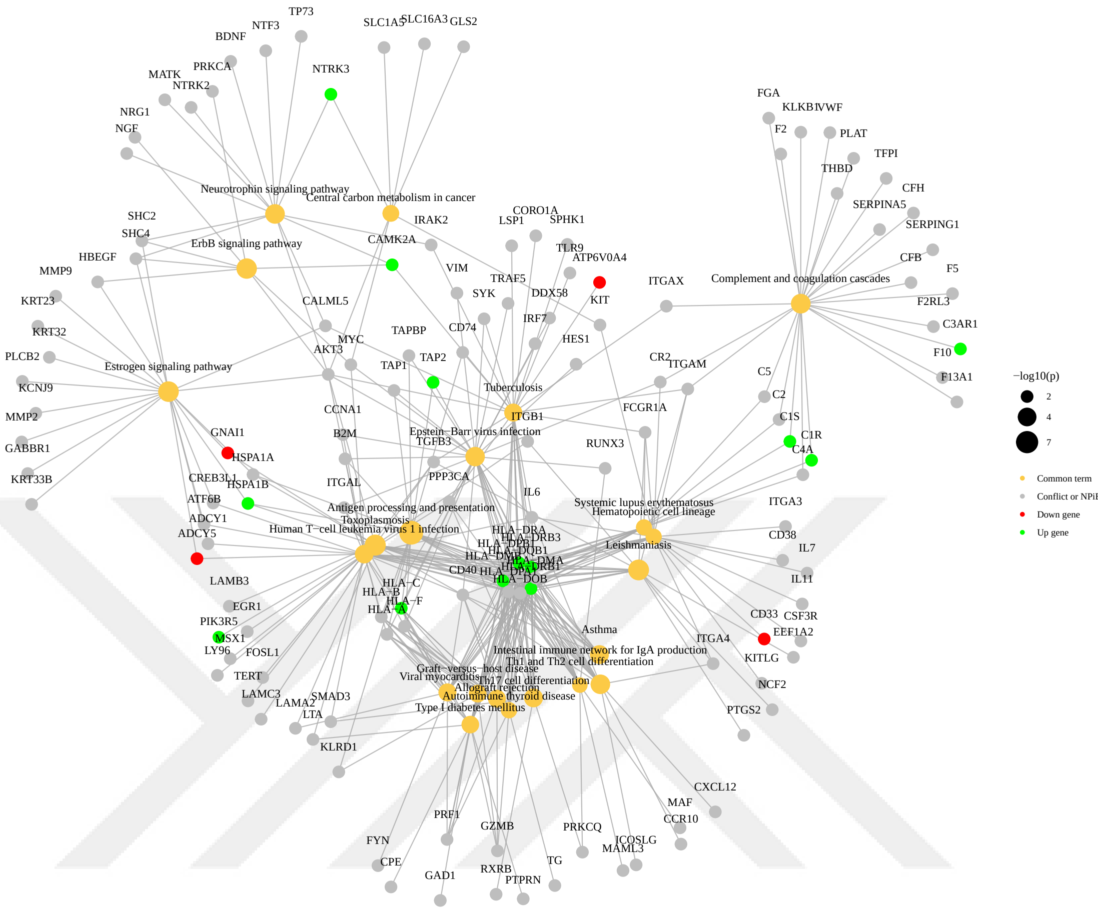

Figure 26: Intersection of most enriched pathways from the determined DEGs of Epirubicin and Irinotecan differential expression analysis.

In this figure, the intersection of the most significant (combined p-value assessment by Fisher's method, p-value ≤ 0.05) commonly enriched KEGG pathways are visualized as yellow hubs. The nodes are representing commonly upregulated DEGs (green), commonly down-regulated DEGs (red), and "conflict or NPiB (Not Present in Both)" DEGs (grey) which were involved in the enrichment of the connected pathway hub. Preferred DEG cutoff of false discovery rate (FDR) < 0.05 and absolute fold change ≥ 1.5. The size of the hubs is reversely proportional with their respective combined p-values for the commonly enriched pathways in the comparison of the two above mentioned drug comparisons.

4.9. EGFR Signaling Targeting Drugs

There are 3 drugs that target EGFR signaling pathway among the curated 52 drugs. The following results are interpretations of the detailed gene expression profile of sensitive TNBC cells versus resistant TNBC cells to those 3 drugs.

4.9.1. Afatinib results

Differential expression analysis results yielded 415 DEGs in the comparison of Afatinib sensitive 8 TNBC cell lines versus resistant 9 cell lines. Active sub-network based pathway enrichment analysis found 19 enriched KEGG pathways. The most significantly enriched 10 pathways and included DEGs are visualized in **Figure 27**.

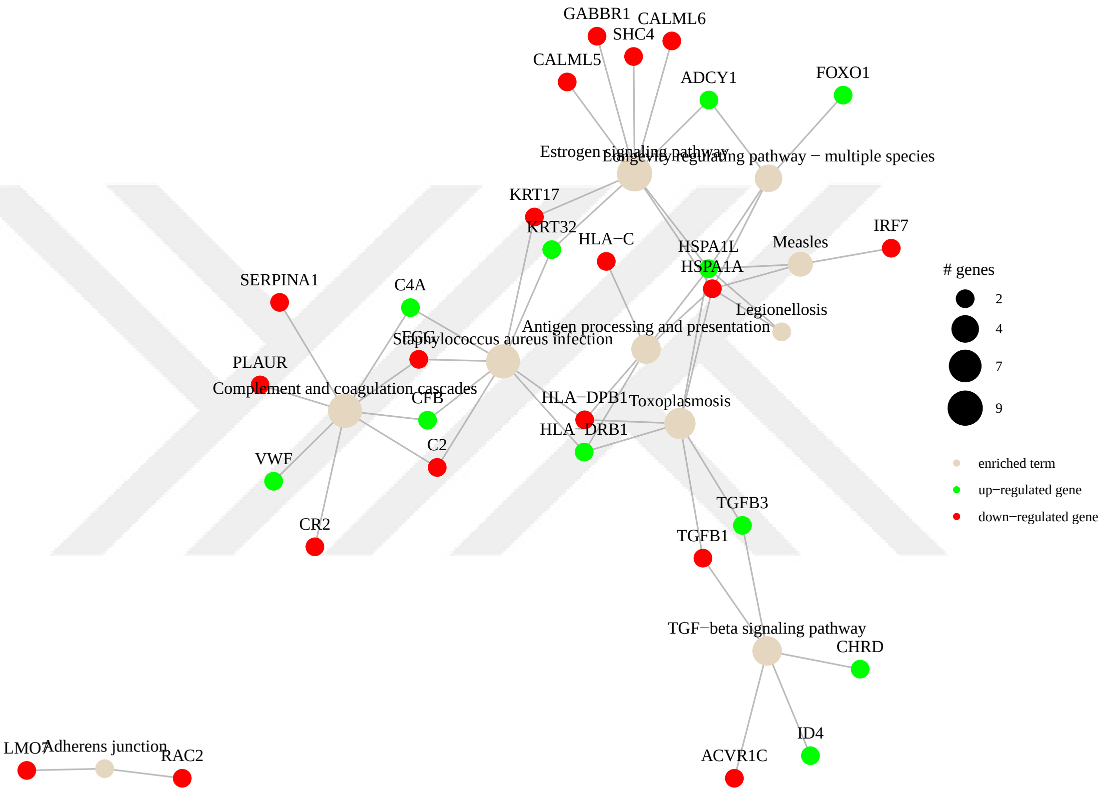

Figure 27: Reduced network of most enriched pathways for the sensitive TNBC cells versus resistant TNBC cells to Afatinib.

In this figure significantly enriched top10 KEGG pathways are visualized as gray hubs (p-value < 0.05). Nodes are representing either upregulated DEGs (green) or down-regulated DEGs (red) which were involved in the enrichment of the connected hub pathway. Preferred DEG cutoff of false discovery rate (FDR) < 0.05 and $\log_2$ absolute fold change ≥ 1.5. These hubs and nodes are not all of the found significant elements. For full list, please look up the relevant section of the supplemental appendix.

4.9.2. Lapatinib results

Differential expression analysis results yielded 322 DEGs in the comparison of Lapatinib sensitive 9 TNBC cell lines versus resistant 8 cell lines. Active sub-network based pathway enrichment analysis found 12 enriched KEGG pathways. The most significantly enriched 10 pathways and included DEGs are visualized in **Figure 28**.

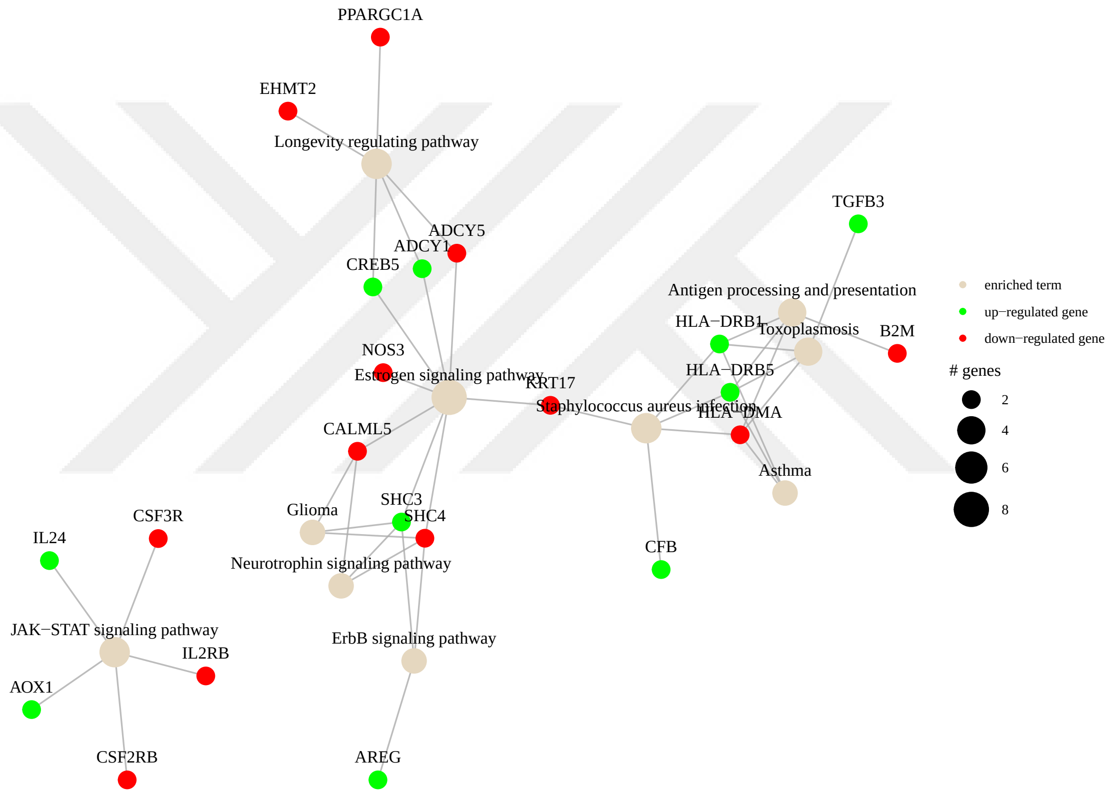

Figure 28: Reduced network of most enriched pathways for the sensitive TNBC cells versus resistant TNBC cells to Lapatinib.

In this figure significantly enriched top10 KEGG pathways are visualized as gray hubs (p-value < 0.05). Nodes are representing either upregulated DEGs (green) or down-regulated DEGs (red) which were involved in the enrichment of the connected hub pathway. Preferred DEG cutoff of false discovery rate (FDR) < 0.05 and $\log_2$ absolute fold change ≥ 1.5. These hubs and nodes are not all of the found significant elements. For full list, please look up the relevant section of the supplemental appendix.

4.9.3. Sapitinib results

Differential expression analysis results yielded 653 DEGs in the comparison of Sapitinib sensitive 3 TNBC cell lines versus resistant 14 cell lines. Active sub-network based pathway enrichment analysis found 38 enriched KEGG pathways. The most significantly enriched 10 pathways and included DEGs are visualized in **Figure 29**.

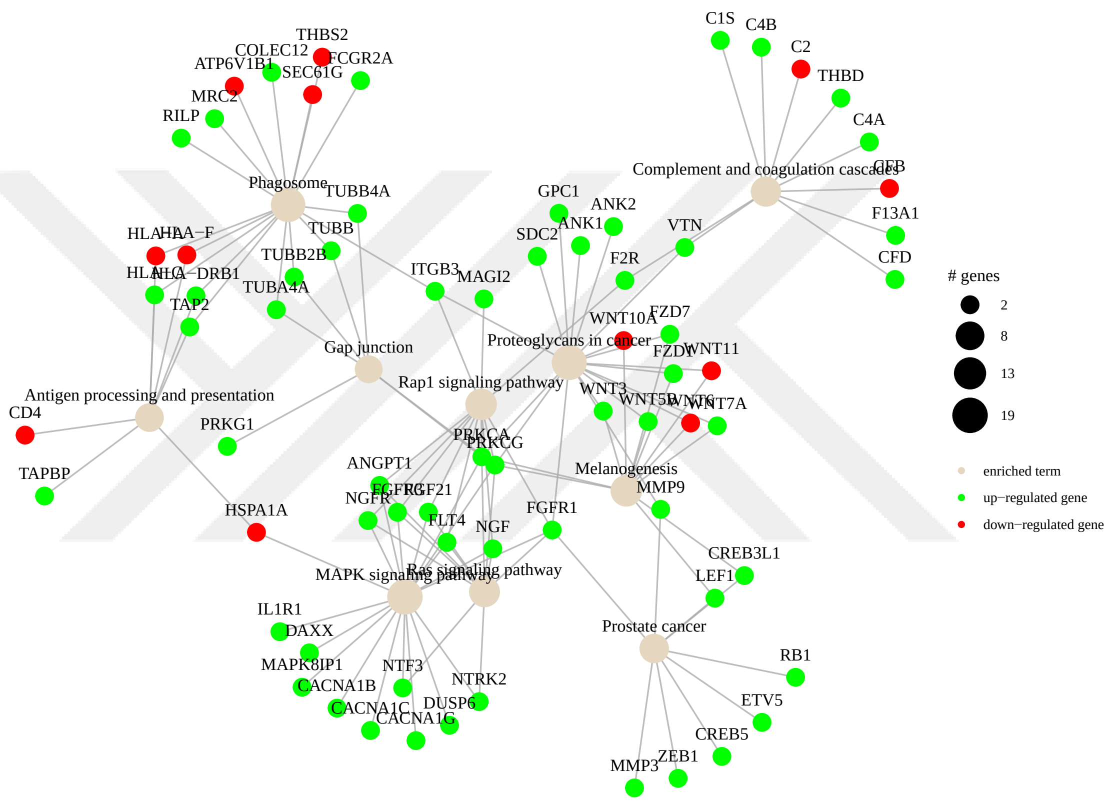

Figure 29: Reduced network of most enriched pathways for the sensitive TNBC cells versus resistant TNBC cells to Sapitinib.

In this figure significantly enriched top10 KEGG pathways are visualized as gray hubs (p-value < 0.05). Nodes are representing either upregulated DEGs (green) or down-regulated DEGs (red) which were involved in the enrichment of the connected hub pathway. Preferred DEG cutoff of false discovery rate (FDR) < 0.05 and $\log_2$ absolute fold change ≥ 1.5. These hubs and nodes are not all of the found significant elements. For full list, please look up the relevant section of the supplemental appendix.

4.9.4. The intersection of Afatinib and Sapitinib

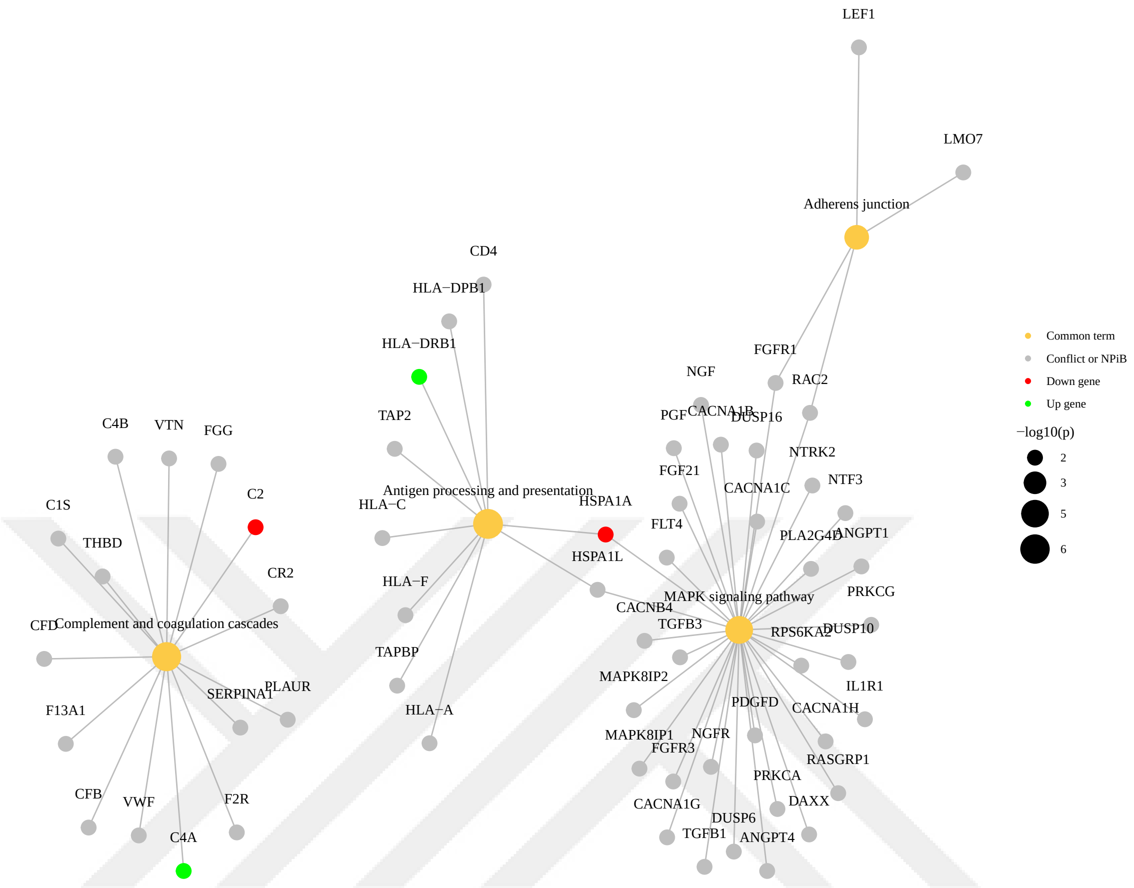

Figure 30: Intersection of most enriched pathways from the determined DEGs of Afatinib and Sapitinib differential expression analysis.

In this figure, the intersection of the most significant (combined p-value assessment by Fisher's method, p-value ≤ 0.05) commonly enriched KEGG pathways are visualized as yellow hubs. The nodes are representing commonly upregulated DEGs (green), commonly down-regulated DEGs (red), and "conflict or NPiB (Not Present in Both)" DEGs (grey) which were involved in the enrichment of the connected pathway hub. Preferred DEG cutoff of false discovery rate (FDR) < 0.05 and absolute fold change ≥ 1.5. The size of the hubs is reversely proportional with their respective combined p-values for the commonly enriched pathways in the comparison of the two above mentioned drug comparisons.

4.10. ERK/MAPK Signaling Targeting Drugs

There are 2 drugs that target ERK/MAPK signaling pathway among the curated 52 drugs. The following results are interpretations of the detailed gene expression profile of sensitive TNBC cells versus resistant TNBC cells to those 2 drugs.

4.10.1. Trametinib results

Differential expression analysis results yielded 653 DEGs in the comparison of Trametinib sensitive 3 TNBC cell lines versus resistant 14 cell lines. Active sub-network based pathway enrichment analysis found 38 enriched KEGG pathways. The most significantly enriched 10 pathways and included DEGs are visualized in **Figure 31**.

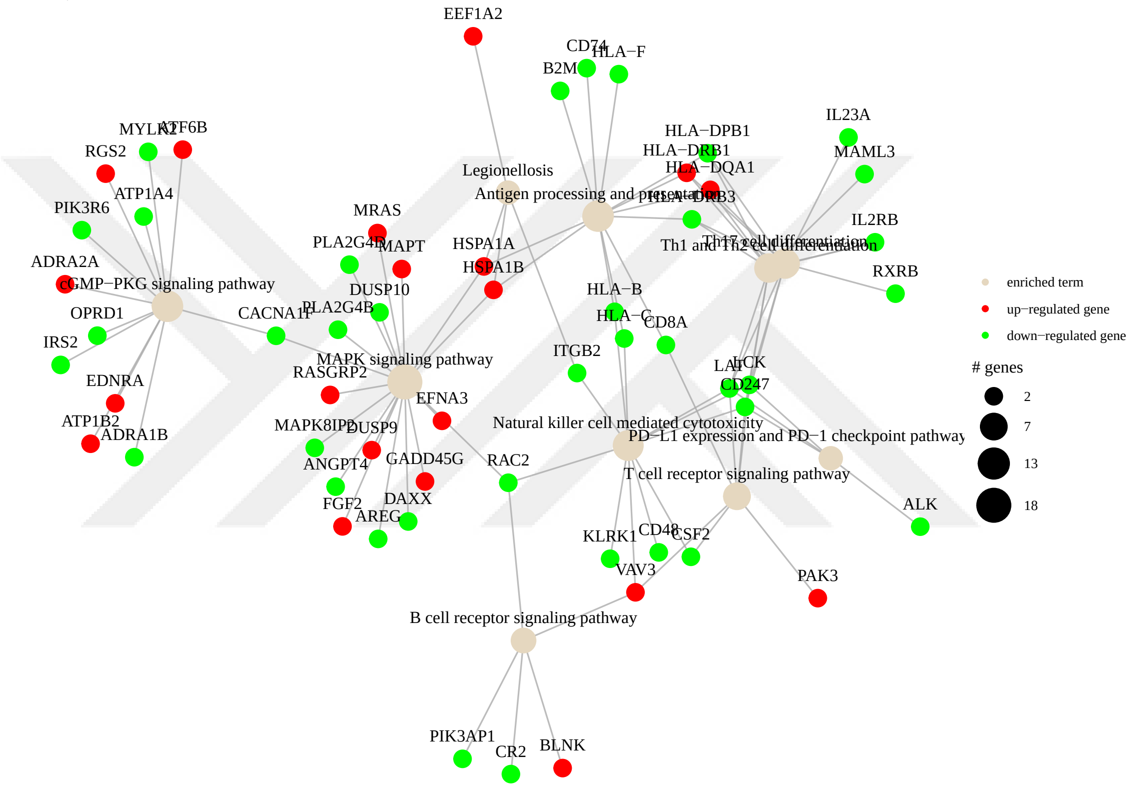

Figure 31: Reduced network of most enriched pathways for the sensitive TNBC cells versus resistant TNBC cells to Trametinib.

In this figure significantly enriched top10 KEGG pathways are visualized as gray hubs (p-value < 0.05). Nodes are representing either upregulated DEGs (green) or down-regulated DEGs (red) which were involved in the enrichment of the connected hub pathway. Preferred DEG cutoff of false discovery rate (FDR) < 0.05 and $\log_2$ absolute fold change ≥ 1.5. These hubs and nodes are not all of the found significant elements. For full list, please look up the relevant section of the supplemental appendix.

4.10.2. VX-11e results

Differential expression analysis results yielded 882 DEGs in the comparison of VX-11e sensitive 3 TNBC cell lines versus resistant 14 cell lines. Active sub-network based pathway enrichment analysis found 41 enriched KEGG pathways. The most significantly enriched 10 pathways and included DEGs are visualized in **Figure 32**.

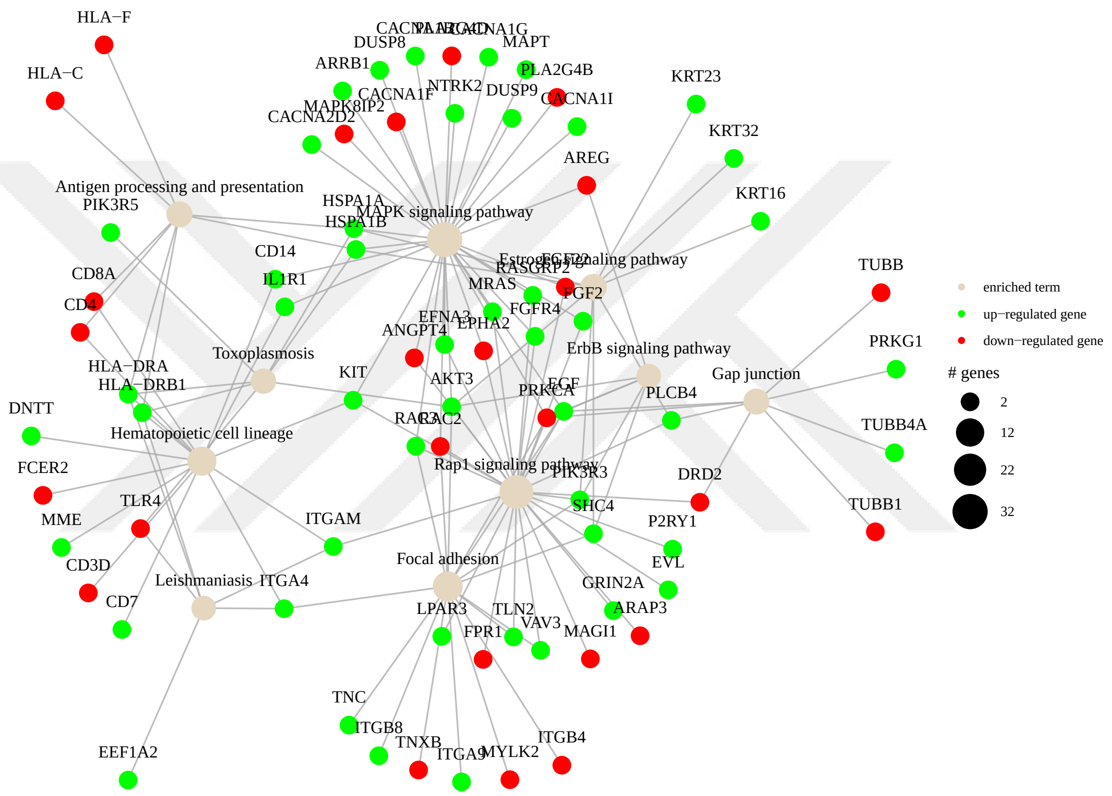

Figure 32: Reduced network of most enriched pathways for the sensitive TNBC cells versus resistant TNBC cells to VX-11e.

In this figure significantly enriched top10 KEGG pathways are visualized as gray hubs (p-value < 0.05). Nodes are representing either upregulated DEGs (green) or down-regulated DEGs (red) which were involved in the enrichment of the connected hub pathway. Preferred DEG cutoff of false discovery rate (FDR) < 0.05 and $\log_2$ absolute fold change ≥ 1.5. These hubs and nodes are not all of the found significant elements. For full list, please look up the relevant section of the supplemental appendix.

4.10.3. The intersection of Trametinib and VX-11e

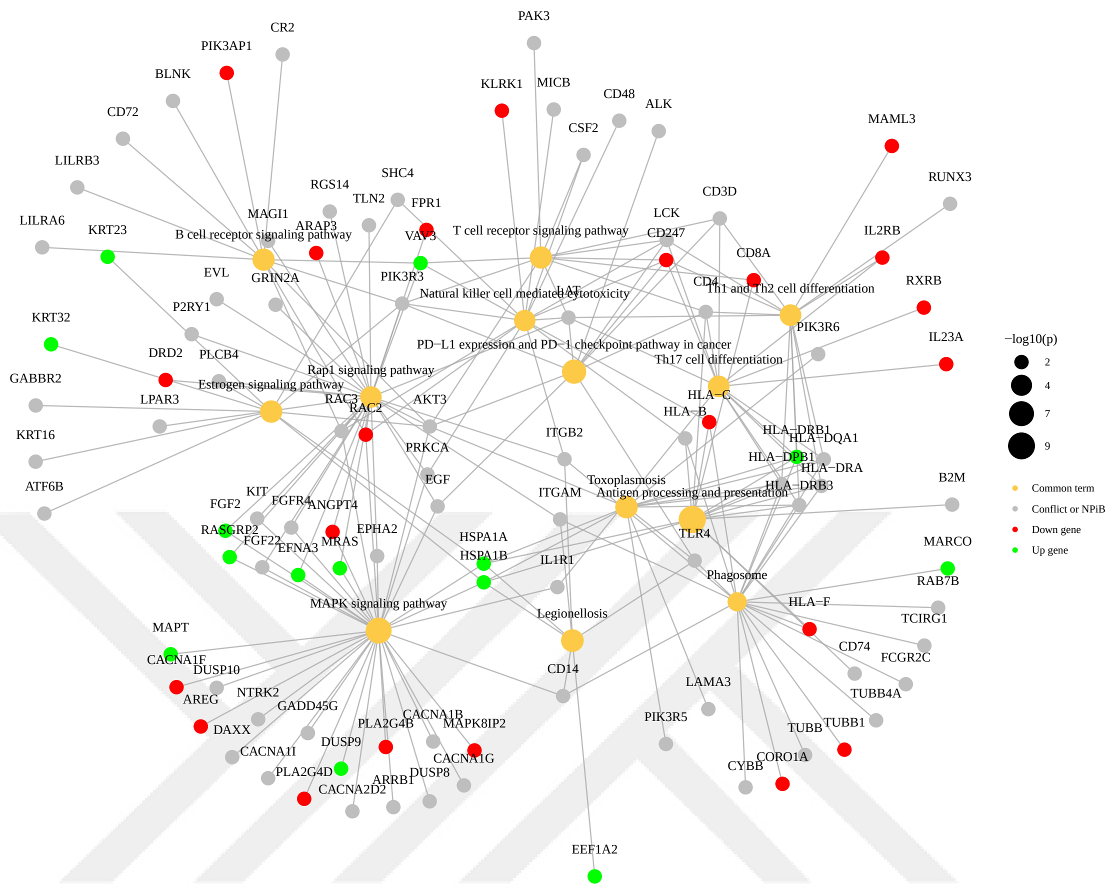

Figure 33: Intersection of most enriched pathways from the determined DEGs of Afatinib and Sapitinib differential expression analysis.

In this figure, the intersection of the most significant (combined p-value assessment by Fisher's method, p-value ≤ 0.05) commonly enriched KEGG pathways are visualized as yellow hubs. The nodes are representing commonly upregulated DEGs (green), commonly down-regulated DEGs (red), and "conflict or NPiB (Not Present in Both)" DEGs (grey) which were involved in the enrichment of the connected pathway hub. Preferred DEG cutoff of false discovery rate (FDR) < 0.05 and absolute fold change ≥ 1.5. The size of the hubs is reversely proportional with their respective combined p-values for the commonly enriched pathways in the comparison of the two above mentioned drug comparisons.

4.11. Genome Integrity Targeting Drugs

There are 3 drugs that target genome integrity among the curated 52 drugs. The following results are interpretations of the detailed gene expression profile of sensitive TNBC cells versus resistant TNBC cells to those 3 drugs.

4.11.1. AZD6738 results

Differential expression analysis results yielded 663 DEGs in the comparison of AZD6738 sensitive 10 TNBC cell lines versus resistant 7 cell lines. Active sub-network based pathway enrichment analysis found 21 enriched KEGG pathways. The most significantly enriched 10 pathways and included DEGs are visualized in **Figure 34**.

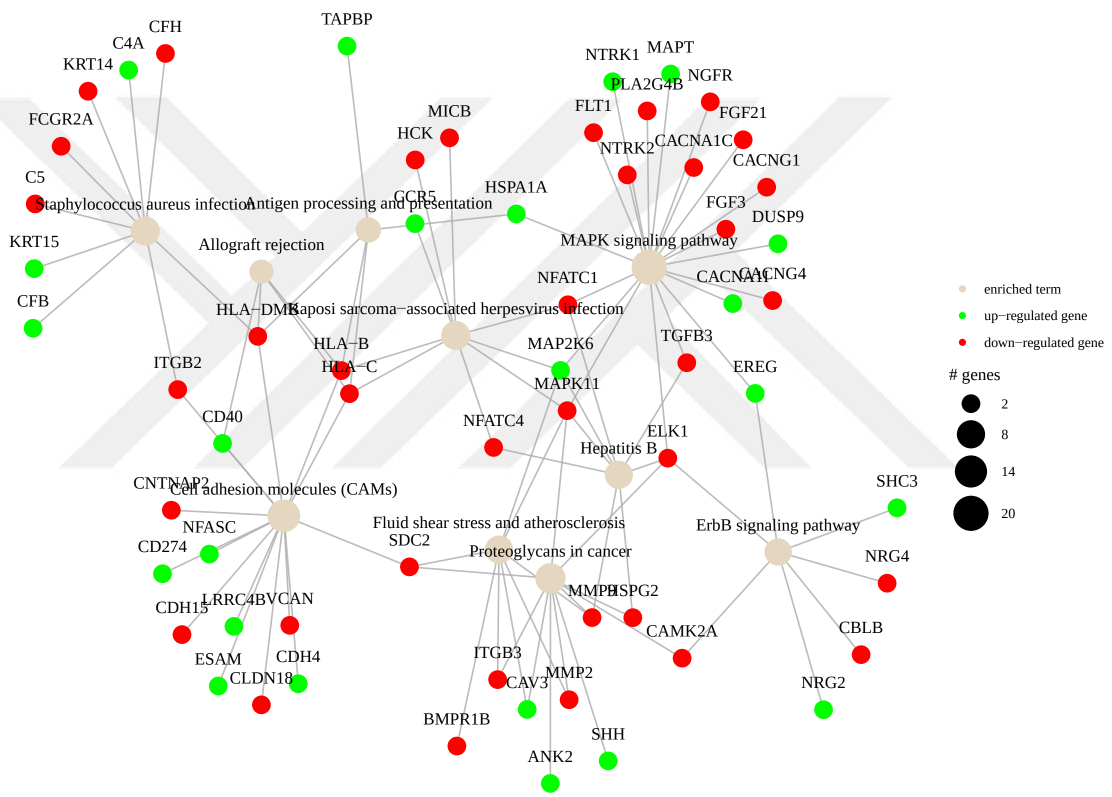

Figure 34: Reduced network of most enriched pathways for the sensitive TNBC cells versus resistant TNBC cells to AZD6738.

In this figure significantly enriched top10 KEGG pathways are visualized as gray hubs (p-value < 0.05). Nodes are representing either upregulated DEGs (green) or down-regulated DEGs (red) which were involved in the enrichment of the connected hub pathway. Preferred DEG cutoff of false discovery rate (FDR) < 0.05 and $\log_2$ absolute fold change ≥ 1.5. These hubs and nodes are not all of the found significant elements. For full list, please look up the relevant section of the supplemental appendix.

4.11.2. NU7441 results

Differential expression analysis results yielded 751 DEGs in the comparison of NU7441 sensitive 6 TNBC cell lines versus resistant 11 cell lines. Active sub-network based pathway enrichment analysis found 31 enriched KEGG pathways. The most significantly enriched 10 pathways and included DEGs are visualized in **Figure 35**.

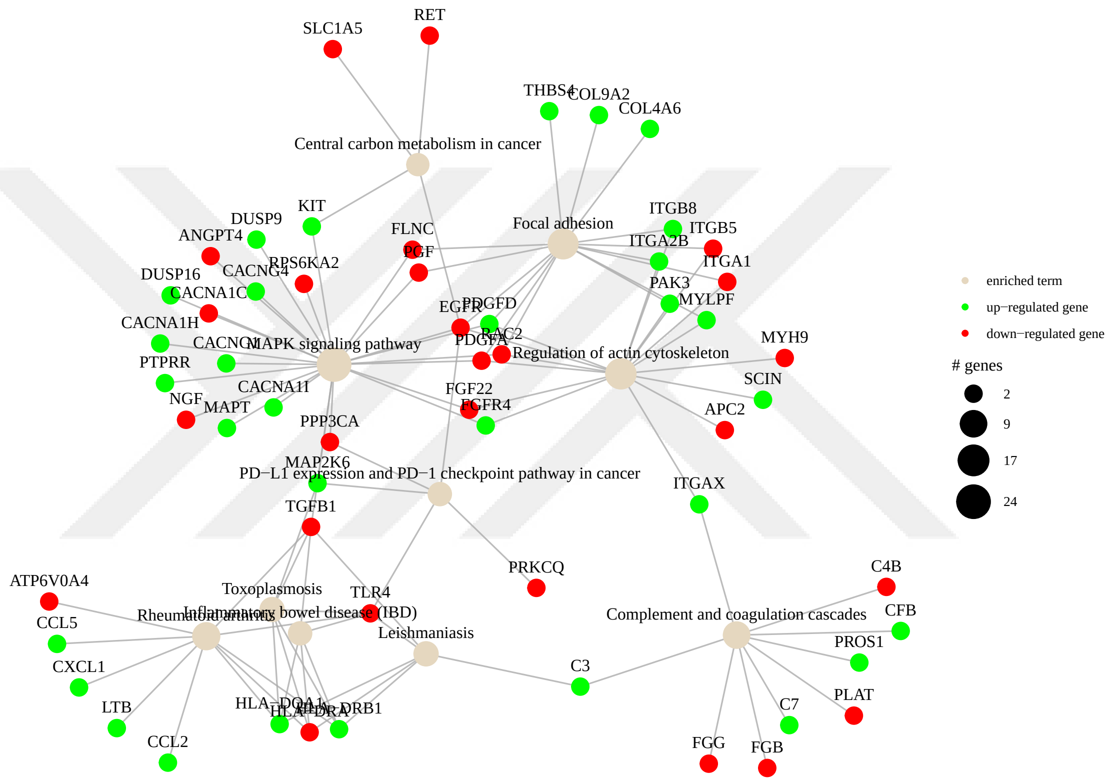

Figure 35: Reduced network of most enriched pathways for the sensitive TNBC cells versus resistant TNBC cells to NU7441.

In this figure significantly enriched top10 KEGG pathways are visualized as gray hubs (p-value < 0.05). Nodes are representing either upregulated DEGs (green) or down-regulated DEGs (red) which were involved in the enrichment of the connected hub pathway. Preferred DEG cutoff of false discovery rate (FDR) < 0.05 and $\log_2$ absolute fold change ≥ 1.5. These hubs and nodes are not all of the found significant elements. For full list, please look up the relevant section of the supplemental appendix.

4.11.3. VE821 results

Differential expression analysis results yielded 1137 DEGs in the comparison of VE821 sensitive 3 TNBC cell lines versus resistant 14 cell lines. Active sub-network based pathway enrichment analysis found 37 enriched KEGG pathways. The most significantly enriched 10 pathways and included DEGs are visualized in **Figure 36**.

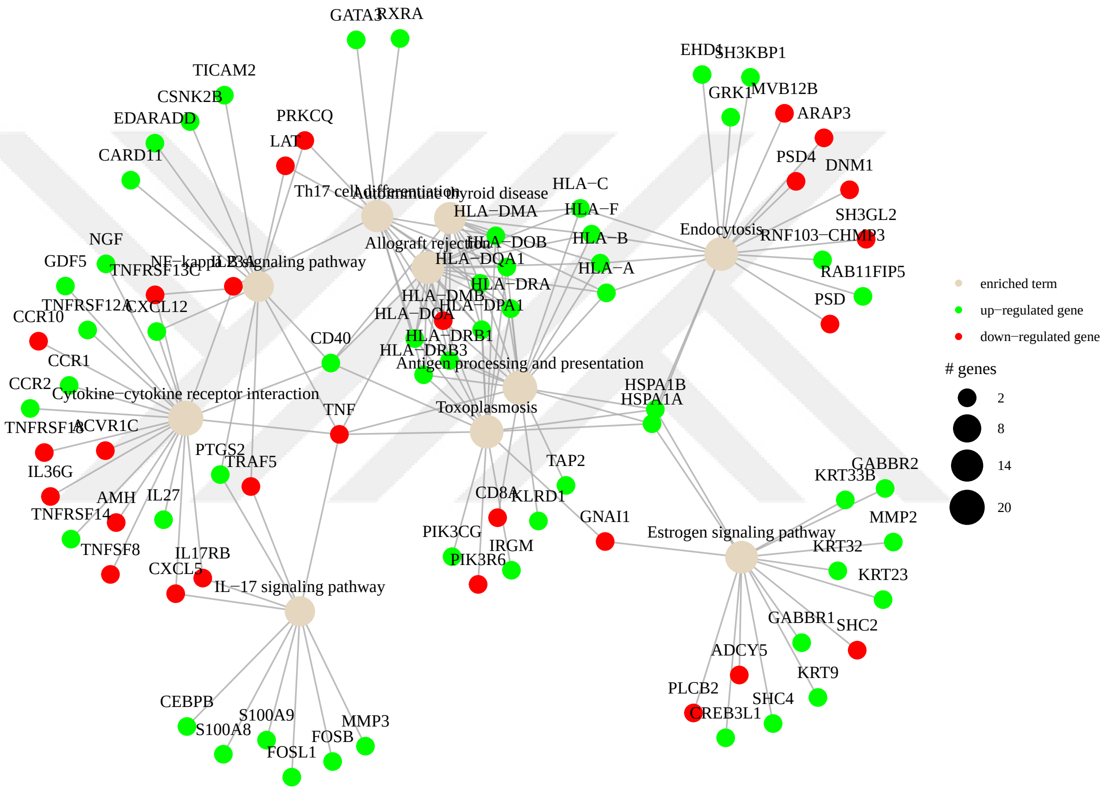

Figure 36: Reduced network of most enriched pathways for the sensitive TNBC cells versus resistant TNBC cells to VE821.

In this figure significantly enriched top10 KEGG pathways are visualized as gray hubs (p-value < 0.05). Nodes are representing either upregulated DEGs (green) or down-regulated DEGs (red) which were involved in the enrichment of the connected hub pathway. Preferred DEG cutoff of false discovery rate (FDR) < 0.05 and $\log_2$ absolute fold change ≥ 1.5. These hubs and nodes are not all of the found significant elements. For full list, please look up the relevant section of the supplemental appendix.

4.11.4. The intersection of NU7441 and VE821

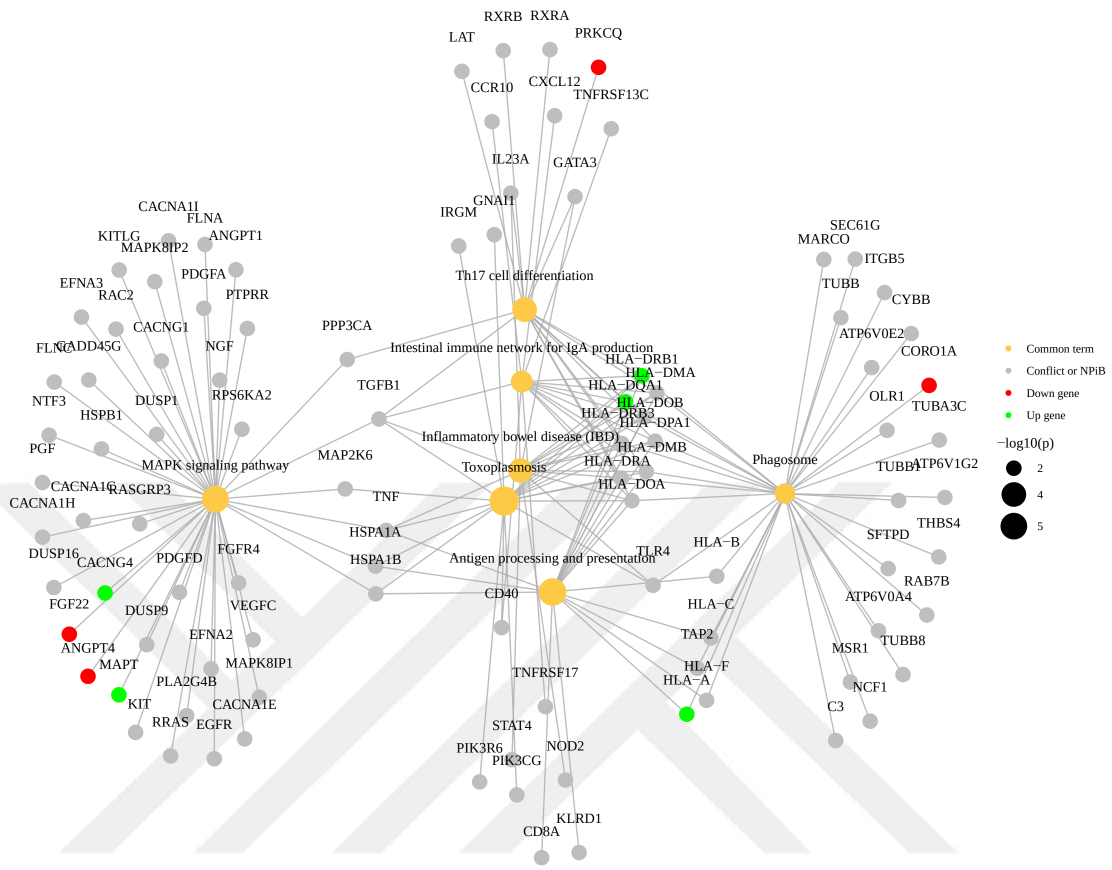

Figure 37: Intersection of most enriched pathways from the determined DEGs of NU7441 and VE821 differential expression analysis.

In this figure, the intersection of the most significant (combined p-value assessment by Fisher's method, p-value ≤ 0.05) commonly enriched KEGG pathways are visualized as yellow hubs. The nodes are representing commonly upregulated DEGs (green), commonly down-regulated DEGs (red), and "conflict or NPiB (Not Present in Both)" DEGs (grey) which were involved in the enrichment of the connected pathway hub. Preferred DEG cutoff of false discovery rate (FDR) < 0.05 and absolute fold change ≥ 1.5. The size of the hubs is reversely proportional with their respective combined p-values for the commonly enriched pathways in the comparison of the two above mentioned drug comparisons.

4.12. IGF1R Signaling Targeting Drugs

There are 2 drugs that target IGF1R signaling pathway among the curated 52 drugs. The following results are interpretations of the detailed gene expression profile of sensitive TNBC cells versus resistant TNBC cells to those 2 drugs.

4.12.1. BMS-536924 results

Differential expression analysis results yielded 665 DEGs in the comparison of BMS-536924 sensitive 10 TNBC cell lines versus resistant 7 cell lines. Active sub-network based pathway enrichment analysis found 17 enriched KEGG pathways. The most significantly enriched 10 pathways and included DEGs are visualized in **Figure 38**.

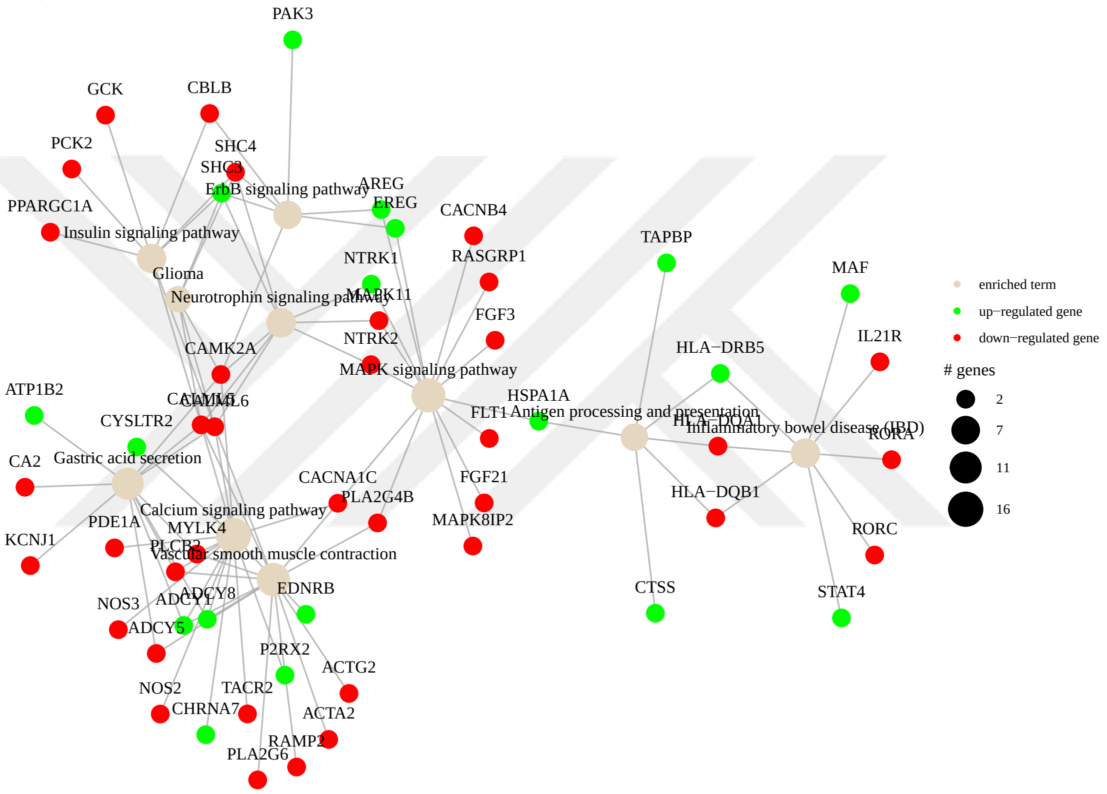

Figure 38: Reduced network of most enriched pathways for the sensitive TNBC cells versus resistant TNBC cells to BMS-536924.

In this figure significantly enriched top10 KEGG pathways are visualized as gray hubs (p-value < 0.05). Nodes are representing either upregulated DEGs (green) or down-regulated DEGs (red) which were involved in the enrichment of the connected hub pathway. Preferred DEG cutoff of false discovery rate (FDR) < 0.05 and $\log_2$ absolute fold change ≥ 1.5. These hubs and nodes are not all of the found significant elements. For full list, please look up the relevant section of the supplemental appendix.

4.12.2. NVP-ADW742 results

Differential expression analysis results yielded 608 DEGs in the comparison of NVP-ADW742 sensitive 5 TNBC cell lines versus resistant 12 cell lines. Active sub-network based pathway enrichment analysis found 12 enriched KEGG pathways. The most significantly enriched 10 pathways and included DEGs are visualized in **Figure 39**.

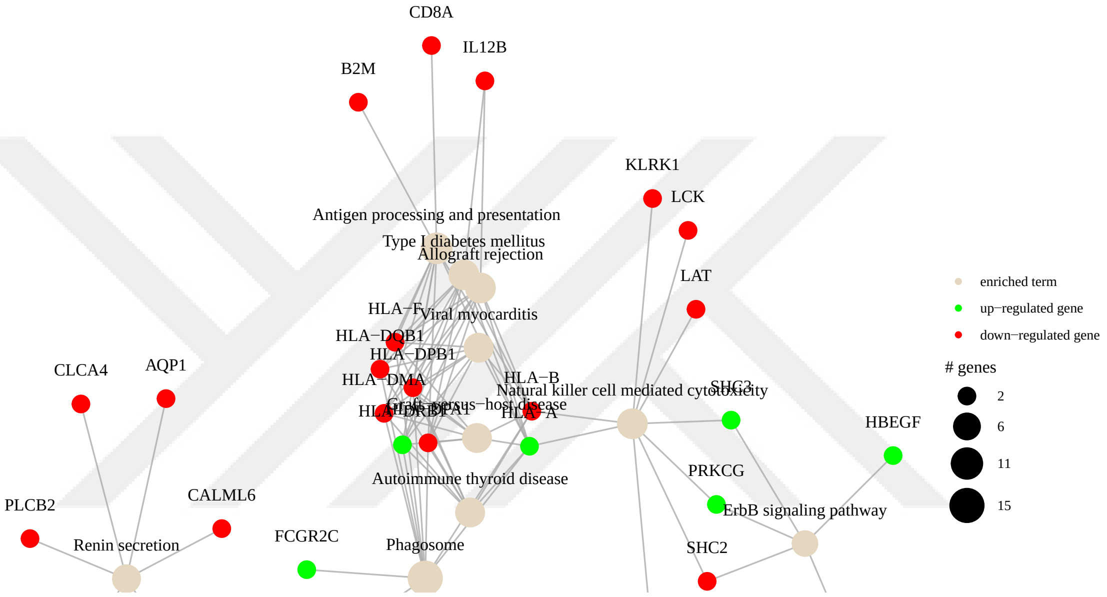

Figure 39: Reduced network of most enriched pathways for the sensitive TNBC cells versus resistant TNBC cells to AVP-ADW742.

In this figure significantly enriched top10 KEGG pathways are visualized as gray hubs (p-value < 0.05). Nodes are representing either upregulated DEGs (green) or down-regulated DEGs (red) which were involved in the enrichment of the connected hub pathway. Preferred DEG cutoff of false discovery rate (FDR) < 0.05 and $\log_2$ absolute fold change ≥ 1.5. These hubs and nodes are not all of the found significant elements. For full list, please look up the relevant section of the supplemental appendix.

4.12.3. The intersection of BMS-536924 and NVP-ADW742

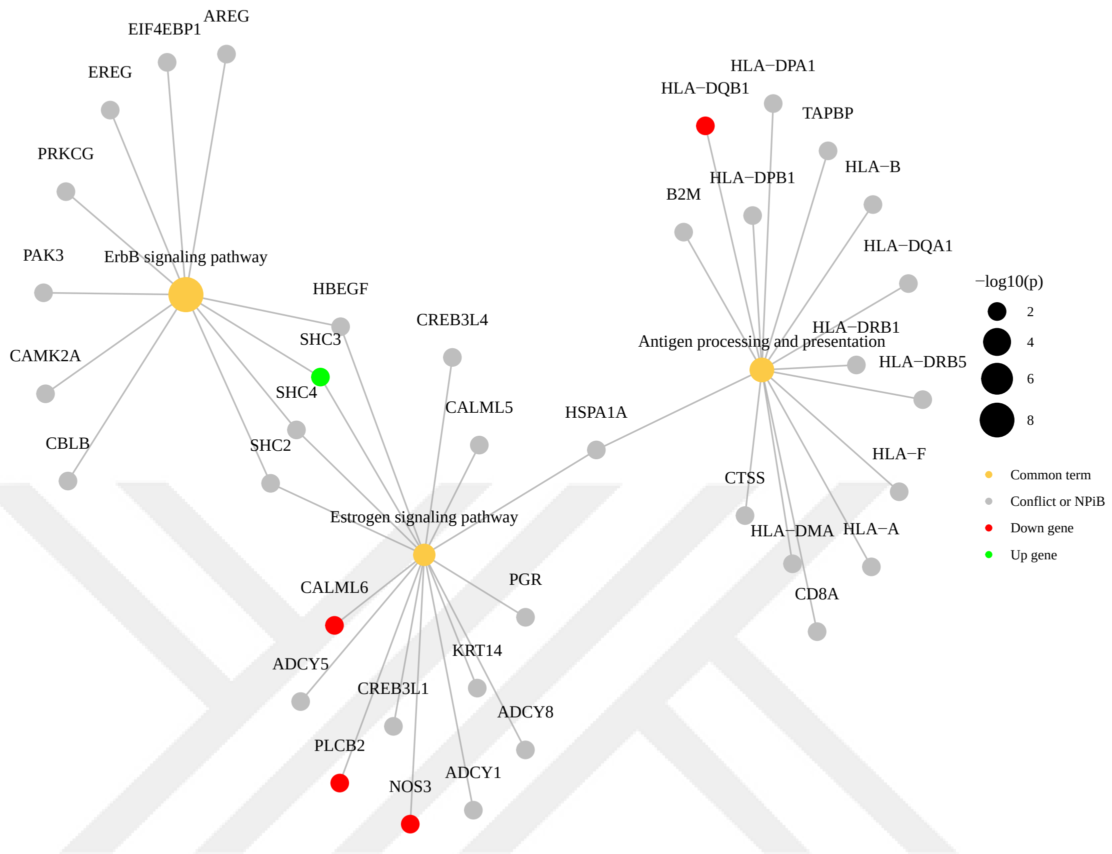

Figure 40: Intersection of most enriched pathways from the determined DEGs of BMS-536924 and NVP-ADW742 differential expression analysis.

In this figure, the intersection of the most significant (combined p-value assessment by Fisher's method, p-value ≤ 0.05) commonly enriched KEGG pathways are visualized as yellow hubs. The nodes are representing commonly upregulated DEGs (green), commonly down-regulated DEGs (red), and "conflict or NPiB (Not Present in Both)" DEGs (grey) which were involved in the enrichment of the connected pathway hub. Preferred DEG cutoff of false discovery rate (FDR) < 0.05 and absolute fold change ≥ 1.5. The size of the hubs is reversely proportional with their respective combined p-values for the commonly enriched pathways in the comparison of the two above mentioned drug comparisons.

4.13. Mitosis Targeting Drugs

There are 6 drugs that target mitosis regulation among the curated 52 drugs of this study. The following results are interpretations of the detailed gene expression profile of sensitive TNBC cells versus resistant TNBC cells to those 6 drugs.

4.13.1. Alisertib results

Differential expression analysis results yielded 839 DEGs in the comparison of Alisertib sensitive 7 TNBC cell lines versus resistant 10 cell lines. Active sub-network based pathway enrichment analysis found 47 enriched KEGG pathways. The most significantly enriched 10 pathways and included DEGs are visualized in **Figure 41**.

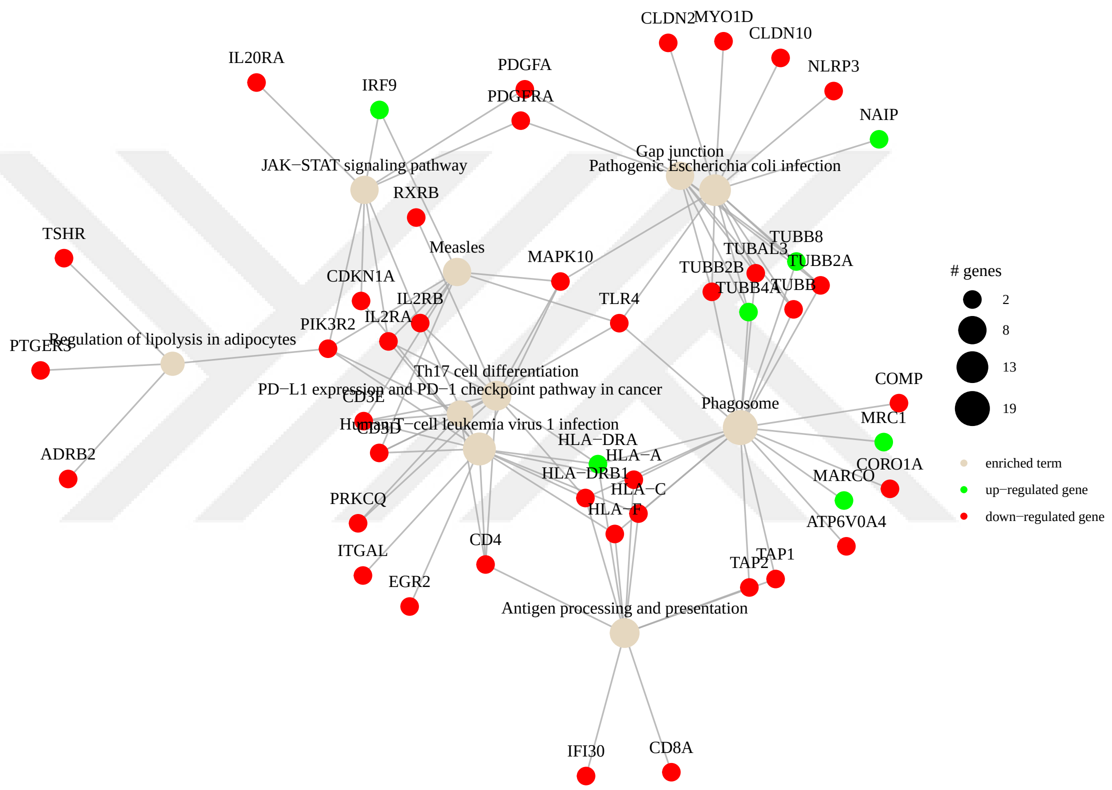

Figure 41: Reduced network of most enriched pathways for the sensitive TNBC cells versus resistant TNBC cells to Alisertib.

In this figure significantly enriched top10 KEGG pathways are visualized as gray hubs (p-value < 0.05). Nodes are representing either upregulated DEGs (green) or down-regulated DEGs (red) which were involved in the enrichment of the connected hub pathway. Preferred DEG cutoff of false discovery rate (FDR) < 0.05 and $\log_2$ absolute fold change ≥ 1.5. These hubs and nodes are not all of the found significant elements. For full list, please look up the relevant section of the supplemental appendix.

4.13.2. Paclitaxel results

Differential expression analysis results yielded 763 DEGs in the comparison of Paclitaxel sensitive 11 TNBC cell lines versus resistant 6 cell lines. Active sub-network based pathway enrichment analysis found 46 enriched KEGG pathways. The most significantly enriched 10 pathways and included DEGs are visualized in **Figure 42**.

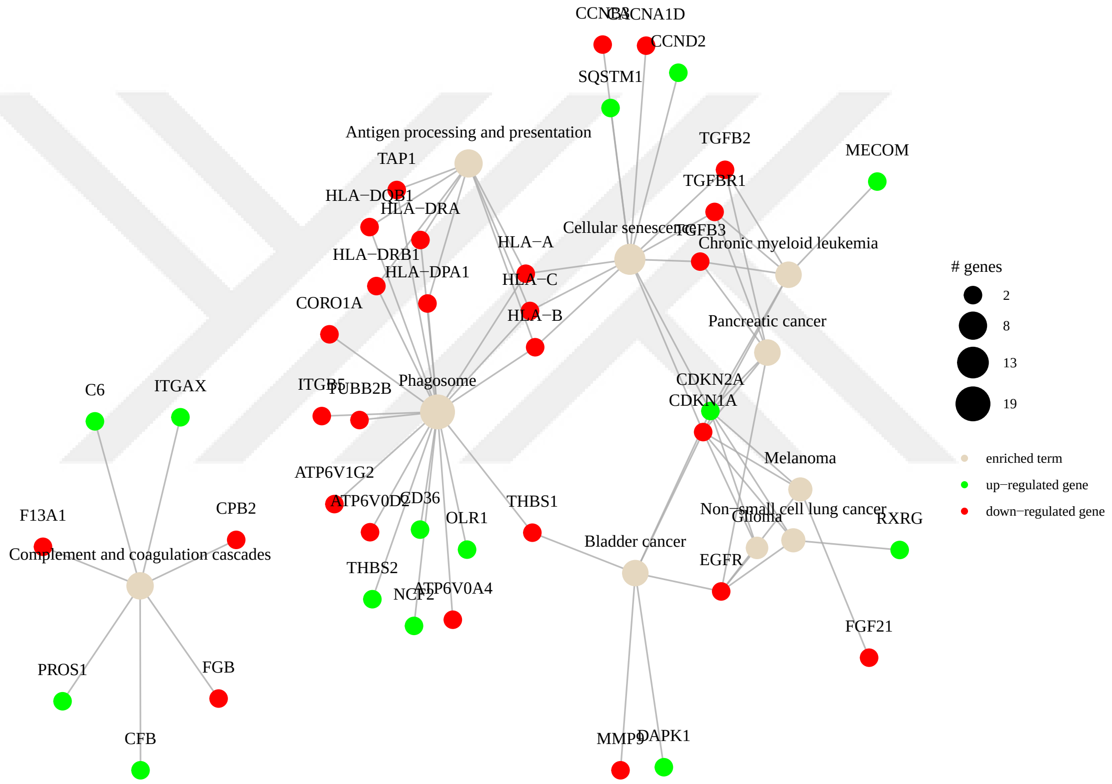

Figure 42: Reduced network of most enriched pathways for the sensitive TNBC cells versus resistant TNBC cells to Paclitaxel.

In this figure significantly enriched top10 KEGG pathways are visualized as gray hubs (p-value < 0.05). Nodes are representing either upregulated DEGs (green) or down-regulated DEGs (red) which were involved in the enrichment of the connected hub pathway. Preferred DEG cutoff of false discovery rate (FDR) < 0.05 and $\log_2$ absolute fold change ≥ 1.5. These hubs and nodes are not all of the found significant elements. For full list, please look up the relevant section of the supplemental appendix.

4.13.3. Tozasertib results

Differential expression analysis results yielded 1166 DEGs in the comparison of Tozasertib sensitive 4 TNBC cell lines versus resistant 13 cell lines. Active sub-network based pathway enrichment analysis found 92 enriched KEGG pathways. The most significantly enriched 10 pathways and included DEGs are visualized in.

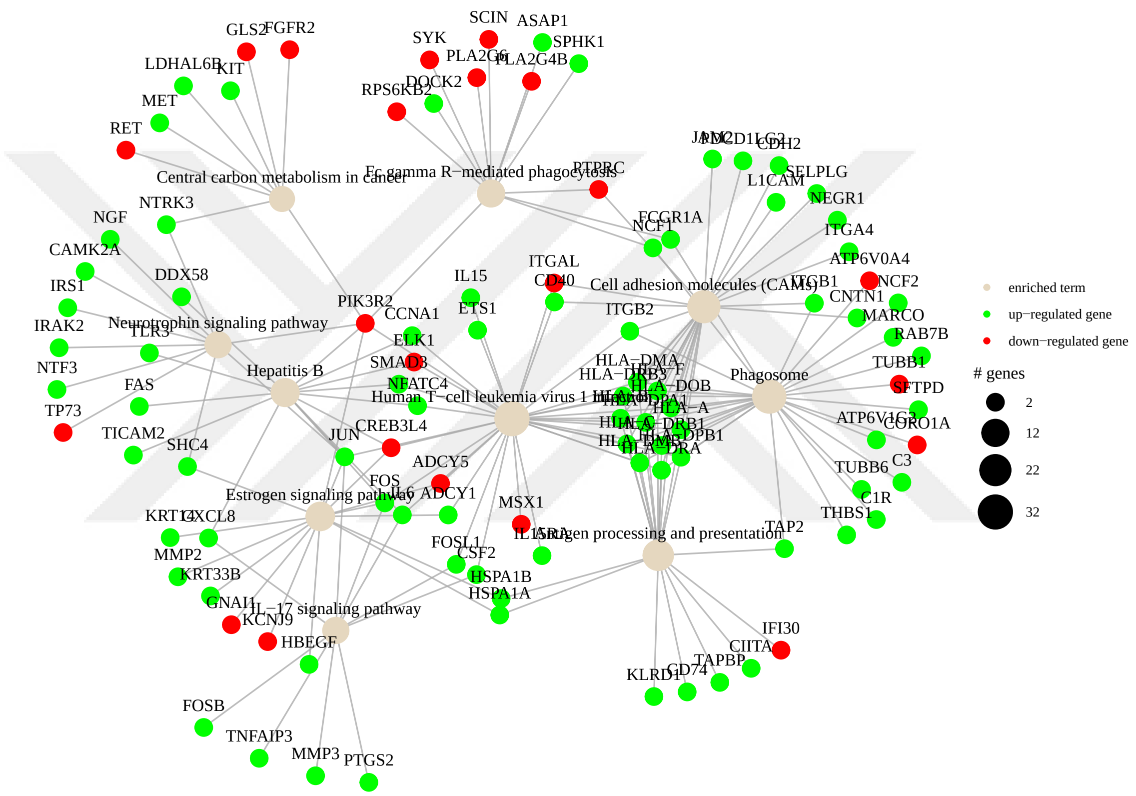

Figure 43: Reduced network of most enriched pathways for the sensitive TNBC cells versus resistant TNBC cells to Tozasertib.

In this figure significantly enriched top10 KEGG pathways are visualized as gray hubs (p-value < 0.05). Nodes are representing either upregulated DEGs (green) or down-regulated DEGs (red) which were involved in the enrichment of the connected hub pathway. Preferred DEG cutoff of false discovery rate (FDR) < 0.05 and $\log_2$ absolute fold change ≥ 1.5. These hubs and nodes are not all of the found significant elements. For full list, please look up the relevant section of the supplemental appendix.

4.13.4. Vinblastine results

Differential expression analysis results yielded 464 DEGs in the comparison of Vinblastine sensitive 9 TNBC cell lines versus resistant 8 cell lines. Active sub-network based pathway enrichment analysis found 11 enriched KEGG pathways. The most significantly enriched 10 pathways and included DEGs are visualized in **Figure 44**.

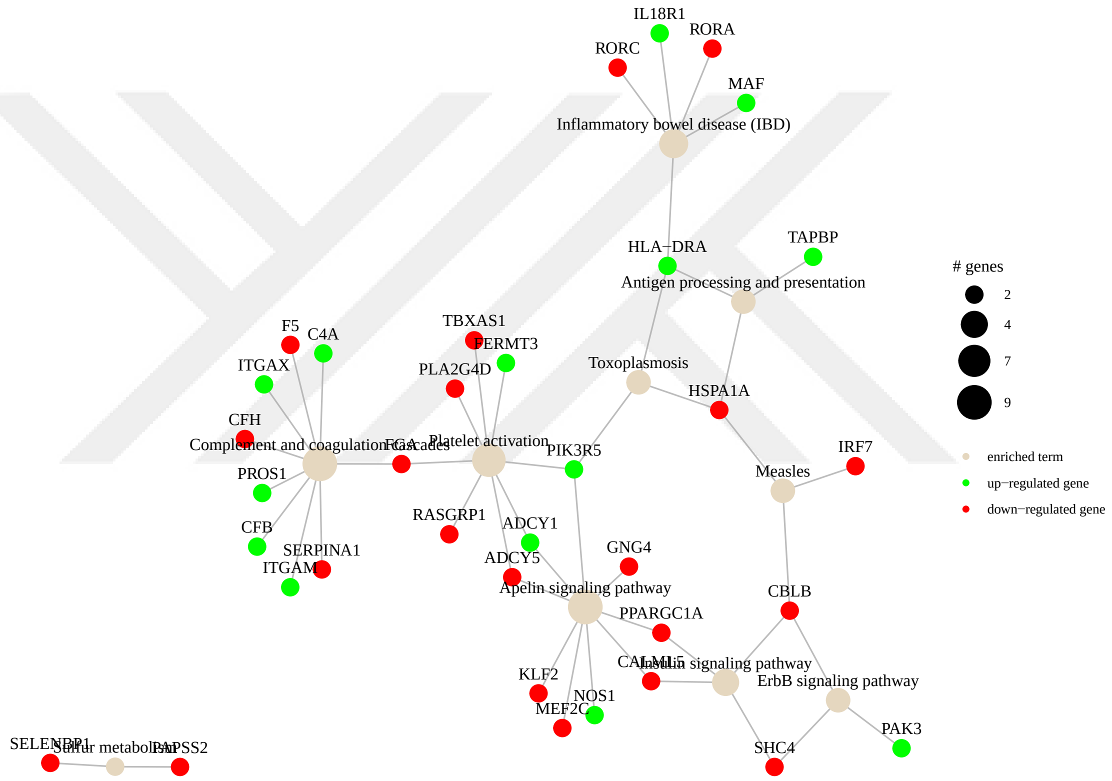

Figure 44: Reduced network of most enriched pathways for the sensitive TNBC cells versus resistant TNBC cells to Vinblastine.

In this figure significantly enriched top10 KEGG pathways are visualized as gray hubs (p-value < 0.05). Nodes are representing either upregulated DEGs (green) or down-regulated DEGs (red) which were involved in the enrichment of the connected hub pathway. Preferred DEG cutoff of false discovery rate (FDR) < 0.05 and $\log_2$ absolute fold change ≥ 1.5. These hubs and nodes are not all of the found significant elements. For full list, please look up the relevant section of the supplemental appendix.

4.13.5. Vinorelbine results

Differential expression analysis results yielded 514 DEGs in the comparison of Vinorelbine sensitive 9 TNBC cell lines versus resistant 8 cell lines. Active sub-network based pathway enrichment analysis found 4 enriched KEGG pathways. The significantly enriched pathways and included DEGs are visualized in **Figure 45**.

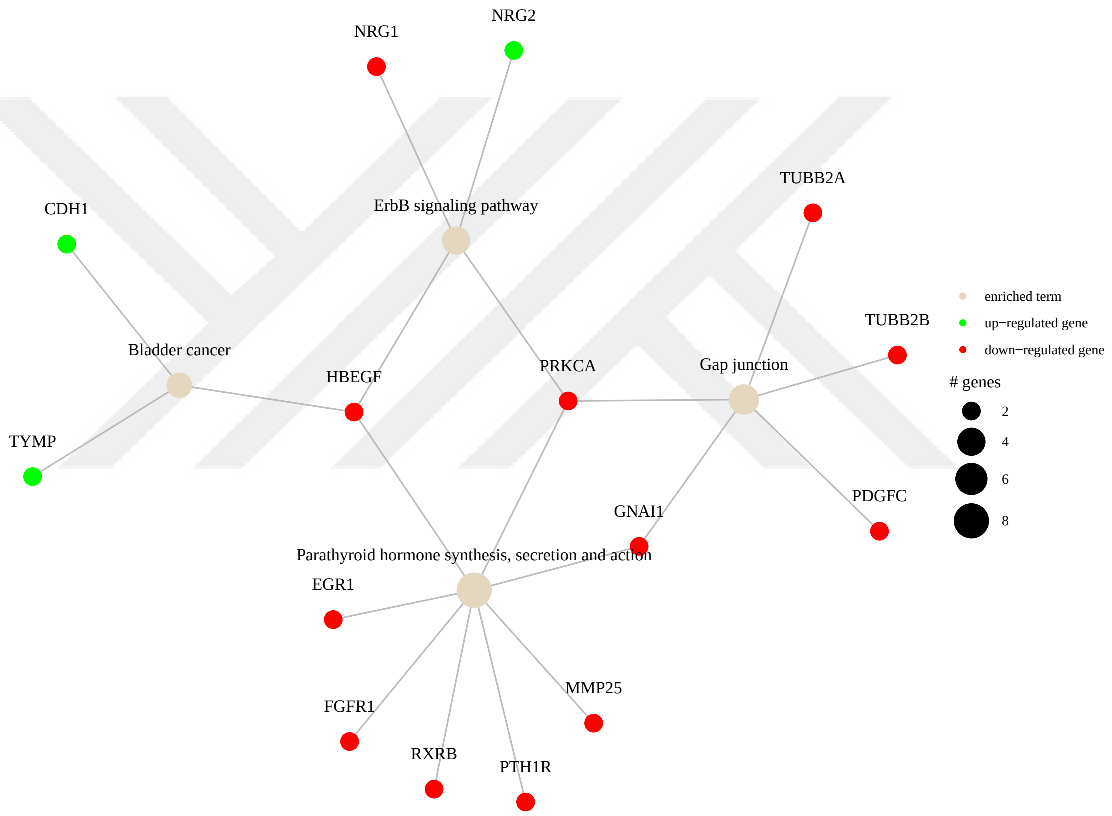

Figure 45: Network of most enriched pathways for the sensitive TNBC cells versus resistant TNBC cells to Vinorelbine.

In this figure significantly enriched KEGG pathways are visualized as gray hubs (p-value < 0.05). Nodes are representing either upregulated DEGs (green) or down-regulated DEGs (red) which were involved in the enrichment of the connected hub pathway. Preferred DEG cutoff of false discovery rate (FDR) < 0.05 and $\log_2$ absolute fold change ≥ 1.5. These hubs and/or nodes are not all of the found significant elements. For full list, please look up the relevant section of the supplemental appendix.

4.13.6. ZM447439 results

Differential expression analysis results yielded 768 DEGs in the comparison of ZM447439 sensitive 4 TNBC cell lines versus resistant 13 cell lines. Active sub-network based pathway enrichment analysis found 47 enriched KEGG pathways. The most significantly enriched 10 pathways and included DEGs are visualized in **Figure 46**.

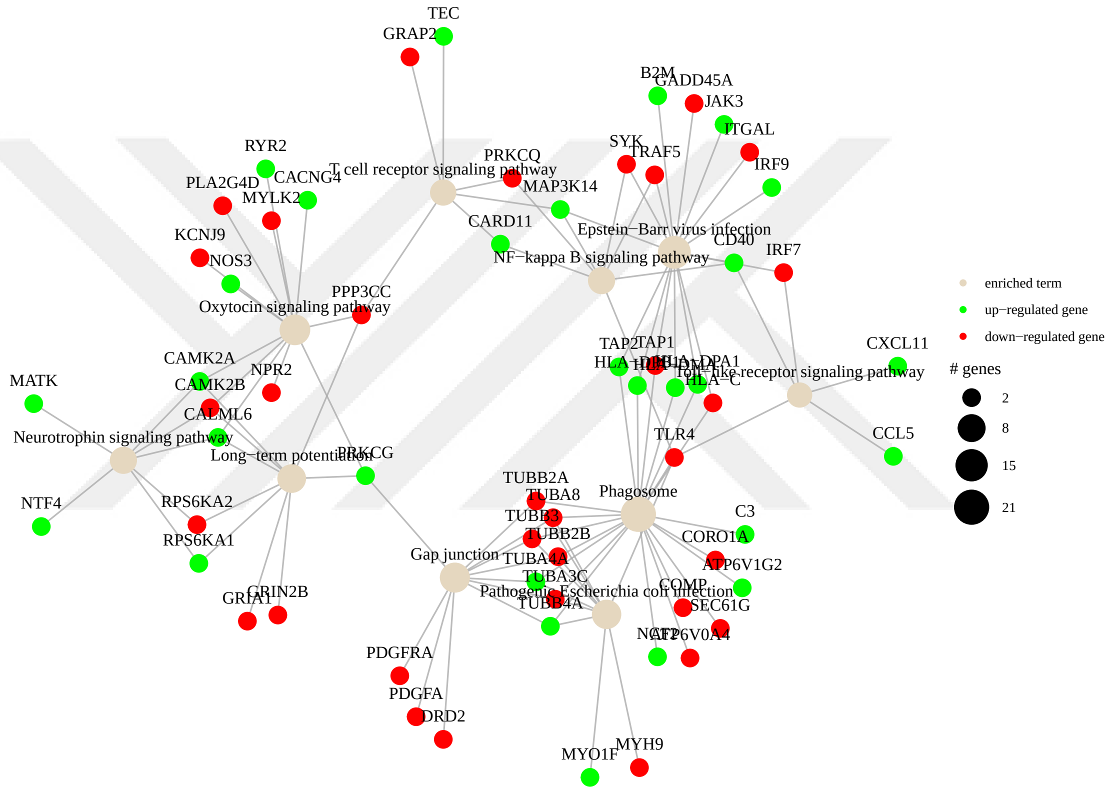

Figure 46: Reduced network of most enriched pathways for the sensitive TNBC cells versus resistant TNBC cells to ZM447439.

In this figure significantly enriched top10 KEGG pathways are visualized as gray hubs (p-value < 0.05). Nodes are representing either upregulated DEGs (green) or down-regulated DEGs (red) which were involved in the enrichment of the connected hub pathway. Preferred DEG cutoff of false discovery rate (FDR) < 0.05 and $\log_2$ absolute fold change ≥ 1.5. These hubs and nodes are not all of the found significant elements. For full list, please look up the relevant section of the supplemental appendix.

4.13.7. The intersection of Alisertib and Tozasertib

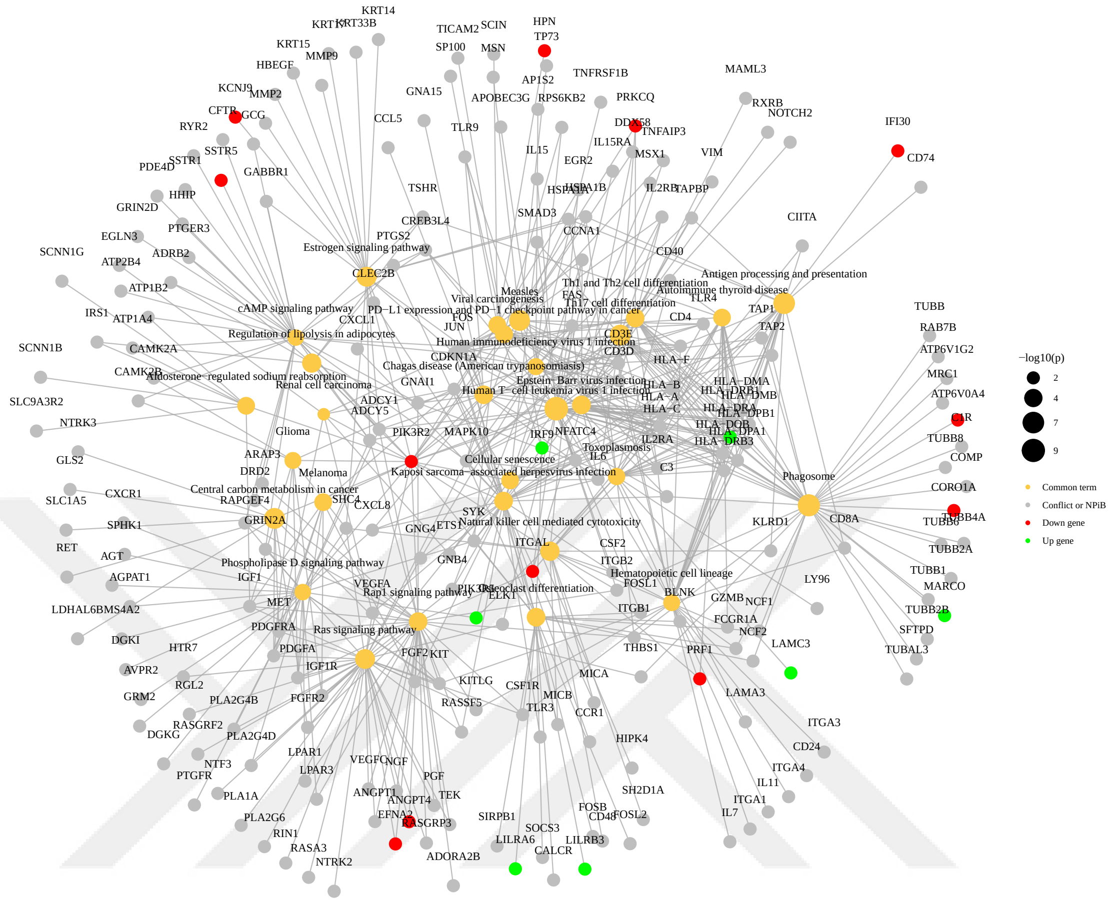

Figure 47: Intersection of most enriched pathways from the determined DEGs of Alisertib and Tozasertib differential expression analysis.

In this figure, the intersection of the most significant (combined p-value assessment by Fisher's method, p-value ≤ 0.05) commonly enriched KEGG pathways are visualized as yellow hubs. The nodes are representing commonly upregulated DEGs (green), commonly down-regulated DEGs (red), and "conflict or NPiB (Not Present in Both)" DEGs (grey) which were involved in the enrichment of the connected pathway hub. Preferred DEG cutoff of false discovery rate (FDR) < 0.05 and absolute fold change ≥ 1.5. The size of the hubs is reversely proportional with their respective combined p-values for the commonly enriched pathways in the comparison of the two above mentioned drug comparisons.

4.14. PI3K/mTOR Signaling Targeting Drugs

9 drugs target PI3K/mTOR signaling pathway among the curated 52 drugs. The following results are interpretations of the detailed gene expression profile of sensitive TNBC cells versus resistant TNBC cells to those 9 drugs.

4.14.1. Afuresertib results

Differential expression analysis results yielded 416 DEGs in the comparison of Afuresertib sensitive 8 TNBC cell lines versus resistant 9 cell lines. Active sub-network based pathway enrichment analysis found 9 enriched KEGG pathways. The significantly enriched pathways and included DEGs are visualized in **Figure 48**.

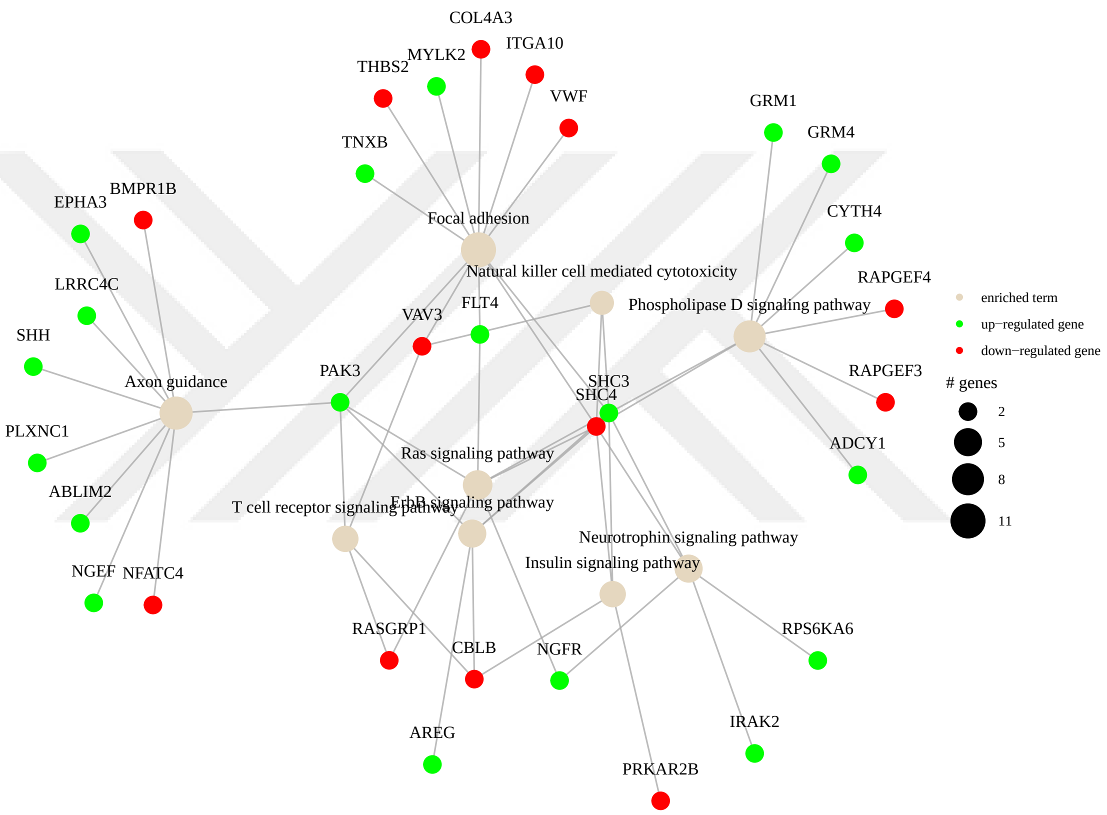

Figure 48: Network of most enriched pathways for the sensitive TNBC cells versus resistant TNBC cells to Afuresertib.

In this figure significantly enriched KEGG pathways are visualized as gray hubs (p-value < 0.05). Nodes are representing either upregulated DEGs (green) or down-regulated DEGs (red) which were involved in the enrichment of the connected hub pathway. Preferred DEG cutoff of false discovery rate (FDR) < 0.05 and $\log_2$ absolute fold change ≥ 1.5. These hubs and/or nodes are not all of the found significant elements. For full list, please look up the relevant section of the supplemental appendix.

4.14.2. AT13148 results

Differential expression analysis results yielded 768 DEGs in the comparison of AT13148 sensitive 3 TNBC cell lines versus resistant 14 cell lines. Active sub-network based pathway enrichment analysis found 33 enriched KEGG pathways. The most significantly enriched 10 pathways and included DEGs are visualized in **Figure 49**.

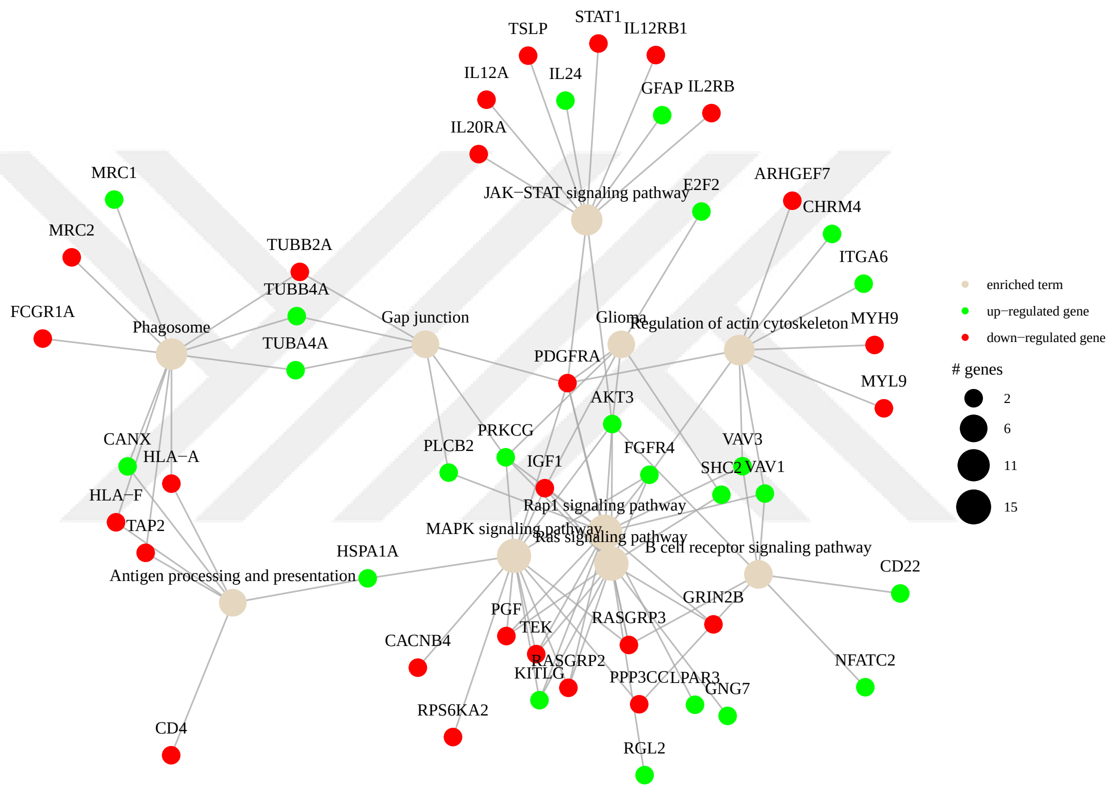

Figure 49: Reduced network of most enriched pathways for the sensitive TNBC cells versus resistant TNBC cells to AT13148.

In this figure significantly enriched top10 KEGG pathways are visualized as gray hubs (p-value < 0.05). Nodes are representing either upregulated DEGs (green) or down-regulated DEGs (red) which were involved in the enrichment of the connected hub pathway. Preferred DEG cutoff of false discovery rate (FDR) < 0.05 and $\log_2$ absolute fold change $\geq$ 1.5. These hubs and nodes are not all of the found significant elements. For full list, please look up the relevant section of the supplemental appendix.

4.14.3. AZD6482 results

Differential expression analysis results yielded 451 DEGs in the comparison of AZD6482 sensitive 3 TNBC cell lines versus resistant 14 cell lines. Active sub-network based pathway enrichment analysis found 33 enriched KEGG pathways. The significantly enriched pathways and included DEGs are visualized in **Figure 50**.

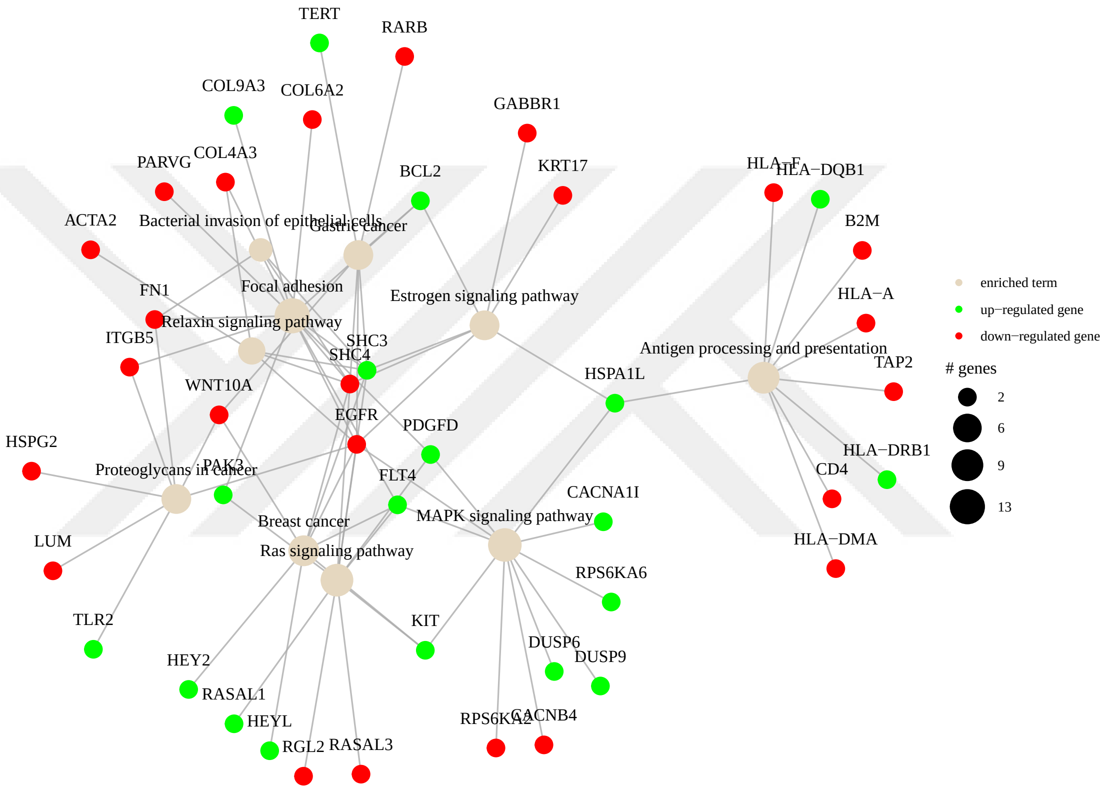

Figure 50: Reduced network of most enriched pathways for the sensitive TNBC cells versus resistant TNBC cells to AZD6482.

In this figure significantly enriched top10 KEGG pathways are visualized as gray hubs (p-value < 0.05). Nodes are representing either upregulated DEGs (green) or down-regulated DEGs (red) which were involved in the enrichment of the connected hub pathway. Preferred DEG cutoff of false discovery rate (FDR) < 0.05 and $\log_2$ absolute fold change $\geq$ 1.5. These hubs and nodes are not all of the found significant elements. For full list, please look up the relevant section of the supplemental appendix.

4.14.4. AZD8055 results

Differential expression analysis results yielded 872 DEGs in the comparison of AZD8055 sensitive 10 TNBC cell lines versus resistant 7 cell lines. Active sub-network based pathway enrichment analysis found 36 enriched KEGG pathways. The most significantly enriched 10 pathways and included DEGs are visualized in **Figure 51**.

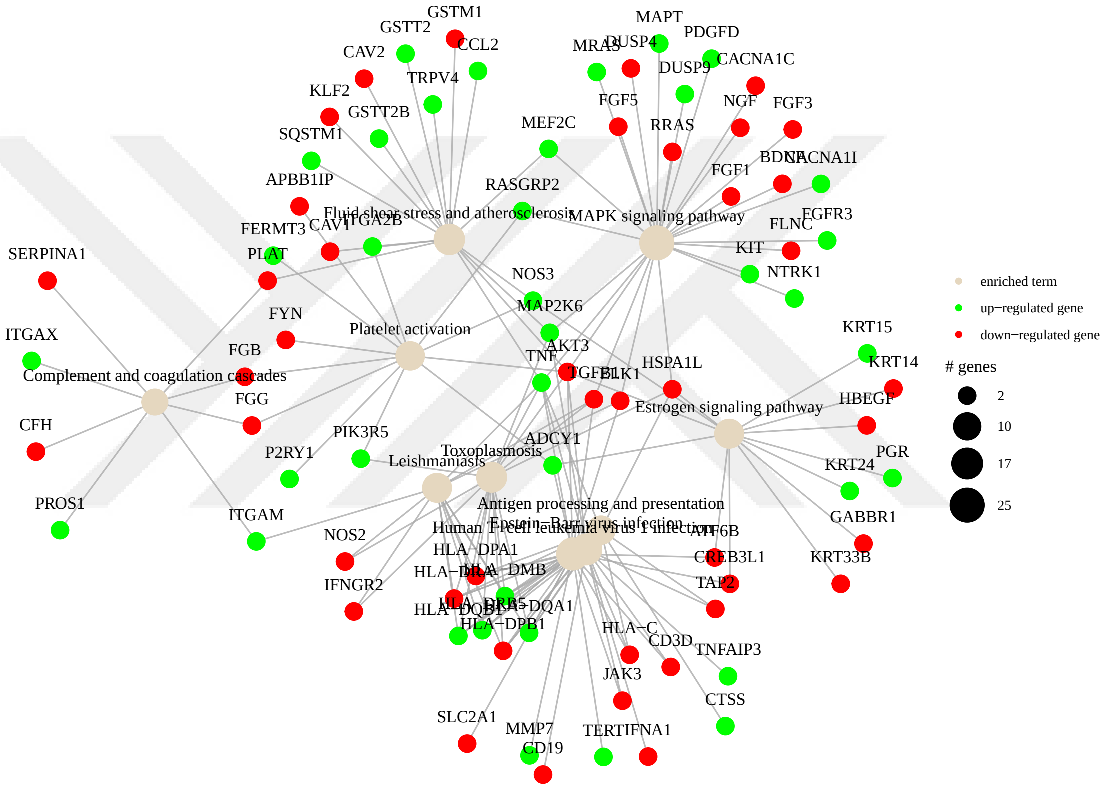

Figure 51: Reduced network of most enriched pathways for the sensitive TNBC cells versus resistant TNBC cells to AZD8055.

In this figure significantly enriched top10 KEGG pathways are visualized as gray hubs (p-value < 0.05). Nodes are representing either upregulated DEGs (green) or down-regulated DEGs (red) which were involved in the enrichment of the connected hub pathway. Preferred DEG cutoff of false discovery rate (FDR) < 0.05 and $\log_2$ absolute fold change ≥ 1.5. These hubs and nodes are not all of the found significant elements. For full list, please look up the relevant section of the supplemental appendix.

4.14.5. AZD8186 results

Differential expression analysis results yielded 486 DEGs in the comparison of AZD8186 sensitive 6 TNBC cell lines versus resistant 11 cell lines. Active sub-network based pathway enrichment analysis found 42 enriched KEGG pathways. The most significantly enriched 10 pathways and included DEGs are visualized in **Figure 52**.

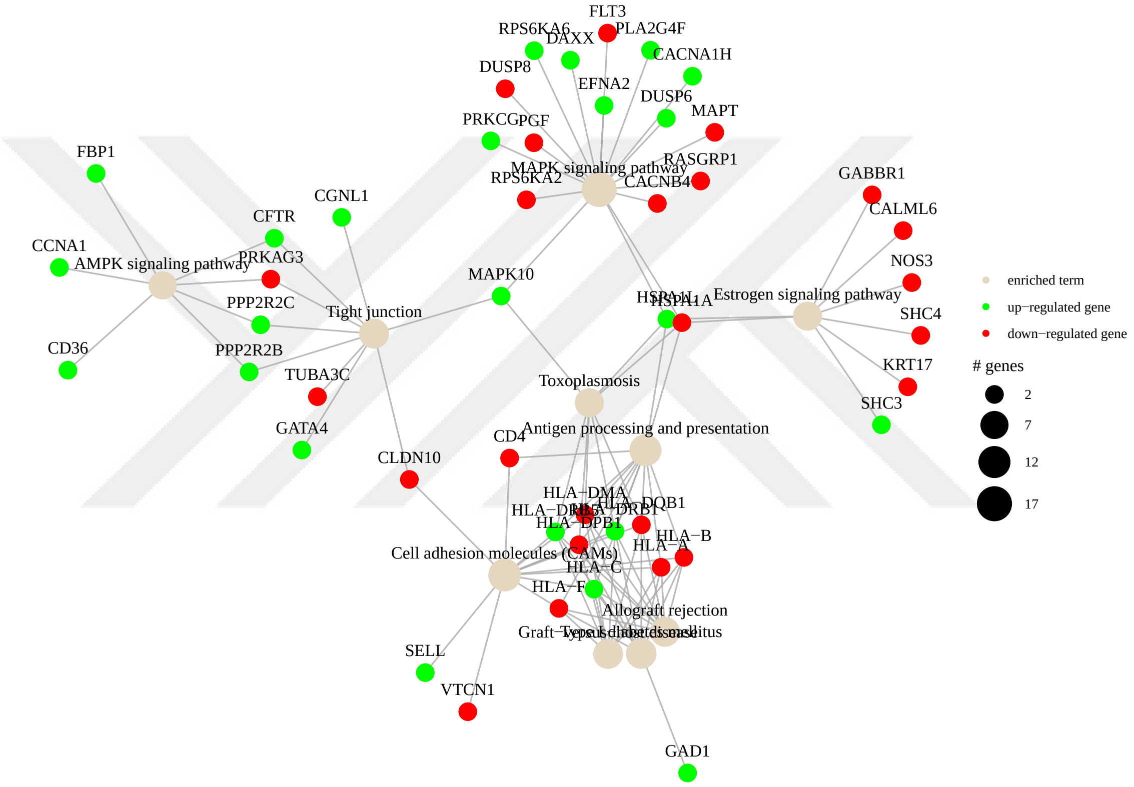

Figure 52: Reduced network of most enriched pathways for the sensitive TNBC cells versus resistant TNBC cells to AZD8186.

In this figure significantly enriched top10 KEGG pathways are visualized as gray hubs (p-value < 0.05). Nodes are representing either upregulated DEGs (green) or down-regulated DEGs (red) which were involved in the enrichment of the connected hub pathway. Preferred DEG cutoff of false discovery rate (FDR) < 0.05 and $\log_2$ absolute fold change ≥ 1.5. These hubs and nodes are not all of the found significant elements. For full list, please look up the relevant section of the supplemental appendix.

4.14.6. Dactolisib results

Differential expression analysis results yielded 620 DEGs in the comparison of Dactolisib sensitive 12 TNBC cell lines versus resistant 5 cell lines. Active sub-network based pathway enrichment analysis found 65 enriched KEGG pathways. The most significantly enriched 10 pathways and included DEGs are visualized in **Figure 53**.

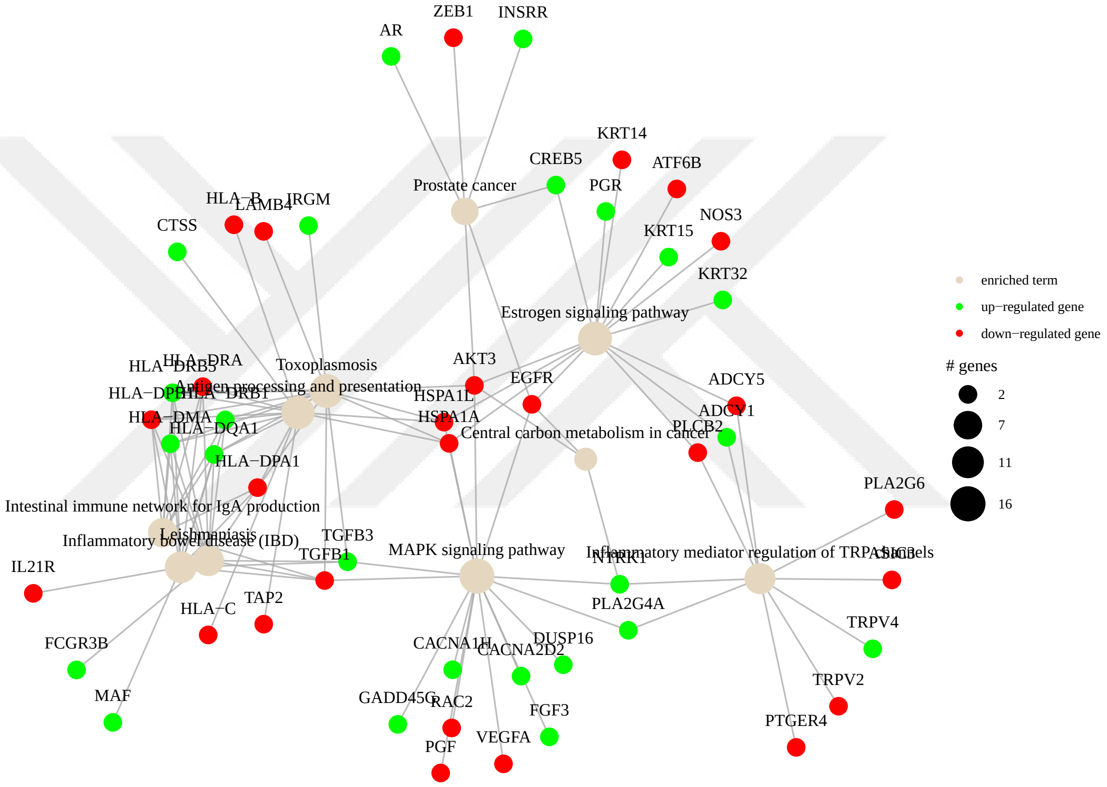

Figure 53: Reduced network of most enriched pathways for the sensitive TNBC cells versus resistant TNBC cells to Dactolisib.

In this figure significantly enriched top10 KEGG pathways are visualized as gray hubs (p-value < 0.05). Nodes are representing either upregulated DEGs (green) or down-regulated DEGs (red) which were involved in the enrichment of the connected hub pathway. Preferred DEG cutoff of false discovery rate (FDR) < 0.05 and $\log_2$ absolute fold change ≥ 1.5. These hubs and nodes are not all of the found significant elements. For full list, please look up the relevant section of the supplemental appendix.

4.14.7. Ipatasertib results

Differential expression analysis results yielded 752 DEGs in the comparison of Ipatasertib sensitive 6 TNBC cell lines versus resistant 11 cell lines. Active sub-network based pathway enrichment analysis found 26 enriched KEGG pathways. The most significantly enriched 10 pathways and included DEGs are visualized in **Figure 54**.

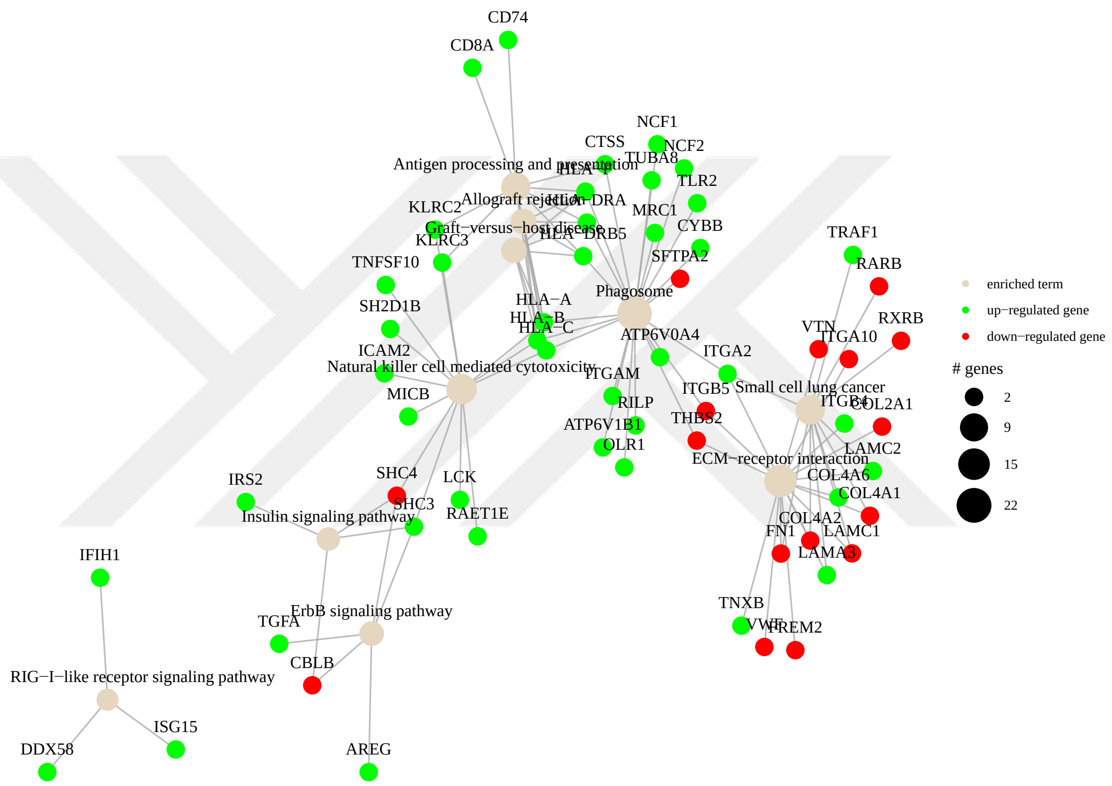

Figure 54: Reduced network of most enriched pathways for the sensitive TNBC cells versus resistant TNBC cells to Ipatasertib.

In this figure significantly enriched top10 KEGG pathways are visualized as gray hubs (p-value < 0.05). Nodes are representing either upregulated DEGs (green) or down-regulated DEGs (red) which were involved in the enrichment of the connected hub pathway. Preferred DEG cutoff of false discovery rate (FDR) < 0.05 and $\log_2$ absolute fold change ≥ 1.5. These hubs and nodes are not all of the found significant elements. For full list, please look up the relevant section of the supplemental appendix.

4.14.8. MK-2206 results

Differential expression analysis results yielded 920 DEGs in the comparison of MK-2206 sensitive 6 TNBC cell lines versus resistant 11 cell lines. Active sub-network based pathway enrichment analysis found 32 enriched KEGG pathways. The most significantly enriched 10 pathways and included DEGs are visualized in **Figure 55**.

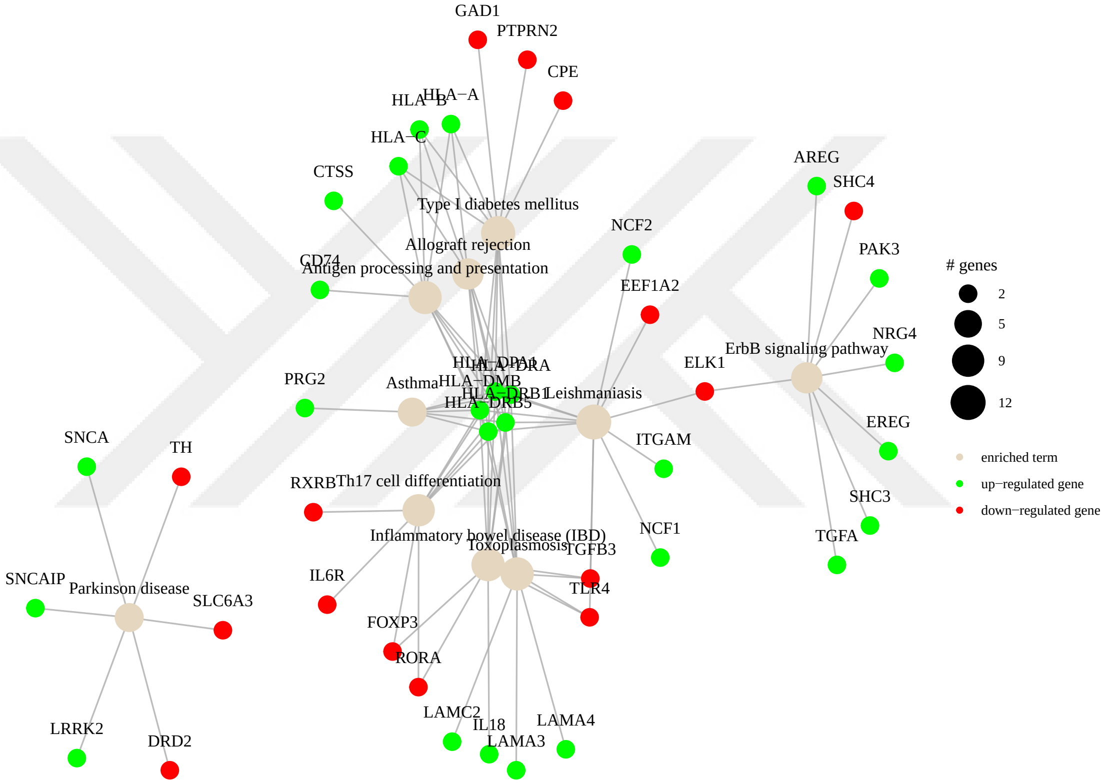

Figure 55: Reduced network of most enriched pathways for the sensitive TNBC cells versus resistant TNBC cells to MK-2206.

In this figure significantly enriched top10 KEGG pathways are visualized as gray hubs (p-value < 0.05). Nodes are representing either upregulated DEGs (green) or down-regulated DEGs (red) which were involved in the enrichment of the connected hub pathway. Preferred DEG cutoff of false discovery rate (FDR) < 0.05 and $\log_2$ absolute fold change ≥ 1.5. These hubs and nodes are not all of the found significant elements. For full list, please look up the relevant section of the supplemental appendix.

4.14.9. OSI-027 results

Differential expression analysis results yielded 703 DEGs in the comparison of OSI-027 sensitive 14 TNBC cell lines versus resistant 3 cell lines. Active sub-network based pathway enrichment analysis found 22 enriched KEGG pathways. The most significantly enriched 10 pathways and included DEGs are visualized in **Figure 56**.

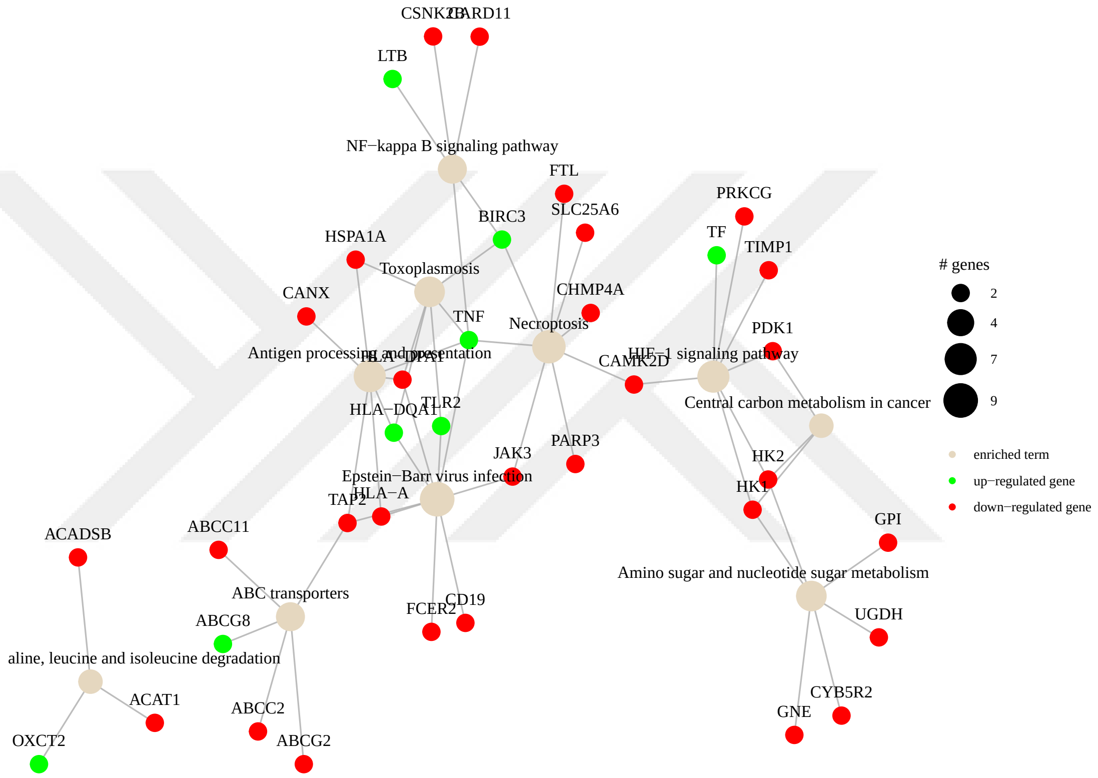

Figure 56: Reduced network of most enriched pathways for the sensitive TNBC cells versus resistant TNBC cells to OSI-027.

In this figure significantly enriched top10 KEGG pathways are visualized as gray hubs (p-value < 0.05). Nodes are representing either upregulated DEGs (green) or down-regulated DEGs (red) which were involved in the enrichment of the connected hub pathway. Preferred DEG cutoff of false discovery rate (FDR) < 0.05 and $\log_2$ absolute fold change ≥ 1.5. These hubs and nodes are not all of the found significant elements. For full list, please look up the relevant section of the supplemental appendix.

4.14.10. Taselisib results

Differential expression analysis results yielded 786 DEGs in the comparison of Taselisib sensitive 10TNBC cell lines versus resistant 7 cell lines. Active sub-network based pathway enrichment analysis found 24 enriched KEGG pathways. The most significantly enriched 10 pathways and included DEGs are visualized in **Figure 57**.

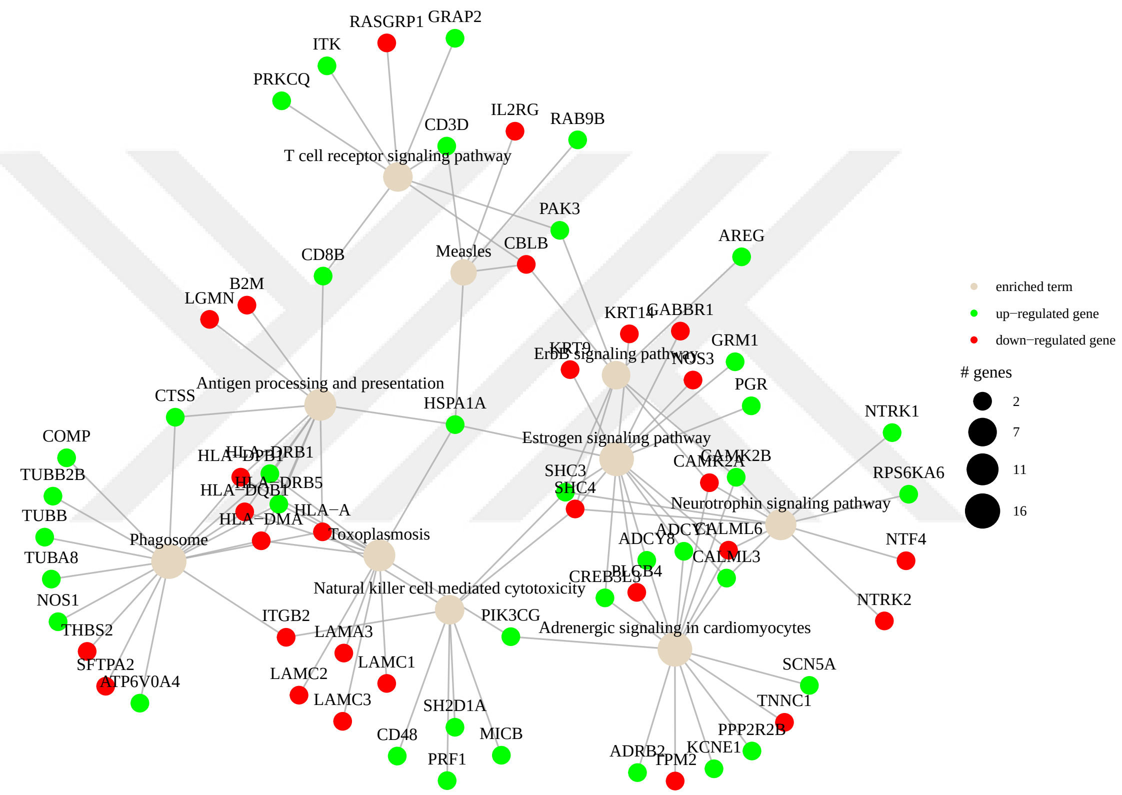

Figure 57: Reduced network of most enriched pathways for the sensitive TNBC cells versus resistant TNBC cells to Taselisib.

In this figure significantly enriched top10 KEGG pathways are visualized as gray hubs (p-value < 0.05). Nodes are representing either upregulated DEGs (green) or down-regulated DEGs (red) which were involved in the enrichment of the connected hub pathway. Preferred DEG cutoff of false discovery rate (FDR) < 0.05 and $\log_2$ absolute fold change ≥ 1.5. These hubs and nodes are not all of the found significant elements. For full list, please look up the relevant section of the supplemental appendix.

4.14.11. The intersection of AZD8186 and Dactolisib

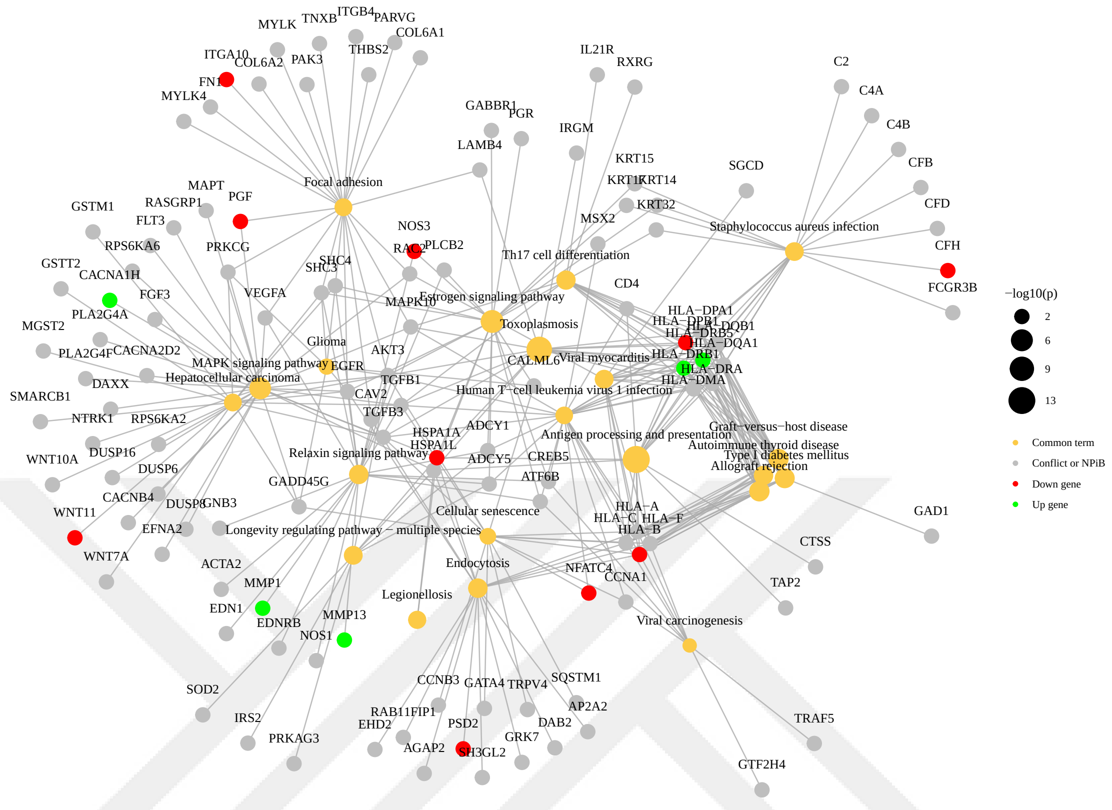

Figure 58: Intersection of most enriched pathways from the determined DEGs of AZD8186 and Dactolisib differential expression analysis.

In this figure, the intersection of the most significant (combined p-value assessment by Fisher's method, p-value ≤ 0.05) commonly enriched KEGG pathways are visualized as yellow hubs. The nodes are representing commonly upregulated DEGs (green), commonly down-regulated DEGs (red), and "conflict or NPiB (Not Present in Both)" DEGs (grey) which were involved in the enrichment of the connected pathway hub. Preferred DEG cutoff of false discovery rate (FDR) < 0.05 and absolute fold change ≥ 1.5. The size of the hubs is reversely proportional with their respective combined p-values for the commonly enriched pathways in the comparison of the two above mentioned drug comparisons.

4.15. RTK Signaling Targeting Drugs

There are 3 drugs that target RTK signaling pathway among the curated 52 drugs. The following results are interpretations of the detailed gene expression profile of sensitive TNBC cells versus resistant TNBC cells to those 3 drugs.

4.15.1. AZD4547 results

Differential expression analysis results yielded 757 DEGs in the comparison of AZD4547 sensitive 7 TNBC cell lines versus resistant 10 cell lines. Active sub-network based pathway enrichment analysis found 29 enriched KEGG pathways. The most significantly enriched 10 pathways and included DEGs are visualized in **Figure 59**.

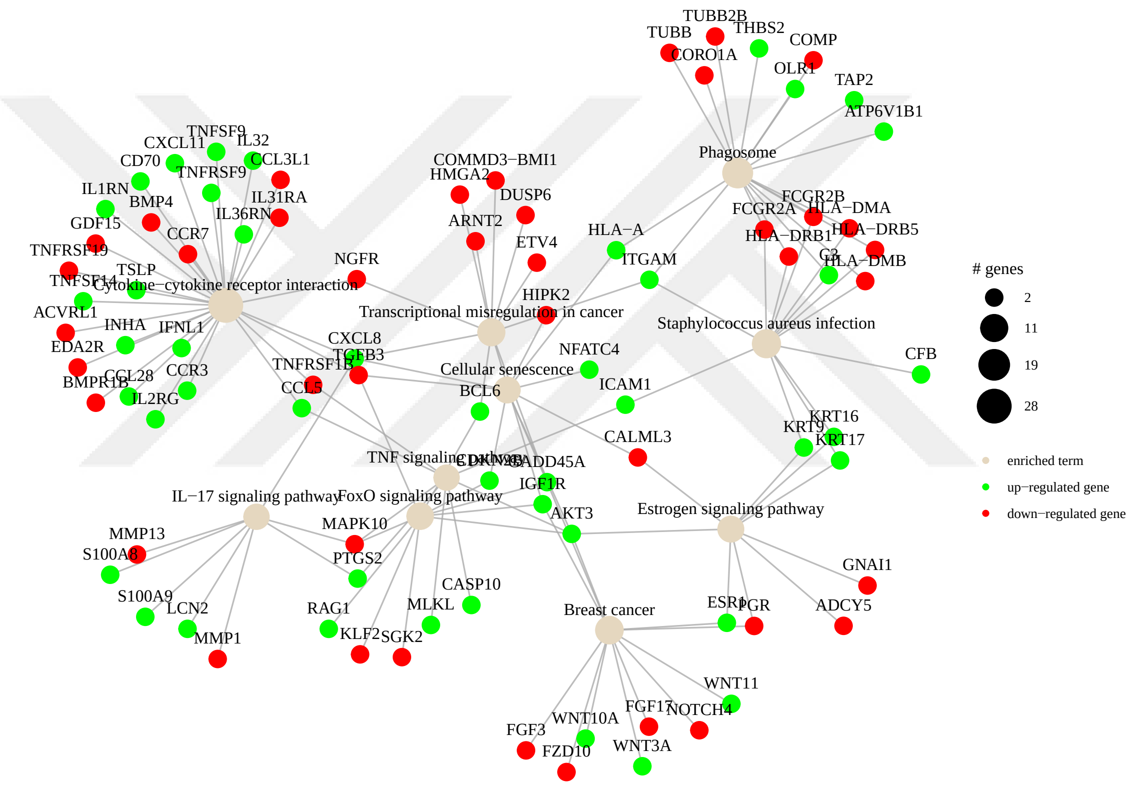

Figure 59: Reduced network of most enriched pathways for the sensitive TNBC cells versus resistant TNBC cells to AZD4547.

In this figure significantly enriched top10 KEGG pathways are visualized as gray hubs (p-value < 0.05). Nodes are representing either upregulated DEGs (green) or down-regulated DEGs (red) which were involved in the enrichment of the connected hub pathway. Preferred DEG cutoff of false discovery rate (FDR) < 0.05 and $\log_2$ absolute fold change $\geq$ 1.5. These hubs and nodes are not all of the found significant elements. For full list, please look up the relevant section of the supplemental appendix.

4.15.2. Cediranib results

Differential expression analysis results yielded 629 DEGs in the comparison of Cediranib sensitive 10 TNBC cell lines versus resistant 7 cell lines. Active sub-network based pathway enrichment analysis found 65 enriched KEGG pathways. The most significantly enriched 10 pathways and included DEGs are visualized in **Figure 60**.

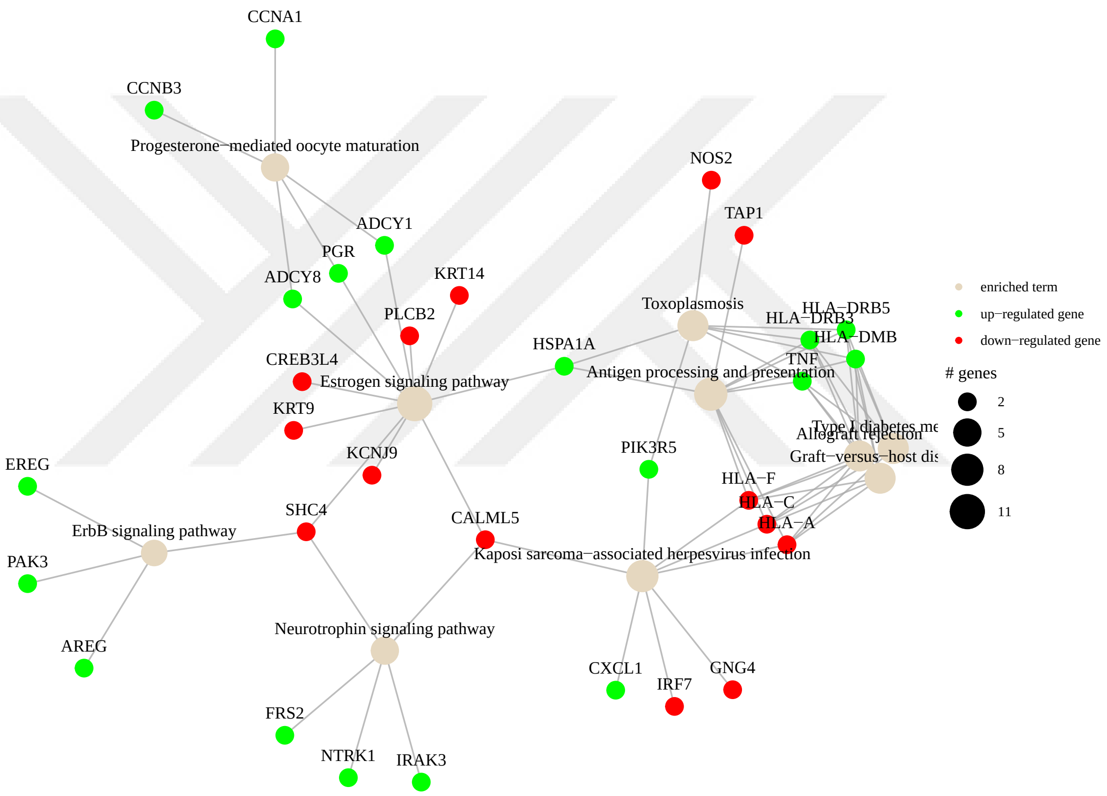

Figure 60: Reduced network of most enriched pathways for the sensitive TNBC cells versus resistant TNBC cells to Cediranib.

In this figure significantly enriched top10 KEGG pathways are visualized as gray hubs (p-value < 0.05). Nodes are representing either upregulated DEGs (green) or down-regulated DEGs (red) which were involved in the enrichment of the connected hub pathway. Preferred DEG cutoff of false discovery rate (FDR) < 0.05 and $\log_2$ absolute fold change ≥ 1.5. These hubs and nodes are not all of the found significant elements. For full list, please look up the relevant section of the supplemental appendix.

4.15.3. Crizotinib results

Differential expression analysis results yielded 839 DEGs in the comparison of Crizotinib sensitive 4 TNBC cell lines versus resistant 13 cell lines. Active sub-network based pathway enrichment analysis found 68 enriched KEGG pathways. The most significantly enriched 10 pathways and included DEGs are visualized in **Figure 61**.

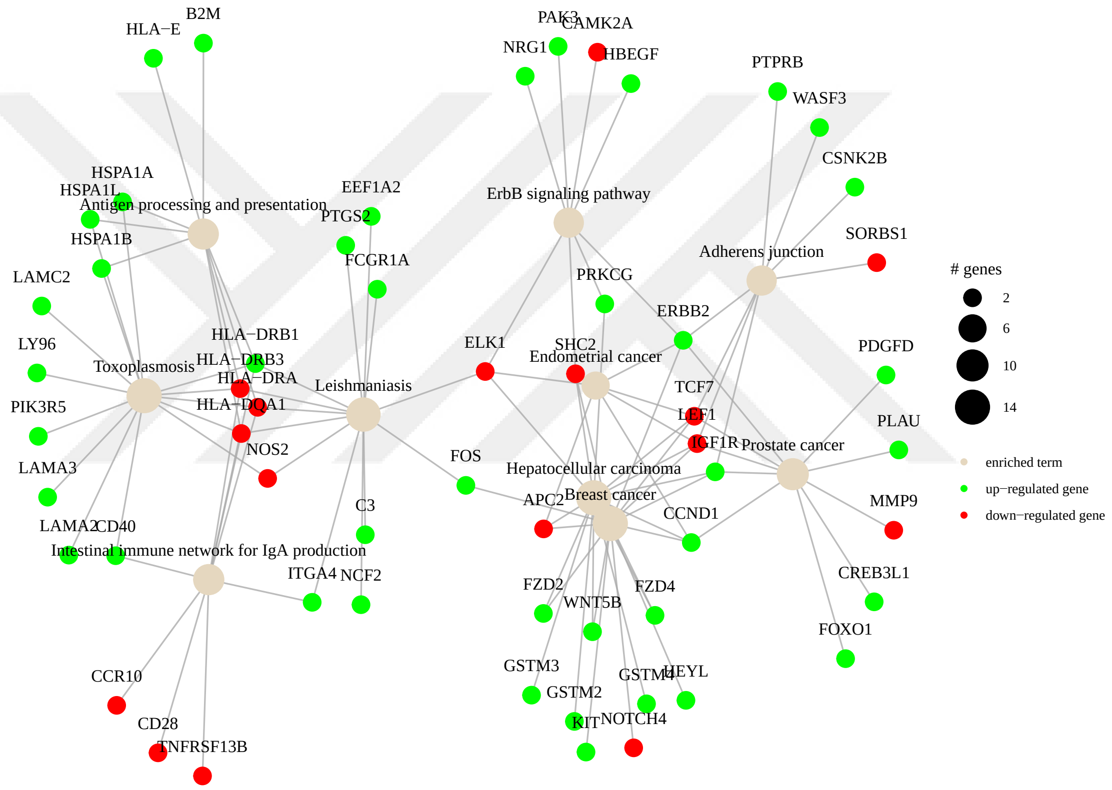

Figure 61: Reduced network of most enriched pathways for the sensitive TNBC cells versus resistant TNBC cells to Crizotinib.

In this figure significantly enriched top10 KEGG pathways are visualized as gray hubs (p-value < 0.05). Nodes are representing either upregulated DEGs (green) or down-regulated DEGs (red) which were involved in the enrichment of the connected hub pathway. Preferred DEG cutoff of false discovery rate (FDR) < 0.05 and $\log_2$ absolute fold change ≥ 1.5. These hubs and nodes are not all of the found significant elements. For full list, please look up the relevant section of the supplemental appendix.

4.15.4. The intersection of Crizotinib and AZD4547

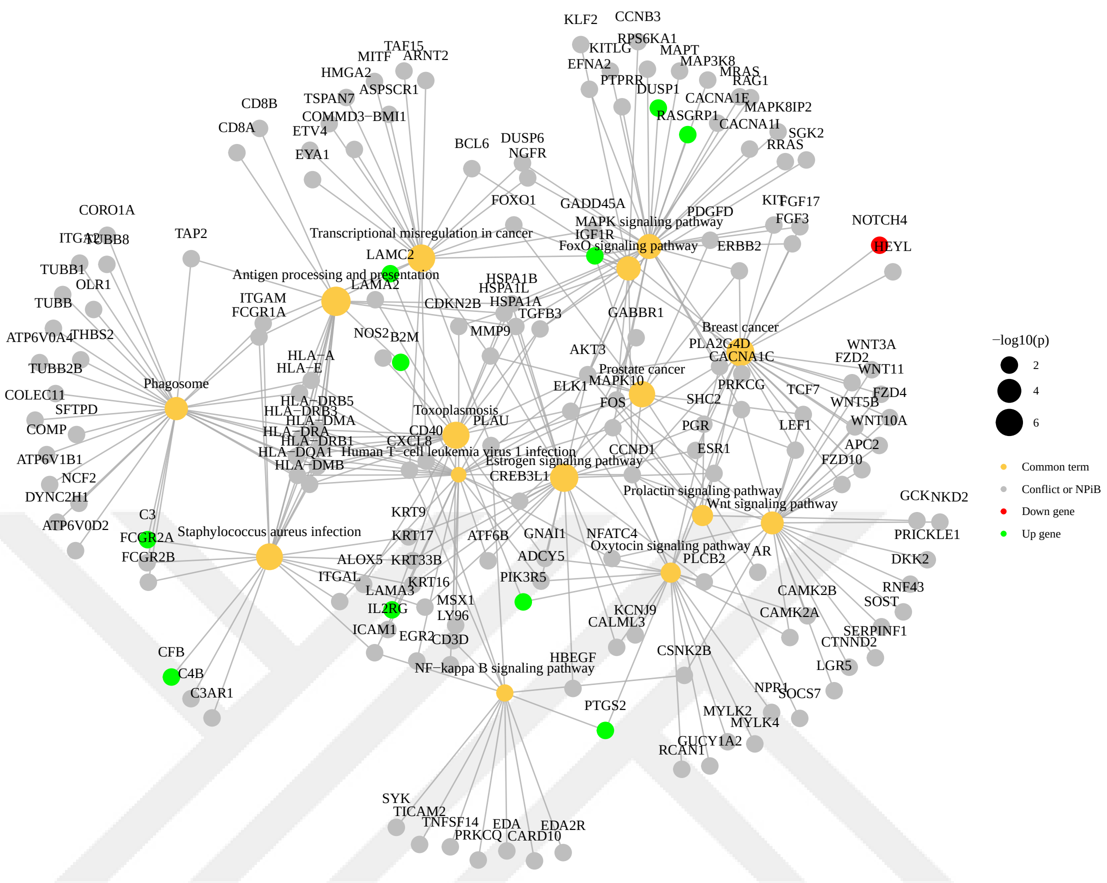

Figure 62: Intersection of most enriched pathways from the determined DEGs of Crizotinib and AZD4547 differential expression analysis.

In this figure, the intersection of the most significant (combined p-value assessment by Fisher's method, p-value ≤ 0.05) commonly enriched KEGG pathways are visualized as yellow hubs. The nodes are representing commonly upregulated DEGs (green), commonly down-regulated DEGs (red), and "conflict or NPiB (Not Present in Both)" DEGs (grey) which were involved in the enrichment of the connected pathway hub. Preferred DEG cutoff of false discovery rate (FDR) < 0.05 and absolute fold change ≥ 1.5. The size of the hubs is reversely proportional with their respective combined p-values for the commonly enriched pathways in the comparison of the two above mentioned drug comparisons.

4.16. Wnt Signaling Targeting Drugs

There are 2 drugs that target the Wnt signaling pathway among the curated 52 drugs. The following results are interpretations of the detailed gene expression profile of sensitive TNBC cells versus resistant TNBC cells to those 2 drugs.

4.16.1. AZ6102 results

Differential expression analysis results yielded 838 DEGs in the comparison of AZ6102 sensitive 6 TNBC cell lines versus resistant 11 cell lines. Active sub-network based pathway enrichment analysis found 48 enriched KEGG pathways. The most significantly enriched 10 pathways and included DEGs are visualized in **Figure 63**.

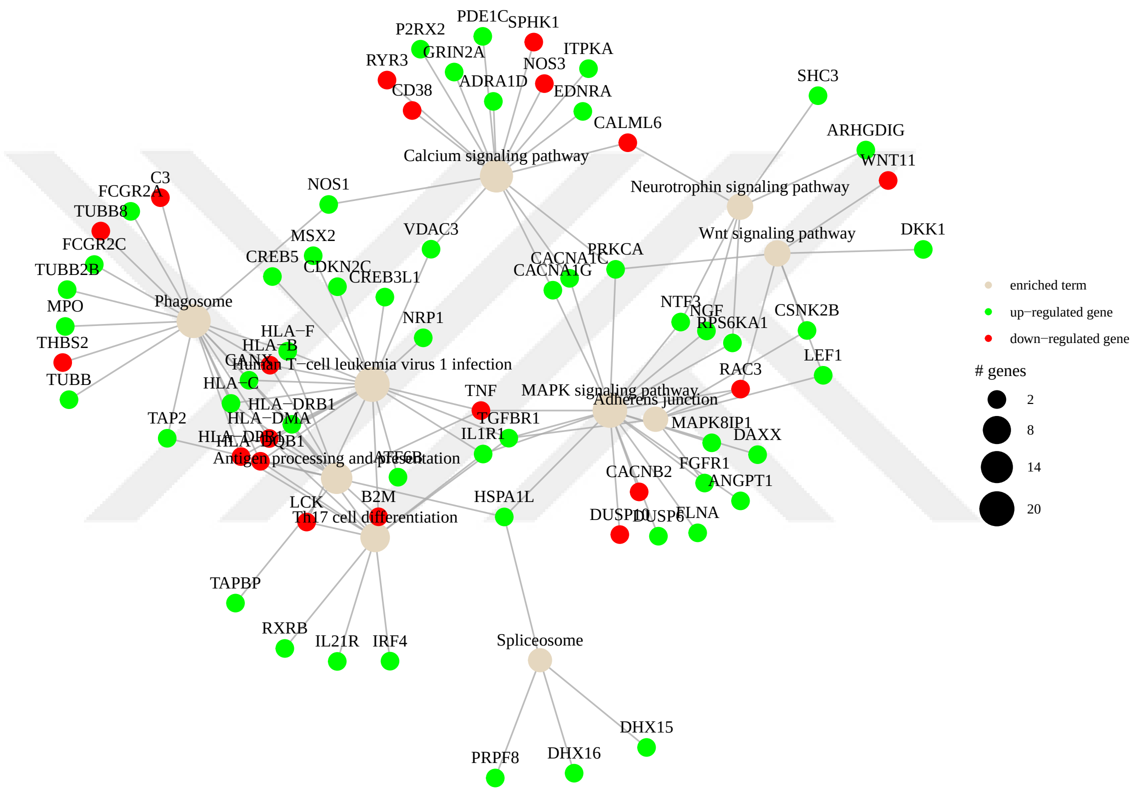

Figure 63: Reduced network of most enriched pathways for the sensitive TNBC cells versus resistant TNBC cells to AZ6102.

In this figure significantly enriched top10 KEGG pathways are visualized as gray hubs (p-value < 0.05). Nodes are representing either upregulated DEGs (green) or down-regulated DEGs (red) which were involved in the enrichment of the connected hub pathway. Preferred DEG cutoff of false discovery rate (FDR) < 0.05 and $\log_2$ absolute fold change ≥ 1.5. These hubs and nodes are not all of the found significant elements. For full list, please look up the relevant section of the supplemental appendix

4.16.2. WIKI4 results

Differential expression analysis results yielded 620 DEGs in the comparison of WIKI4 sensitive 3 TNBC cell lines versus resistant 14 cell lines. Active sub-network based pathway enrichment analysis found 18 enriched KEGG pathways. The most significantly enriched 10 pathways and included DEGs are visualized in **Figure 64**.

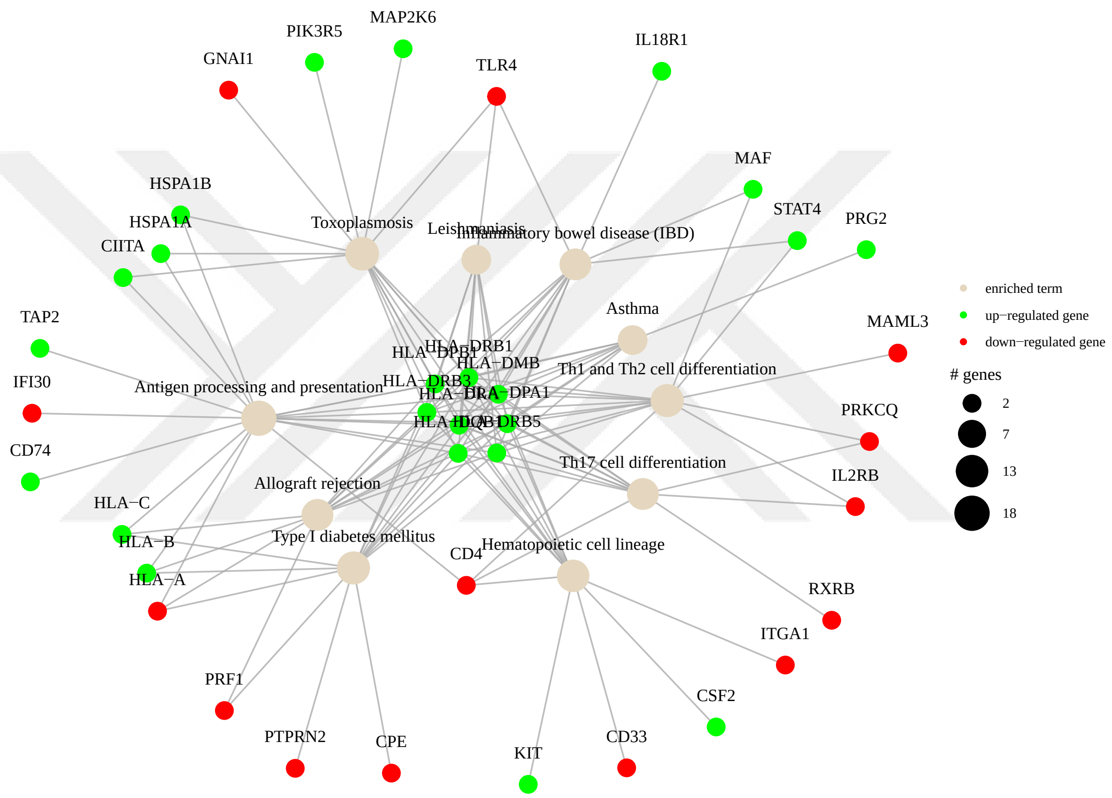

Figure 64: Reduced network of most enriched pathways for the sensitive TNBC cells versus resistant TNBC cells to WIKI4.

In this figure significantly enriched top10 KEGG pathways are visualized as gray hubs (p-value < 0.05). Nodes are representing either upregulated DEGs (green) or down-regulated DEGs (red) which were involved in the enrichment of the connected hub pathway. Preferred DEG cutoff of false discovery rate (FDR) < 0.05 and $\log_2$ absolute fold change ≥ 1.5. These hubs and nodes are not all of the found significant elements. For full list, please look up the relevant section of the supplemental appendix

4.16.3. The intersection of AZ6102 and WIKI4

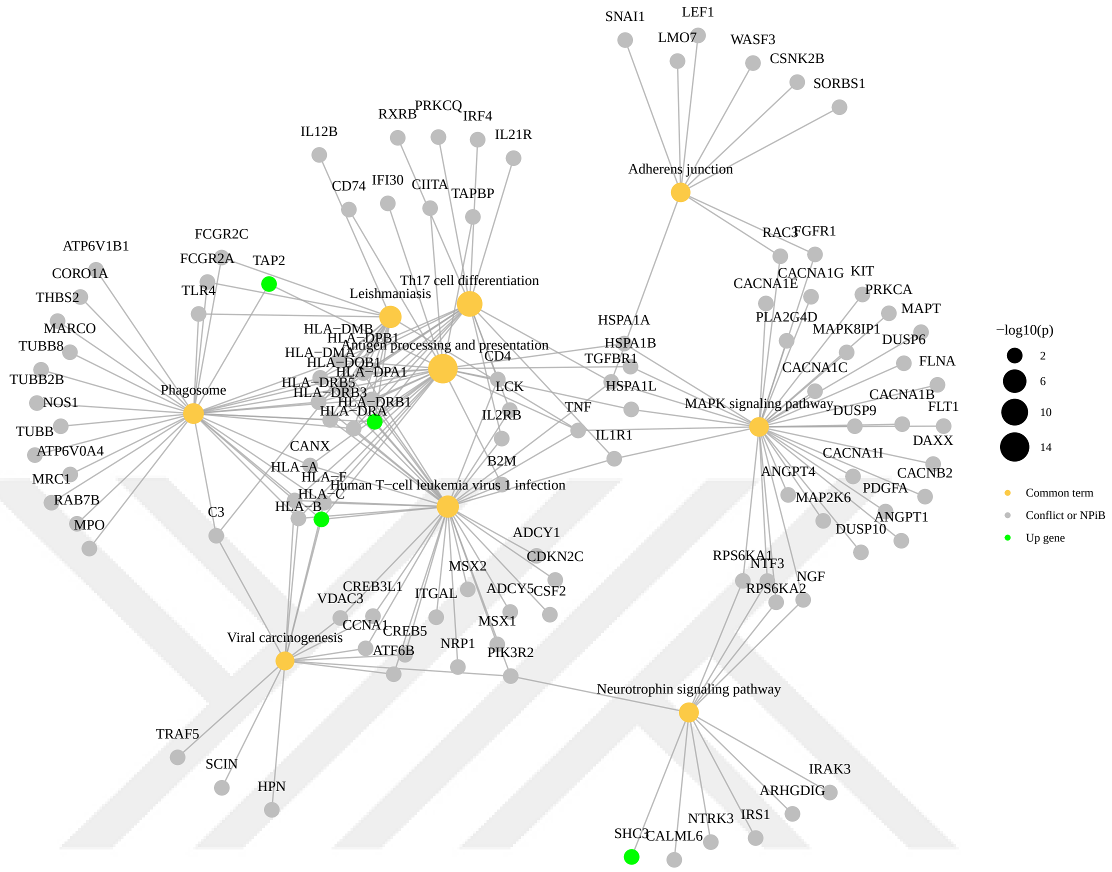

Figure 65: Intersection of most enriched pathways from the determined DEGs of AZ6102 and WIKI4 differential expression analysis.

In this figure, the intersection of the most significant (combined p-value assessment by Fisher's method, p-value ≤ 0.05) commonly enriched KEGG pathways are visualized as yellow hubs. The nodes are representing commonly upregulated DEGs (green), commonly down-regulated DEGs (red), and "conflict or NPiB (Not Present in Both)" DEGs (grey) which were involved in the enrichment of the connected pathway hub. Preferred DEG cutoff of false discovery rate (FDR) < 0.05 and absolute fold change ≥ 1.5. The size of the hubs is reversely proportional with their respective combined p-values for the commonly enriched pathways in the comparison of the two above mentioned drug comparisons.

4.17. Other Drugs

5 drugs have not been linked with a target pathway among the curated 52 drugs by GDSC. The following results are interpretations of the detailed gene expression profile of sensitive TNBC cells versus resistant TNBC cells to those 5 drugs.

4.17.1. AZD5363 results

Differential expression analysis results yielded 583 DEGs in the comparison of AZD5363 sensitive 7 TNBC cell lines versus resistant 10 cell lines. Active sub-network based pathway enrichment analysis found 31 enriched KEGG pathways. The most significantly enriched 10 pathways and included DEGs are visualized in **Figure 66**.

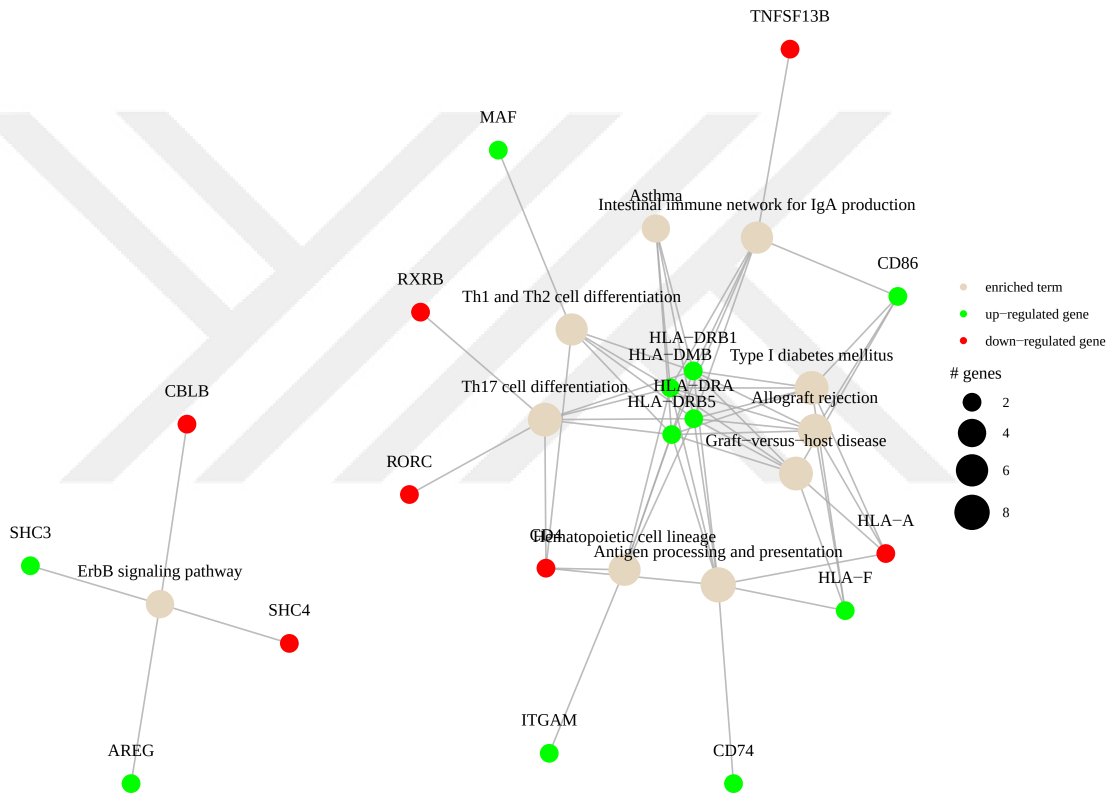

Figure 66: Reduced network of most enriched pathways for the sensitive TNBC cells versus resistant TNBC cells to AZD5363.

In this figure significantly enriched top10 KEGG pathways are visualized as gray hubs (p-value < 0.05). Nodes are representing either upregulated DEGs (green) or down-regulated DEGs (red) which were involved in the enrichment of the connected hub pathway. Preferred DEG cutoff of false discovery rate (FDR) < 0.05 and $\log_2$ absolute fold change ≥ 1.5. These hubs and nodes are not all of the found significant elements. For full list, please look up the relevant section of the supplemental appendix.

4.17.2. Dasatinib results

Differential expression analysis results yielded 750 DEGs in the comparison of Dasatinib sensitive 4 TNBC cell lines versus resistant 13 cell lines. Active sub-network based pathway enrichment analysis found 70 enriched KEGG pathways. The most significantly enriched 10 pathways and included DEGs are visualized in **Figure 67**.

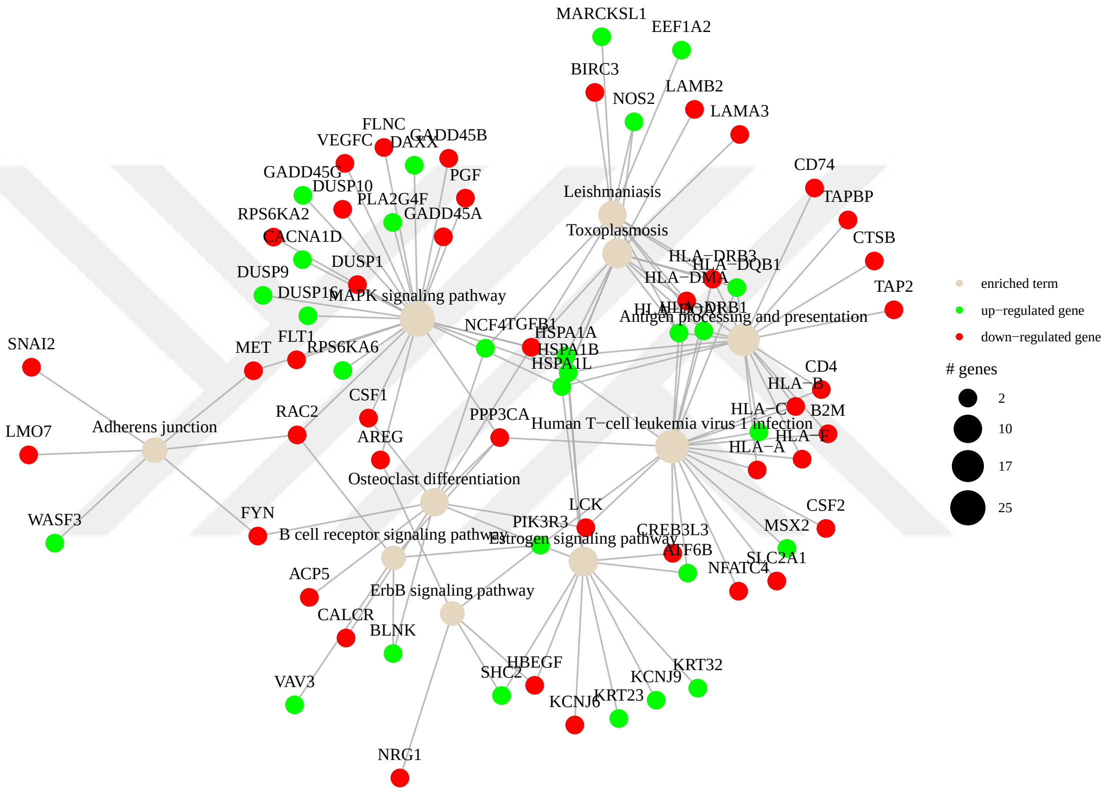

Figure 67: Reduced network of most enriched pathways for the sensitive TNBC cells versus resistant TNBC cells to Dasatinib.

In this figure significantly enriched top10 KEGG pathways are visualized as gray hubs (p-value < 0.05). Nodes are representing either upregulated DEGs (green) or down-regulated DEGs (red) which were involved in the enrichment of the connected hub pathway. Preferred DEG cutoff of false discovery rate (FDR) < 0.05 and $\log_2$ absolute fold change ≥ 1.5. These hubs and nodes are not all of the found significant elements. For full list, please look up the relevant section of the supplemental appendix.

4.17.3. Sorafenib results

Differential expression analysis results yielded 684 DEGs in the comparison of Sorafenib sensitive 8 TNBC cell lines versus resistant 9 cell lines. Active sub-network based pathway enrichment analysis found 24 enriched KEGG pathways. The most significantly enriched 10 pathways and included DEGs are visualized in **Figure 68**.

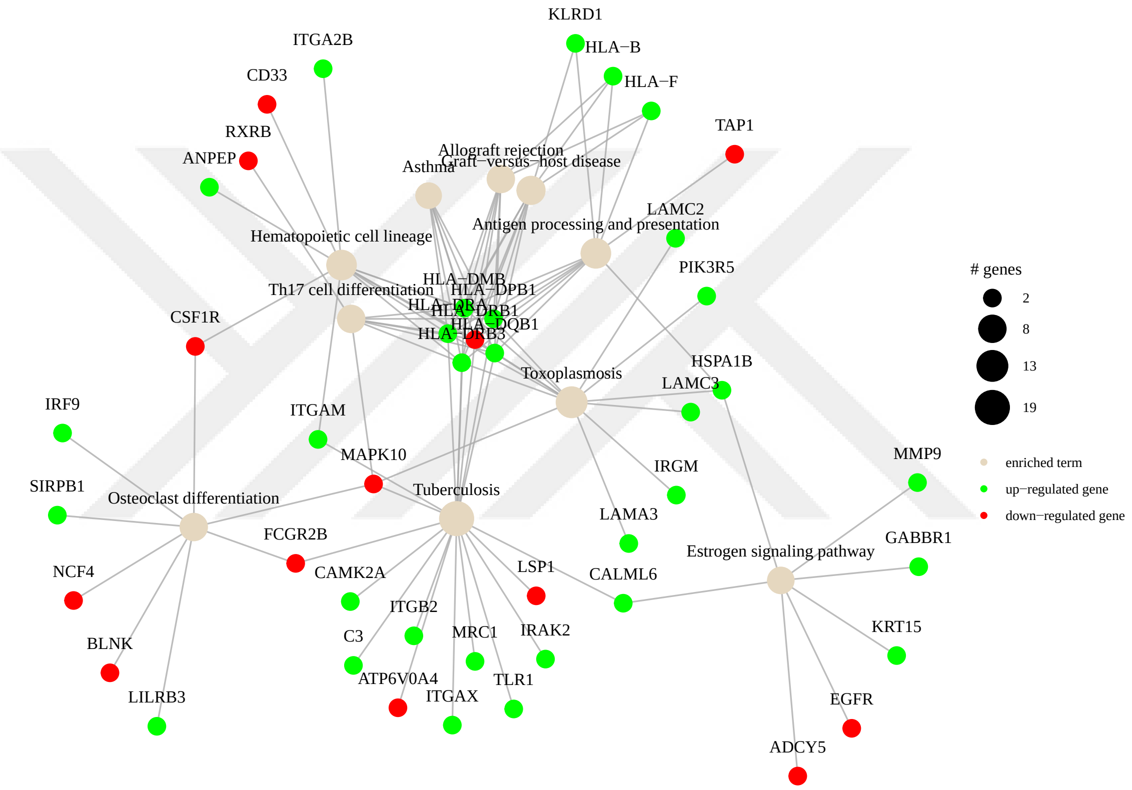

Figure 68: Reduced network of most enriched pathways for the sensitive TNBC cells versus resistant TNBC cells to Sorafenib.

In this figure significantly enriched top10 KEGG pathways are visualized as gray hubs (p-value < 0.05). Nodes are representing either upregulated DEGs (green) or down-regulated DEGs (red) which were involved in the enrichment of the connected hub pathway. Preferred DEG cutoff of false discovery rate (FDR) < 0.05 and $\log_2$ absolute fold change ≥ 1.5. These hubs and nodes are not all of the found significant elements. For full list, please look up the relevant section of the supplemental appendix

4.17.4. YK-4-279 results

Differential expression analysis results yielded 557 DEGs in the comparison of YK-4-279 sensitive 10 TNBC cell lines versus resistant 7 cell lines. Active sub-network based pathway enrichment analysis found 15 enriched KEGG pathways. The most significantly enriched 10 pathways and included DEGs are visualized in **Figure 69**.

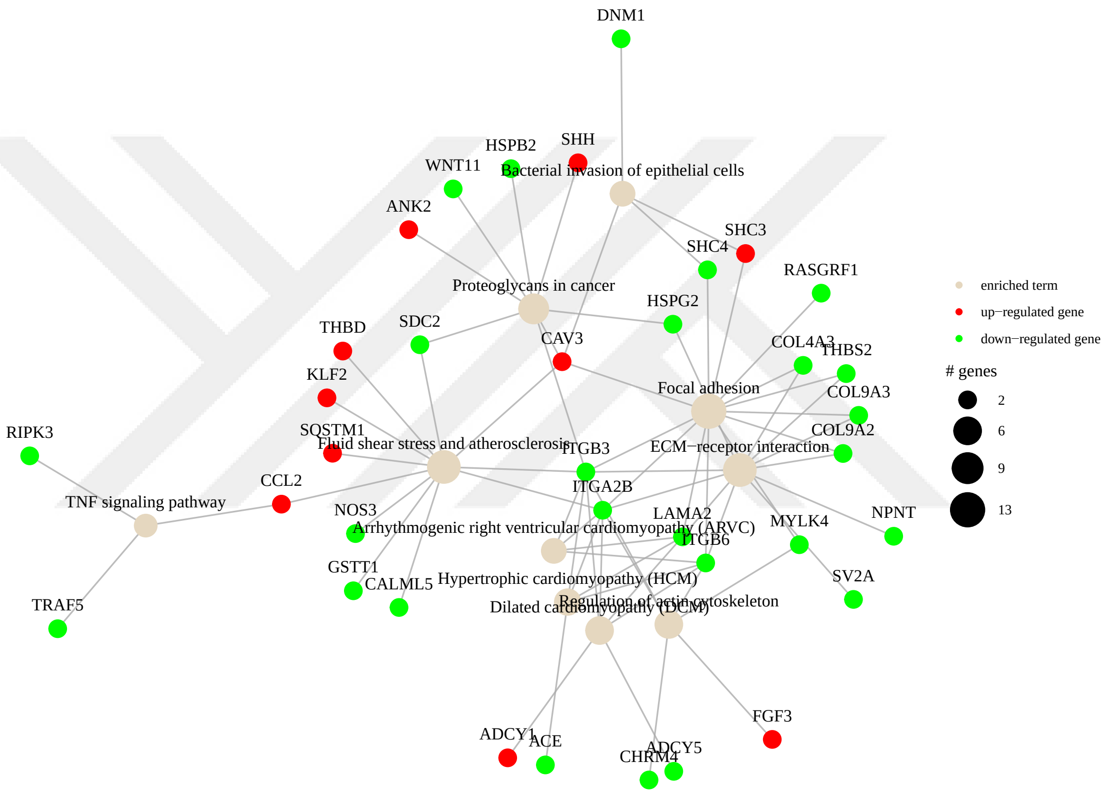

Figure 69: Reduced network of most enriched pathways for the sensitive TNBC cells versus resistant TNBC cells to YK-4-279.

In this figure significantly enriched top10 KEGG pathways are visualized as gray hubs (p-value < 0.05). Nodes are representing either upregulated DEGs (green) or down-regulated DEGs (red) which were involved in the enrichment of the connected hub pathway. Preferred DEG cutoff of false discovery rate (FDR) < 0.05 and $\log_2$ absolute fold change ≥ 1.5. These hubs and nodes are not all of the found significant elements. For full list, please look up the relevant section of the supplemental appendix.

4.17.5. Pevonedistat results

Differential expression analysis results yielded 544 DEGs in the comparison of Pevonedistat sensitive 10 TNBC cell lines versus resistant 7 cell lines. Active sub-network based pathway enrichment analysis found 17 enriched KEGG pathways. The most significantly enriched 10 pathways and included DEGs are visualized in **Figure 70**.

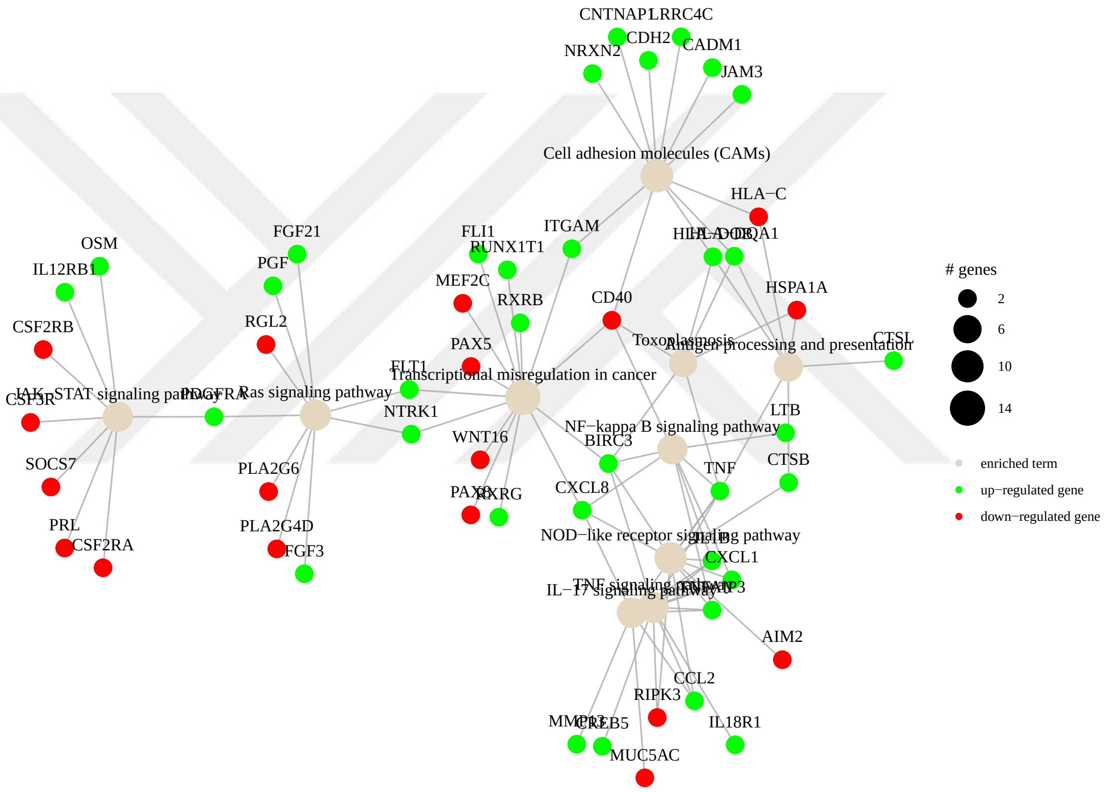

Figure 70: Reduced network of most enriched pathways for the sensitive TNBC cells versus resistant TNBC cells to Pevonedistat.

In this figure significantly enriched top10 KEGG pathways are visualized as gray hubs (p-value < 0.05). Nodes are representing either upregulated DEGs (green) or down-regulated DEGs (red) which were involved in the enrichment of the connected hub pathway. Preferred DEG cutoff of false discovery rate (FDR) < 0.05 and $\log_2$ absolute fold change ≥ 1.5. These hubs and nodes are not all of the found significant elements. For full list, please look up the relevant section of the supplemental appendix.

5. DISCUSSION and CONCLUSION

Breast cancer is the second leading cause of death in women and Triple-Negative breast cancer (TNBC) is one of the most aggressive cancer subtypes of breast cancer. Even though the prevalence of TNBC cases among the patients is around 15-20 percent of the whole breast cancer cases; the survival lifespan of the patients is at least 3 times lesser than other sub-type having breast cancer patients.

To better understand the overall resistance mechanisms to a large pool of chemotherapeutic compounds, 52 different drugs' pharmacodynamics measurements on 17 TNBC cell lines were used, and then baseline gene expression profiles of these 17 TNBC cell lines were assessed independently. Then, those 52 drugs investigated by their common targeted pathways and assessed together to unravel the most commonly affected DEGs and most commonly enriched pathways that take a significant role in the respective drugs' resistance mechanisms (**Figure 1**).

In this study, initially, the availability of the transcriptomics data and pharmacodynamics data of TNBC cell lines was looked upon. Even though some studies indicate more than 20 distinct TNBC cell lines **(88)**; for the assessment of combined gene expression and drug-responses of TNBC cells, a consensus 17 TNBC cell lines gathered due to their prevalent usage on recent studies and abundant commercial availability to further reproducibility-wise inquiries.

Baseline gene expression of cells is conventionally used in research as either a negative control group to test the effect of any stimulant applied to investigated cells or to build predictive statistical models by machine-learning-based approaches. In this study, the baseline gene expression of TNBC cells utilized in a novel way to better understand what fundamental expression patterns led them to refractory response to the curated chemotherapeutic compounds.

GDSC consortium's pharmacodynamics data is bulk-downloaded to pool a large number of therapeutic compounds. The idea is covering the wider landscape of the available drugs. Some of the drugs that are included in this study are already commercially available, but some are still experimental drugs or pre-release phase of the commercial candidate drugs for the pharmaceutical companies. The inconvenient nomenclature of some drug molecules (i.e. BDP-00009066 and NVP-ADW742) is clearly explained by this being-experimental of these drugs.

As it is explained in section 3.2 Pharmacodynamics Data, some of the drugs that are conventionally used in the clinics may be filtered out either in the TNBC sample distribution on response groups or some of the missing dosage measurements might be led to being uninvolved of the drug in the data pool of curated 52 drugs.

Our first approach was the investigation of drug similarities for these drugs. SMILES notation of the chemical formula of these compounds used to convert them to easily computationally manageable way and then generated a hierarchical cluster for them to observe how quantifiably similar each of 52 drugs with each other. Most similar 4 drug pairs selected from the dendrogram of **Figure 2**. Then those are investigated for their common pathway enrichment analysis from their respective DEGs. Those most similar 4 drug pairs are "AZD4547 and ZM447439", "AZD6738 and Pevonedistat", "NVP-ADW742 and WIKI4", and "Afatinib and Sapitinib". The first three pairs are presented in section 4.1. Drug Similarity by SMILES. The last most similar drug pair is presented on page 49 because that pair is overlapping as one of the most similar drug-pair and most enriched pathways having drug comparison in their targeted metabolic pathway.

Results of similarity-based comparison of drug responses of the TNBC cell lines are quite variable for the compared most similar drug pairs. The expectation was to see much more overlapping commonly upregulated or downregulated genes in the intersection network results of the enriched KEGG pathways by respective DEGs of investigated two drugs. in section 4.1. Drug Similarity by SMILES.

Then, targeted pathways of the curated drug molecules were focused on and put into classes according to the drugs' targeted metabolic pathways. Among 52 different chemotherapeutic compounds, 15 common pathway target groups were observed. As a possible resistance mechanism to investigated targeted pathway drug groups, dysregulation of the most enriched metabolic pathways in each case might be causal factors on the resistant phenotype to investigated drugs.

To emphasize one more time, there were no stimulant applied gene expression data available for these TNBC cell lines, overlapping with the investigated drugs and the main idea was covering a quite large landscape of drugs. Quantitative interpretation of the baseline gene expression of these cells with the drug responses is the statistically relevant explanation of why some cells are more refractory to some drugs while the others are much sensitive.

Even though these 17 TNBC cell lines are immortalized entities and they bear a great number of mutations on themselves as a reason and/or consequence of being cancerous cells, the information of these mutations can be combined with expression patterns of TNBC cells. Using solely mRNA information of the cells cannot provide additional support for is there any upstream molecular events occurs that lead to dysregulation of the mRNA product or not. On the other hand, all of the transcribed mRNAs are not translated to proteins there are post-transcriptional regulation mechanisms like miRNA regulation. Better to investigate all of these aspects in a much comprehensive integrative multi-omics study. That is a further aim and one of the to-dos of this thesis study.

To conclude, most prevalently enriched found pathways in sensitive TNBC cells versus resistant TNBC cells are MAPK signaling, estrogen signaling, ErbB signaling, and PI3K/mTOR signaling which are all greatly involved in cancer biology. The determined DEGs are highly differing for each of the drug response comparison and also again varies in intersections of the most enriched pathways and DEGS for targeted pathway groups but the enriched pathways are substantially consistent. This phenomenon is, almost independent from the distribution and cell members of sensitive cells or resistant cells, and the drug. DEGs are almost different in all cases but their involvement in the metabolic pathways is ending up the enrichment of mostly the same pathways as can be seen in intersection results.

6. SUPPLEMENTARY APPENDIX

All processed data and written R codes are grouped for different work packages in this study can be found in the dedicated folder on GitHub **(89)**.

The results of the differential expression analyses, the determined DEGs for the comparison of the sensitive cell lines versus the resistant cell lines to 52 therapeutic compounds, detailed full-size images of all the figures and supplementary figures that elaborate them, and processed data that is used to obtain the main results were deposited on the dedicated project on “figshare” platform for to maintain reproducibility and additional insight to readers **(90)**.

7. REFERENCES

1. Siegel RL, Miller KD, Jemal A. Cancer statistics, 2020. CA Cancer J Clin. 2020;70(1):7–30.

2. Jhan J-R, Andrechek ER. Effective personalized therapy for breast cancer based on predictions of cell signaling pathway activation from gene expression analysis. Oncogene. 2017 22;36(25):3553–61.

3. Harbeck N, Gnant M. Breast cancer. Lancet Lond Engl. 2017 18;389(10074):1134–50.

4. Kennecke H, Yerushalmi R, Woods R, Cheang MCU, Voduc D, Speers CH, et al. Metastatic behavior of breast cancer subtypes. J Clin Oncol Off J Am Soc Clin Oncol. 2010 Jul 10;28(20):3271–7.

5. Tyanova S, Albrechtsen R, Kronqvist P, Cox J, Mann M, Geiger T. Proteomic maps of breast cancer subtypes. Nat Commun. 2016 Jan 4;7:10259.

6. Dumitrescu RG. Interplay between genetic and epigenetic changes in breast cancer subtypes. Methods Mol Biol Clifton NJ. 2018;1856:19–34.

7. Dai X, Xiang L, Li T, Bai Z. Cancer hallmarks, biomarkers and breast cancer molecular subtypes. J Cancer. 2016;7(10):1281–94.

8. Shi Y, Jin J, Ji W, Guan X. Therapeutic landscape in mutational triple negative breast cancer. Mol Cancer. 2018 14;17(1):99.

9. Vagia E, Mahalingam D, Cristofanilli M. The landscape of targeted therapies in TNBC. Cancers. 2020 Apr 8;12(4).

10. Bianchini G, Balko JM, Mayer IA, Sanders ME, Gianni L. Triple-negative breast cancer: challenges and opportunities of a heterogeneous disease. Nat Rev Clin Oncol. 2016 Nov;13(11):674–90.

11. Dent R, Trudeau M, Pritchard KI, Hanna WM, Kahn HK, Sawka CA, et al. Triple-negative breast cancer: clinical features and patterns of recurrence. Clin Cancer Res Off J Am Assoc Cancer Res. 2007 Aug 1;13(15 Pt 1):4429–34.

12. Yin L, Duan J-J, Bian X-W, Yu S-C. Triple-negative breast cancer molecular subtyping and treatment progress. Breast Cancer Res BCR. 2020 Jun 9;22(1):61.

13. Hooke R, Allestry J, Martyn J. Micrographia, or some physiological descriptions of minute bodies made by magnifying glasses with observations and inquiries thereupon [Internet]. London : Printed by Jo. Martyn and Ja. Allestry, printers to the Royal Society ... ,; 1665. 323 p. Available from: https://www.biodiversitylibrary.org/bibliography/904

14. Turner Wm. The cell theory, past and present. J Anat Physiol. 1890 Jan;24(Pt 2):253–87.

15. Harvey A. On the fœtus in utero, as inoculating the maternal with the peculiarities of the paternal organism. Glasg Med J. 1859 Jan;6(24):385–407.

16. Buxton BH. Photographs of a series of sections of an early human embryo. J Anat Physiol. 1899 Apr;33(Pt 3):381-526.29.

17. Thompson P. Description of a human embryo of twenty-three paired somites. J Anat Physiol. 1907 Apr;41(Pt 3):159–71.

18. Matthews AP. Artifically produced mitotic division in unfertilized arbacia eggs. J Boston Soc Med Sci. 1900 Oct 16;5(1):13–7.

19. Lambert RA. Comparative studies upon cancer cells and normal cells : ii. The character of growth in vitro with special reference to cell division. J Exp Med. 1913 May 1;17(5):499–510.

20. Spain KC, Loeb L. A quantitative analysis of the influence of the size of the defect on wound healing in the skin of the Guinea pig. J Exp Med. 1916 Jan 1;23(1):107–22.

21. Loeb L, Fleisher MS. The growth of tissues in the test tube under experimentally varied conditions with special reference to mitotic cell proliferation. J Med Res. 1919 Sep;40(3):509–50.

22. Chung K-T, Nilson EH, Case MJ, Marr AG, Hungate RE. Estimation of growth rate from the mitotic index. Appl Microbiol. 1973 May;25(5):778–80.

23. Carleton A. A rhythmical periodicity in the mitotic division of animal cells. J Anat. 1934 Jan;68(Pt 2):251–63.

24. Hoffman JG. Wright's hypothesis: Its relation to volume growth of tissue cells and mitotic index. Science. 1947 Oct 10;106(2754):343–4.

25. Fraser RS, Moreno F. Rates of synthesis of polyadenylated messenger RNA and ribosomal RNA during the cell cycle of Schizosaccharomyces pombe. With an Appendix: Calculation of the pattern of protein accumulation from observed changes in the rate of messenger RNA synthesis. J Cell Sci. 1976 Aug;21(3):497–521.

26. Baisch H, Göhde W, Linden WA. Analysis of PCP-data to determine the fraction of cells in the various phases of cell cycle. Radiat Environ Biophys. 1975 Jun 1;12(1):31–9.

27. Bashford EF, Murray JA. The significance of the zoological distribution, the nature of the mitoses, and the transmissibility of cancer. Br Med J. 1904 Jan 30;1(2248):269–71.

28. Comings DE. A general theory of carcinogenesis. Proc Natl Acad Sci U S A. 1973 Dec;70(12):3324–8.

29. Hartley A-V, Lu T. Modulating the modulators: Regulation of protein arginine methyltransferases by post-translational modifications. Drug Discov Today. 2020 Jul 3;

30. DeLeo AB, Appella E. The p53 saga: Early steps in the development of tumor immunotherapy. J Immunol Baltim Md 1950. 2020 May 1;204(9):2321–8.

31. Roy D, Sheng GY, Herve S, Carvalho E, Mahanty A, Yuan S, et al. Interplay between cancer cell cycle and metabolism: Challenges, targets and therapeutic opportunities. Biomed Pharmacother Biomedecine Pharmacother. 2017 May;89:288–96.

32. Sobočan M, Smolle MA, Schatz C, Haybaeck J. The interplay of tumor stroma and translational factors in endometrial cancer. Cancers. 2020 Jul 27;12(8).

33. Fazio A, Owusu Obeng E, Rusciano I, Marvi MV, Zoli M, Mongiorgi S, et al. Subcellular localization relevance and cancer-associated mechanisms of diacylglycerol kinases. Int J Mol Sci. 2020 Jul 26;21(15).

34. Azad T, Rezaei R, Surendran A, Singaravelu R, Boulton S, Dave J, et al. Hippo signaling pathway as a central mediator of receptors tyrosine kinases (RTKs) in tumorigenesis. Cancers. 2020 Jul 24;12(8).

35. Tang K, Jia Y-N, Yu B, Liu H-M. Medicinal chemistry strategies for the development of protein tyrosine phosphatase SHP2 inhibitors and PROTAC degraders. Eur J Med Chem. 2020 Jul 23;204:112657.

36. Czarnecka AM, Bartnik E, Fiedorowicz M, Rutkowski P. Targeted therapy in melanoma and mechanisms of resistance. Int J Mol Sci. 2020 Jun 27;21(13).

37. Amirani E, Hallajzadeh J, Asemi Z, Mansournia MA, Yousefi B. Effects of chitosan and oligochitosans on the phosphatidylinositol 3-kinase-AKT pathway in cancer therapy. Int J Biol Macromol. 2020 Jul 18;164:456–67.

38. Schaefer T, Steiner R, Lengerke C. SOX2 and p53 expression control converges in PI3K/AKT signaling with versatile implications for stemness and cancer. Int J Mol Sci. 2020 Jul 11;21(14).

39. Kokal M, Mirzakhani K, Pungsrinont T, Baniahmad A. Mechanisms of androgen receptor agonist and antagonist - Mediated cellular senescence in prostate cancer. Cancers. 2020 Jul 8;12(7).

40. In der Stroth L, Tharehalli U, Günes C, Lechel A. Telomeres and telomerase in the development of liver cancer. Cancers. 2020 Jul 24;12(8).

41. Park H-A, Brown SR, Kim Y. Cellular mechanisms of circulating tumor cells during breast cancer metastasis. Int J Mol Sci. 2020 Jul 17;21(14).

42. Menck K, Sivaloganathan S, Bleckmann A, Binder C. Microvesicles in cancer: Small size, large potential. Int J Mol Sci. 2020 Jul 28;21(15).

43. Filip S, Vymetalkova V, Petera J, Vodickova L, Kubecek O, John S, et al. Distant metastasis in colorectal cancer patients - Do we have new predicting clinicopathological and molecular biomarkers? A comprehensive review. Int J Mol Sci. 2020 Jul 24;21(15).

44. Davis OCM. Some observations on the mechanism of drug action. Br Med J. 1922 Jul 1;2(3209):11–2.

45. Torda C, Wolff HG. Experimental studies on headache: Pharmacodynamics of urine excreted during migraine headache and its relation to 17-Ketosteroid content. J Clin Invest. 1943 Nov;22(6):853–8.

46. Forssman S, Lindsten T. A contribution to the pharmacodynamics of malonic, succinic, citric, aconitic, alpha-ketoglutaric and glutamic acid. Acta Pharmacol Toxicol (Copenh). 1946;2(4):329–42.

47. Meroni PL, Valentini G, Ayala F, Cattaneo A, Valesini G. New strategies to address the pharmacodynamics and pharmacokinetics of tumor necrosis factor (TNF) inhibitors: A systematic analysis. Autoimmun Rev. 2015 Sep;14(9):812–29.

48. Yoshida M, Hoshi A, Kuretani K, Kanai T, Ichino M. Action of 5-fluorocyclocytidine on cultured L-5178Y cells. Gan. 1975 Oct;66(5):561–4.

49. Zeng H, Zhu X, Tian Q, Yan Y, Zhang L, Yan M, et al. In vivo antitumor effects of carboxymethyl chitosan-conjugated triptolide after oral administration. Drug Deliv. 2020 Dec;27(1):848–54.

50. Polak S, Wiśniowska B, Glinka A, Fijorek K, Mendyk A. Slow delayed rectifying potassium current (IKs) - Analysis of the in vitro inhibition data and predictive model development. J Appl Toxicol JAT. 2013 Aug;33(8):723–39.

51. Condelli N, Caruso MC, Galgano F, Russo D, Milella L, Favati F. Prediction of the antioxidant activity of extra virgin olive oils produced in the Mediterranean area. Food Chem. 2015 Jun 15;177:233–9.

52. Rajput A, Kumar A, Kumar M. Computational identification of inhibitors using QSAR approach against Nipah virus. Front Pharmacol. 2019;10:71.

53. Frankish A, Diekhans M, Ferreira A-M, Johnson R, Jungreis I, Loveland J, et al. GENCODE Reference annotation for the human and mouse genomes. Nucleic Acids Res. 2019 Jan 8;47(D1):D766–73.

54. Tassinari V, Cesarini V, Silvestris DA, Scafidi A, Cucina L, Gallo A. MicroRNA editing detection and function: A combined in silico and experimental approach for the identification and validation of putative oncogenic targets. Methods Mol Biol Clifton NJ. 2021;2181:253–67.

55. Diroma MA, Ciaccia L, Pesole G, Picardi E. Bioinformatics resources for RNA editing. Methods Mol Biol Clifton NJ. 2021;2181:177–91.

56. Lander ES, Linton LM, Birren B, Nusbaum C, Zody MC, Baldwin J, et al. Initial sequencing and analysis of the human genome. Nature. 2001 Feb;409(6822):860–921.

57. Werner T. Next generation sequencing in functional genomics. Brief Bioinform. 2010 Sep;11(5):499–511.

58. Mortazavi A, Williams BA, McCue K, Schaeffer L, Wold B. Mapping and quantifying mammalian transcriptomes by RNA-Seq. Nat Methods. 2008 Jul;5(7):621–8.

59. Zhao S, Ye Z, Stanton R. Misuse of RPKM or TPM normalization when comparing across samples and sequencing protocols. RNA N Y N. 2020 Aug;26(8):903–9.

60. Nguyen KL, Grondin A, Courtois B, Gantet P. Next-generation sequencing accelerates crop gene discovery. Trends Plant Sci. 2019;24(3):263–74.

61. Kulkarni A, Anderson AG, Merullo DP, Konopka G. Beyond bulk: A review of single cell transcriptomics methodologies and applications. Curr Opin Biotechnol. 2019;58:129–36.

62. van Kuijk K, Kuppe C, Betsholtz C, Vanlandewijck M, Kramann R, Sluimer JC. Heterogeneity and plasticity in healthy and atherosclerotic vasculature explored by single-cell sequencing. Cardiovasc Res. 2019 Oct 1;115(12):1705–15.

63. Kim D, Chung KB, Kim T-G. Application of single-cell RNA sequencing on human skin: Technical evolution and challenges. J Dermatol Sci. 2020 Jun 12;

64. Hsu LL, Culhane AC. Impact of data preprocessing on integrative matrix factorization of single cell data. Front Oncol. 2020;10:973.

65. Li Z, Tyler WA, Haydar TF. Lessons from single cell sequencing in CNS cell specification and function. Curr Opin Genet Dev. 2020 Jul 14;65:138–43.

66. Wu Y, Zhang K. Tools for the analysis of high-dimensional single-cell RNA sequencing data. Nat Rev Nephrol. 2020 Jul;16(7):408–21.

67. Lehmann BD, Bauer JA, Chen X, Sanders ME, Chakravarthy AB, Shyr Y, et al. Identification of human triple-negative breast cancer subtypes and preclinical models for selection of targeted therapies. J Clin Invest. 2011 Jul;121(7):2750–67.

68. Iorio et al. F. GDSC - Extended methods [Internet]. Available from: https://www.cancerrxgene.org/gdsc1000/GDSC1000_WebResources//Home_files/Extended%20Methods.html#8

69. Iorio et al. F. Genomics of drug sensitivity in cancer v2 [Internet]. [cited 2020 Aug 4]. Available from: https://www.cancerrxgene.org/

70. Iorio F, Knijnenburg TA, Vis DJ, Bignell GR, Menden MP, Schubert M, et al. A landscape of pharmacogenomic interactions in cancer. Cell. 2016 Jul 28;166(3):740–54.

71. Ghandi M, Huang FW, Jané-Valbuena J, Kryukov GV, Lo CC, McDonald ER, et al. Next-generation characterization of the Cancer Cell Line Encyclopedia. Nature. 2019;569(7757):503–8.

72. Homo sapiens (ID 523380) - BioProject - NCBI [Internet]. [cited 2020 Aug 4]. Available from: https://www.ncbi.nlm.nih.gov/bioproject/PRJNA523380/

73. Klijn C, Durinck S, Stawiski EW, Haverty PM, Jiang Z, Liu H, et al. A comprehensive transcriptional portrait of human cancer cell lines. Nat Biotechnol. 2015 Mar;33(3):306–12.

74. EGAS00001000610 project of European Genome-phenome Archive [Internet]. [cited 2020 Aug 4]. Available from: https://www.ebi.ac.uk/ega/studies/EGAS00001000610

75. FastQC: A quality control tool for high throughput sequence data - Babraham Bioinformatics [Internet]. [cited 2020 Aug 4]. Available from: http://www.bioinformatics.babraham.ac.uk/projects/fastqc/

76. Bushnell B, Rood J, Singer E. BBMerge - Accurate Paired Shotgun Read Merging via Overlap. PloS One. 2017;12(10):e0185056.

77. Dobin A, Davis CA, Schlesinger F, Drenkow J, Zaleski C, Jha S, et al. STAR: ultrafast universal RNA-seq aligner. Bioinforma Oxf Engl. 2013 Jan 1;29(1):15–21.

78. GTEx & TOPMed data production and analysis pipelines [Internet]. GitHub. [cited 2020 Aug 4]. Available from: https://github.com/broadinstitute/gtex-pipeline

79. Ensembl’s reference data of the FTP server interface [Internet]. [cited 2020 Aug 4]. Available from: http://www.ensembl.org/info/data/ftp/index.html

80. Patro R, Duggal G, Love MI, Irizarry RA, Kingsford C. Salmon provides fast and bias-aware quantification of transcript expression. Nat Methods. 2017 Apr;14(4):417–9.

81. R Core Team. R: A language and environment for statistical computing [Internet]. Vienna, Austria: R Foundation for Statistical Computing; 2020. Available from: https://www.R-project.org/

82. Soneson C, Love MI, Robinson MD. Differential analyses for RNA-seq: Transcript-level estimates improve gene-level inferences. F1000Research. 2015 Dec 30;4:1521.

83. Love MI, Huber W, Anders S. Moderated estimation of fold change and dispersion for RNA-seq data with DESeq2. Genome Biol. 2014 Dec 5;15(12):550.

84. Ulgen E, Ozisik O, Sezerman OU. pathfindR: An R package for comprehensive identification of enriched pathways in omics data through active subnetworks. Front Genet [Internet]. 2019 [cited 2020 Aug 4];10. Available from: https://www.frontiersin.org/articles/10.3389/fgene.2019.00858/full

85. PubChem. PubChem digital library [Internet]. [cited 2020 Aug 4]. Available from: https://pubchem.ncbi.nlm.nih.gov/

86. Backman TWH, Cao Y, Girke T. ChemMine tools: an online service for analyzing and clustering small molecules. Nucleic Acids Res. 2011 Jul 1;39(suppl_2):W486–91.

87. ChemMine tools [Internet]. [cited 2020 Aug 4]. Available from: https://chemminetools.ucr.edu/

88. Dai X, Cheng H, Bai Z, Li J. Breast cancer cell line classification and its relevance with breast tumor subtyping. J Cancer. 2017 Sep 12;8(16):3131–41.

89. Ekren R. Supplementary codes to the transcriptomics-based investigation of drug resistance mechanisms in triple-negative breast cancer cell lines [Internet]. 2020 [cited 2020 Jul 28]. Available from: https://github.com/rekren/TNBC

90. Ekren R. Supplementary appendix to the transcriptomics-based investigation of drug resistance mechanisms in triple-negative breast cancer cell lines [Internet]. [cited 2020 Jul 28]. Available from: https://figshare.com/projects/Transcriptomics-Based_Investigation_of_Drug_Resistance_Mechanisms_in_Triple-Negative_Breast_Cancer_Cell_Lines/85226

8. CURRICULUM VITAE

Personal Information

Name	Rüçhan	**Surname**	Ekren
Place of Birth	Balıkesir	**Date of Birth**	22/06/1991
Nationality	T.R	**Telephone**	05342883326
e-mail	ruchanekren(et)gmail.com		

Education

	Name of the Graduated School	**Graduation Year**
M.Sc.	Acıbadem Mehmet Ali Aydınlar University	2020
B.Sc.	Izmir Institute of Technology	2017
High School	Susurluk Anatolian High School	2009

Languages	**Reading**	**Writing**	**Listening**
English	Professional Proficiency	Professional Proficiency	Professional Proficiency
Turkish	Native	Native	Native

Exam	**Scores**		
ALES	Quantitative: 75.29	Verbal: 78.54	Equally-Weighted: 77.46
YÖKDİL	83.75		

Computer Skills	Proficiency Level
R Programming Language	Very Good
MS Office	Very Good
GNU/Linux Shell	Good
Python Programming Language	Good

Publications
High-throughput profiling reveals perturbation of ER stress-related genes in atherosclerosis induced by high-cholesterol diet and the protective role of vitamin E" Bozaykut P, Ekren R, Sezerman OU, Gladyshev VN, Ozer N (*Biofactors*, May 2020, https://doi.org/10.1002/biof.1635)
Response Assessment with Molecular characterization of Circulating Tumor Cells and Plasma Micro RNAs profiling in locally advanced Breast Cancer Patients during Neoadjuvant Chemotherapy", Akkiprik M, Koca S, Uğurlu MÜ, Ekren R, Peker Eyüboğlu İ,Alan Ö, Erzik C, Güllü Amuran G, Akın Telli T, Güllüoğlu MB, Sezerman U, Yumuk PF (*Clinical Breast Cancer*, February 2020, https://doi.org/10.1016/j.clbc.2020.02.006)
Ameliorative potential of Lavandula stoechas in metabolic syndrome via multitarget interactions." Kulabas SS, Ipek H, Tufekci AR, Arslan S, Demirtas I, Ekren R, Sezerman U, Tumer TB, (*J Ethnopharmacol*, May 2018, https://doi.org/10.1016/j.jep.2018.04.043)